

## Wild bonobos host geographically restricted malaria parasites including a putative new *Laverania* species

Liu, Weimin; Sherrill-Mix, Scott; Learn, Gerald H.; Scully, Erik J.; Li, Yingying; Avitto, Alexa N.; Loy, Dorothy E.; Lauder, Abigail P.; Sundararaman, Sesh A.; Plenderleith, Lindsey J.; Ndjango, Jean-Bosco N.; Georgiev, Alexander V.; Ahuka-Mundeke, Steve; Peeters, Martine; Bertaolani, Paco; Dupain, Jef; Garai, Cintia; Hart, John A.; Hart, Terese B.; Shaw, George M.; Sharp, Paul M.; Hahn, Beatrice H.

**Nature Communications**

DOI:

[10.1038/s41467-017-01798-5](https://doi.org/10.1038/s41467-017-01798-5)

Published: 01/11/2017

Peer reviewed version

[Cyswllt i'r cyhoeddiad / Link to publication](#)

*Dyfyniad o'r fersiwn a gyhoeddwyd / Citation for published version (APA):*

Liu, W., Sherrill-Mix, S., Learn, G. H., Scully, E. J., Li, Y., Avitto, A. N., Loy, D. E., Lauder, A. P., Sundararaman, S. A., Plenderleith, L. J., Ndjango, J-B. N., Georgiev, A. V., Ahuka-Mundeke, S., Peeters, M., Bertaolani, P., Dupain, J., Garai, C., Hart, J. A., Hart, T. B., ... Hahn, B. H. (2017). Wild bonobos host geographically restricted malaria parasites including a putative new *Laverania* species. *Nature Communications*, 8, [1635]. <https://doi.org/10.1038/s41467-017-01798-5>

### Hawliau Cyffredinol / General rights

Copyright and moral rights for the publications made accessible in the public portal are retained by the authors and/or other copyright owners and it is a condition of accessing publications that users recognise and abide by the legal requirements associated with these rights.

- Users may download and print one copy of any publication from the public portal for the purpose of private study or research.
- You may not further distribute the material or use it for any profit-making activity or commercial gain
- You may freely distribute the URL identifying the publication in the public portal ?

### Take down policy

If you believe that this document breaches copyright please contact us providing details, and we will remove access to the work immediately and investigate your claim.

## **Geographically restricted malaria infections of wild bonobos include a new *Laverania* species**

Weimin Liu<sup>1#</sup>, Scott Sherrill-Mix<sup>1,2#</sup>, Gerald H. Learn<sup>1</sup>, Erik J. Scully<sup>3,4</sup>, Yingying Li<sup>1</sup>, Alexa N. Avitto<sup>1</sup>,  
Dorothy E. Loy<sup>1,2</sup>, Abigail P. Lauder<sup>2</sup>, Sesh A. Sundararaman<sup>1,2</sup>, Lindsey J. Plenderleith<sup>5</sup>,  
Jean-Bosco N. Ndjango<sup>6</sup>, Alexander V. Georgiev<sup>7,8</sup>, Steve Ahuka-Mundeke<sup>9</sup>, Martine Peeters<sup>10</sup>,  
Paco Bertolani<sup>11</sup>, Jef Dupain<sup>12</sup>, Cintia Garai<sup>13</sup>, John A. Hart<sup>13</sup>, Terese B. Hart<sup>13</sup>, George M. Shaw<sup>1,2</sup>,  
Paul M. Sharp<sup>5</sup> and Beatrice H. Hahn<sup>1,2\*</sup>

Departments of <sup>1</sup>Medicine and <sup>2</sup>Microbiology, University of Pennsylvania, Philadelphia, PA 19104, USA;  
<sup>3</sup>Department of Human Evolutionary Biology, Harvard University, Cambridge, MA, USA, 02138;  
<sup>4</sup>Department of Immunology and Infectious Diseases, Harvard T.H. Chan School of Public Health, Boston, MA, USA, 02115; <sup>5</sup>Institute of Evolutionary Biology and Centre for Immunity, Infection and Evolution, University of Edinburgh, Edinburgh EH9 3FL, UK; <sup>6</sup>Department of Ecology and Management of Plant and Animal Resources, Faculty of Sciences, University of Kisangani, Kisangani, Democratic Republic of the Congo; <sup>7</sup>Department of Human Evolutionary Biology, Harvard University, Cambridge, MA 02138, USA; <sup>8</sup>School of Biological Sciences, Bangor University, Bangor, LL57 2UW, UK; <sup>9</sup>Institut National de Recherche Biomedicale, University of Kinshasa, Kinshasa, Democratic Republic of the Congo BP 1197; <sup>10</sup>Unité Mixte Internationale 233/INSERM-U1175, Institut de Recherche pour le Développement and University of Montpellier 1, 34394 Montpellier, France; <sup>11</sup>Leverhulme Centre for Human Evolutionary Studies, University of Cambridge, UK; <sup>12</sup>African Wildlife Foundation Conservation Centre, 00502 Nairobi, Kenya; <sup>13</sup>Lukuru Wildlife Research Foundation, Tshuapa-Lomami-Lualaba Project, Kinshasa, Democratic Republic of the Congo.

<sup>#</sup>W.L. and S.S.-M. contributed equally to this work

\*corresponding author (email address: bhahn@upenn.edu)

**Malaria parasites are widespread among chimpanzees and gorillas, but have not been detected**

in bonobos. Here, we show that bonobos are endemically *Plasmodium* infected, but only in the eastern-most part of their range. Testing 1,556 faecal samples from 11 field sites, we identified high prevalence *Laverania* infections in the Tshuapa-Lomami-Lualaba (TL2) area, but not at other locations across the Congo. TL2 bonobos harbour *P. gaboni*, formerly only found in chimpanzees, as well as a newly discovered species, *Plasmodium lomamiensis*. Phylogenetic relationships among *Laverania* species suggest co-divergence with their gorilla, chimpanzee and bonobo ancestors, providing a timescale for their evolution. Rare co-infections with non-*Laverania* parasites were also observed. The absence of *Plasmodium* from most field sites could not be explained by parasite seasonality, bonobo population structure, or differences in the abundance of faecal plant or microbiome constituents. Thus, the geographic restriction of bonobo *Plasmodium* likely reflects factors that influence parasite transmission.

African great apes are highly endangered, requiring non-invasive approaches to study infectious agents in wild-living communities. To elucidate the origins and evolution of human malaria parasites, we<sup>1-3</sup> and

others<sup>4-6</sup> have developed PCR-based methods that permit the faecal-based detection and molecular characterisation of related parasites in wild-living apes. Such studies have shown that chimpanzees (*Pan troglodytes*) and western gorillas (*Gorilla gorilla*) harbour a plethora of *Plasmodium* parasites, which fall into two major groups<sup>7</sup>. One group (subgenus *Plasmodium*) includes several *Plasmodium* species infecting monkeys as well as ape parasites that are closely related to human *P. malariae*, *P. ovale* and *P. vivax*<sup>7</sup>. Of these, ape *P. vivax* is known to infect both chimpanzees and gorillas, while contemporary human *P. vivax* represents a lineage that emerged from these parasites as it spread out of Africa<sup>2</sup>. The other group (subgenus *Laverania*) includes ape parasites that are most closely related to human *P. falciparum*<sup>7</sup>. There are currently six described ape *Laverania* species, which appear to exhibit strict host specificity in wild ape populations<sup>1,3-5</sup>. These include *P. reichenowi* (also termed C1), *P. gaboni* (C2), and *P. billcollinsi* (C3), which infect chimpanzees, as well as *P. praefalciparum* (G1), *P. adleri* (G2), and *P. blacklocki* (G3), which infect western gorillas. Of these, only the gorilla parasite *P. praefalciparum* has crossed the species barrier to humans, resulting in the emergence of *P. falciparum*<sup>1,7,8</sup>. Although initially based primarily on mitochondrial sequences<sup>1</sup>, this taxonomy of *Laverania* species has subsequently been confirmed by analysis of multiple nuclear gene sequences<sup>3,9</sup>.

*Laverania* infections have been documented at multiple locations throughout the ranges of chimpanzees and western lowland gorillas (*G. g. gorilla*), with estimated prevalence rates in infected communities ranging between 22% and 40% (ref. 7). Similarly, ape *P. vivax* is found in all chimpanzee subspecies as well as western and eastern gorillas (*G. beringei*), although estimated prevalence rates are lower, ranging between 4% and 8% (ref. 7). Studies of Asian primate species have shown that the distribution and prevalence of *Plasmodium* infections depends on a number of ecological variables, such as forest cover<sup>10</sup>, population density<sup>11</sup>, vector capacity<sup>12</sup> and environmental conditions<sup>13</sup>, many of which are interrelated. Although the factors that promote and sustain malaria transmission in wild apes remain largely unknown, it is clear that *Plasmodium* species are not uniformly distributed among them. For example, eastern gorillas harbour ape *P. vivax*, but do not seem to carry *Laverania* parasites<sup>1,2</sup>. More strikingly, bonobos (*Pan paniscus*) appear to be free of all known ape *Plasmodium* species, despite the screening of multiple communities<sup>1,2</sup>.

The seeming absence of *Plasmodium* infections from wild bonobos has remained a mystery. First, *Anopheles* vectors, including forest species such as *A. moucheti*, *A. marshallii* and *A. vinckei*, which are known to carry ape *Plasmodium* parasites<sup>14,15</sup> appear to be distributed throughout the bonobo range<sup>16</sup>. Second, bonobos are very closely related to chimpanzees, suggesting a similar susceptibility to *Plasmodium* infection. Third, there is no evidence that bonobos are inherently resistant to *Plasmodium* parasites, since human *P. falciparum* and *P. malariae* have been detected in the blood of several captive individuals<sup>17</sup>. Reasoning that previous studies may have missed infected communities, we conducted a more extensive survey, increasing both the number and geographic diversity of sampled bonobo populations. Here, we show that wild bonobos are, in fact, susceptible to a wide variety of *Plasmodium* parasites, including a previously unknown *Laverania* species that appears to have co-evolved with its host. However, endemic infection was only detected in the eastern-most part of the bonobo range, indicating that most wild-living bonobo communities have lost these parasites.

## Results

**Bonobos are naturally *Laverania* infected.** Bonobos are found in the rain forests of the Congo Basin in the Democratic Republic of the Congo (DRC). Separated from eastern chimpanzees (*P. t. schweinfurthii*) and eastern lowland gorillas (*G. b. graueri*) by the Congo River, their range extends from the Lualaba River in the east, to the Kasai and Sankuru Rivers in the south, and the Lake Tumba and Lake Mai-Ndombe regions in the west (Fig. 1). Initial studies failed to identify *Plasmodium* infections in wild bonobos, but were conducted at only two locations (LK and KR)<sup>1</sup>. Although subsequent surveys included additional bonobo field sites (ML, LA, IK, BN, BJ, TL2), faecal samples were only tested for *P. vivax*-like parasites<sup>2</sup>. Here, we screened these (n=646) as well as newly collected (n=803) faecal samples from the same (LA, IK) and additional (LG, BX, MZ) study sites for *Laverania* infection (Fig. 1). Using conventional (diagnostic) PCR to amplify a 956 bp mitochondrial cytochrome B (*cytB*) fragment<sup>1</sup>, we failed to detect parasite sequences in 1,418 samples from 10 of these 11 locations (Table 1). Surprisingly, however, 16 of 138 faecal specimens from the Tschuapa-Lomami-Lualaba (TL2) project site were *Laverania* positive as determined by direct amplicon sequencing (Table 1).

Reasoning that conventional PCR screening may have missed low-level *Laverania* infection, we retested all available *cytB* negative faecal specimens by subjecting them to an intensified PCR protocol. Since most ape faecal samples contain limited quantities of parasite DNA, we reasoned that testing multiple aliquots of the same DNA preparation would increase the likelihood of parasite detection. To avoid PCR contamination, only initially negative samples were re-tested using the intensified approach. Performing 8 to 10 independent PCR reactions for each DNA sample, we identified 17 additional faecal samples from TL2 to contain *cytB* sequences, resulting in a total of 33 positive specimens from 24 different apes (Table 1). Although in most cases only one or a few replicates yielded an amplification product (Supplementary Table 1), the intensified PCR approach more than doubled the number of positives at the TL2 site, revealing an overall *Laverania* prevalence of 38% (Table 1). However, this was not observed for other bonobo field sites. Intensified PCR of the remaining 1,105 faecal samples identified only a single additional positive specimen from the Kokolopori Bonobo Reserve (KR). Thus, malaria parasites are either absent or below the limits of faecal detection at the vast majority of bonobo field sites.

**A new bonobo-specific *Laverania* species.** Having identified *Laverania* positive bonobo faecal samples, we next sought to molecularly characterise the infecting parasites. Since apes are frequently co-infected with multiple *Plasmodium* species, we used limiting dilution PCR, also called single genome amplification (SGA), to generate mitochondrial *cytB* sequences (956 bp) devoid of *Taq* polymerase-induced artifacts such as *in vitro* recombination<sup>18</sup>. Using this approach, we generated 166 limiting dilution-derived *cytB* sequences from 34 *Laverania* positive bonobo samples, including a unique haplotype from the single positive specimen collected at the KR site (Supplementary Table 2). Phylogenetic analysis showed that these bonobo parasites fell into two well-supported clades within the *Laverania* subgenus (Fig. 2, Supplementary Fig. 1). One of these comprised a sublineage of *P. gaboni* (C2E) previously found to infect eastern chimpanzees (*P. t. schweinfurthii*) in the DRC<sup>3</sup>. Within this sublineage, bonobo and chimpanzee parasite sequences were completely interspersed, indicating that *P. gaboni* productively infects both of these *Pan* species (Fig. 2, Supplementary Fig. 1). The other clade

represented a distinct *Laverania* lineage (B1) that included only bonobo parasites, except for a single *cytB* sequence previously identified<sup>3</sup> in an eastern chimpanzee sample (PApts368) from the Parisi Forest east of the Congo/Lualaba River (Fig. 1).

To determine whether B1 parasites were more widespread among eastern chimpanzees than previously recognised, we used regular and intensified PCR to screen faecal samples (n= 562) from nine such study sites located closest to the bonobo range (Fig. 1). Although this analysis yielded twice as many *Laverania* positive samples as conventional *cytB* PCR (Supplementary Table 3), none of the newly derived parasite sequences fell within the B1 clade (Supplementary Table 4). Instead, eastern chimpanzees were exclusively infected with *P. reichenowi* (C1), *P. gaboni* (C2) and *P. billcollinsi* (C3) (Supplementary Fig. 1). These data indicate that TL2 bonobos harbour a form of *P. gaboni* that is highly prevalent in neighboring eastern chimpanzees as well as a second *Laverania* species that seems to be unique to bonobos.

To characterise the newly identified bonobo parasites in other regions of their genomes, we used SGA to target additional organelle and nuclear loci for analysis (Supplementary Table 2). These included 3.4 kb and 3.3 kb mtDNA fragments, which together span the entire mitochondrial genome; a 390 bp caseinolytic protease M (*clpM*) gene fragment from the apicoplast genome; and three nuclear loci, including portions of genes encoding the erythrocyte binding antigens 165 (*eba165*; 790 bp) and 175 (*eba175*; 394 bp), and the gametocyte surface protein P47 (*p47*; 800 bp). Phylogenetic analyses of 134 newly derived parasite sequences yielded very similar results (with respect to the clustering of parasites into major clades) in all genomic regions (Fig. 3; Supplementary Fig. 2). Except for a single C1 *eba175* sequence indicative of a rare *P. reichenowi* infection (Supplementary Fig. 2d), all other bonobo-derived sequences fell either within *P. gaboni* or the B1 clade (Supplementary Table 2). This new clade was supported by high bootstrap values in all genomic regions analysed, except for the short (394 bp) *eba175* fragment. It also consistently grouped as a sister clade to *P. reichenowi*. These findings, along with the extent of genetic divergence between *P. reichenowi* and the newly identified bonobo parasite clade, argue strongly for the existence of an additional *Laverania* species that is specific for bonobos (Figs. 2 and 3, Supplementary Figs. 1 and 2). The finding of B1 *cytB* (Fig. 2) and

*eba165* (Fig. 3a) parasite sequences in a single chimpanzee faecal sample collected 280 km east of TL2 does not argue against this, since it shows that B1 parasites reached this geographic region, but failed to spread in the resident chimpanzee population (Supplementary Table 4). We propose to name the new bonobo parasite species *Plasmodium lomamiensis* to highlight its discovery in the recently established Lomami National Park.

**TL2 bonobos also harbour non-*Laverania* parasites.** Single genome amplification of bonobo faecal DNA also yielded rare sequences from non-*Laverania* parasites that resulted from primer cross-reactivity (Supplementary Table 2). One such *cytB* sequence clustered with a previously characterised parasite sequence from a chimpanzee sample (DGptt540), forming a well-supported lineage that was only distantly related to human and ape *P. malariae* (Fig. 4a). Two other *clpM* sequences clustered with *P. vivax* parasites, but the amplified fragments were too short to differentiate human and ape *P. vivax* (Fig. 4b). To search for additional non-*Laverania* infections, we used *P. vivax*- and *P. malariae*-specific primers to rescreen bonobo faecal samples from the BX (n=1), KR (n=69), LA (n=199) and TL2 (n=138) field sites using intensified PCR. This analysis confirmed *P. vivax* infection in one bonobo sample, and identified *P. vivax* and *P. ovale curtisi* sequences in two additional samples, all from the TL2 site (Fig. 4c). Further characterisation revealed that the *P. ovale curtisi* positive sample also contained ape *P. vivax* sequences (Fig. 4d). Thus, of 24 *Laverania* positive bonobos at the TL2 site, three also harboured *P. malariae*-, *P. vivax*- and/or *P. ovale*-related parasites, while an additional bonobo exhibited a *P. vivax* mono-infection (Supplementary Table 2). Although the recovered sequences were too short to differentiate human and ape specific parasite lineages, the results show that bonobos, like chimpanzees and gorillas, are frequently infected with multiple *Laverania* and non-*Laverania* species<sup>1,5,7</sup>. However, unlike chimpanzees and gorillas, bonobos appear to become infected with these parasites in only one particular part of their natural range.

**The Lomami River is not a barrier to malaria transmission.** Analysing mitochondrial DNA (mtDNA) sequences to determine the population structure of wild bonobo populations, two previous studies



reported that the Lomami River, but not other tributaries of the Congo River, represents a geographical barrier to bonobo gene flow<sup>19,20</sup>. We thus considered the possibility that bonobos in the western and central regions of the DRC had acquired a malaria protective trait that had not spread to bonobo populations east of the Lomami River. To investigate this, we subjected *Plasmodium* positive and negative samples from TL2 to the same host mtDNA analysis (Supplementary Table 5) and compared the resulting haplotypes to all previously reported bonobo mtDNA sequences (Fig. 5a, Supplementary Fig. 3). Phylogenetic analysis showed that most of the newly derived mtDNA sequences from TL2 (blue) fell into two clades that were exclusively comprised of sequences from bonobos sampled east of the Lomami River (Supplementary Fig. 3b)<sup>19,20</sup>. However, four new TL2 haplotypes representing 15 faecal samples, including four *Laverania* positive specimens, did not fall within these two “eastern” clades (indicated by arrows in Fig. 5a and Supplementary Fig. 3a). Analysis of their GPS coordinates revealed that they were all collected west (TL2-W) of the Lomami River (Fig. 5b). These results thus confirm and extend previous findings showing that bonobos east of the Lomami River represent (at least matrilineally) a genetically isolated population<sup>19,20</sup>. However, this isolation does not explain the geographic restriction of bonobo malaria infections, since *Laverania* positive individuals were found on both sides of the Lomami River. Although it remains unknown how far the *Plasmodium* endemic area extends beyond TL2 in the eastern Congo, it seems clear that the Lomami River itself does not represent a barrier to malaria transmission.

**Climate does not explain the distribution of bonobo malaria.** Because climatic factors such as ambient temperature and rainfall are known to influence malaria transmission in humans<sup>21-23</sup>, we asked whether seasonal differences in *Plasmodium* prevalence could explain the absence of parasite detection at the majority of bonobo study sites. Comparison of sample dates across all field sites revealed no obvious association between faecal parasite positivity and the month of specimen collection (Table 2). For example, samples collected in November and December at the TL2 site included a large fraction of malaria positive specimens, but this was not the case for samples collected during these same months at the IK, KR and LA field sites. To examine the impact of climatic variation on bonobo

parasite detection more directly, we used a statistical model previously shown to be strongly predictive of spatiotemporal variation in *Laverania* infection among wild-living chimpanzees (Erik Scully, unpublished results). This model, which was parameterised using PCR (*cytB*) screening data from 2,436 chimpanzee faecal samples collected at 55 locations across equatorial Africa<sup>7</sup>, showed that ambient temperature, daily temperature fluctuations, and forest cover, but not rainfall, each influenced the probability of *Laverania* detection.

Using only specimens with known sampling dates and GPS coordinates for which land surface temperature and forest cover data were also available (Supplementary Table 6), we estimated the probability of *Laverania* infection for each of the 11 bonobo field sites. Assuming similar climatic influences on chimpanzee and bonobo parasite development and transmission, this analysis showed that at seven sites for which a sufficiently large number of samples were available, bonobos were significantly less frequently *Laverania* infected than predicted by the climate model. For the BN, IK, LA, LK, and MZ sites, the model predicted a less than one in a million probability that a positive sample would not be detected if bonobos at these sites exhibited similar infection patterns as chimpanzees. Moreover, for the KR site, where only one sample was *Laverania* positive, seasonal variation could not explain this very low detection rate (Table 2). The rate of parasite detection at the TL2 site, where 27 of 113 samples with climate data were positive, was lower than, but not significantly different from, that predicted for a chimpanzee study site with similar ecological conditions. The very small sample sizes at BJ and BX sites lacked statistical power to detect differences, and the low predicted probability of infection at the ML site indicated that more sampling during months of higher predicted infection probabilities would be necessary to confidently reject the climate model. Nevertheless, it appears that seasonal or climatic variation in parasite prevalence can be excluded as an explanation for the observed geographic restriction of bonobo *Plasmodium* infections.

**Plant diet is not associated with faecal parasite detection.** Wild apes consume a variety of plants, fruits, barks and piths, some of which have been reported to have antimalarial activity<sup>24-26</sup>. We thus asked whether our inability to detect *Plasmodium* infections at most bonobo field sites was due to the

presence of certain plants, which upon ingestion would reduce parasite titers below the limits of faecal detection. To examine this possibility, we selected a subset of *Laverania* positive (n=18) and negative (n=51) bonobo faecal samples from endemic (TL2) and non-endemic (KR, IK, LG, LK) field sites, and characterised their plant content by targeting two regions of the chloroplast genome for high throughput sequencing (Supplementary Table 7). These comprised a 500 bp fragment of the *rbcL* gene and a 750 bp fragment of the *matK* gene, both of which have been used extensively as barcodes to identify land plants<sup>27-29</sup>, including in stool samples from endangered species<sup>30</sup>. *Laverania* positive (n=14) and negative (n=15) chimpanzee faecal samples were analysed for control (Supplementary Table 7).

Samples were sequenced to a mean depth of 16,054 *matK* and 21,995 *rbcL* paired-end reads, which were clustered into Operational Taxonomic Units (OTUs) and assigned to taxonomic groups by blasting them against a custom *matK* and *rbcL* reference database (Supplementary Fig. 4). Using a permutational multivariate analysis of variance to compare unweighted UniFrac distances<sup>31</sup> as a measure of large scale differences in plant composition, we found small differences between faecal samples from bonobos and chimpanzees (*matK*: 2.0% of variance,  $p=0.003$ ; *rbcL*: 2.8% of variance,  $p<10^{-6}$ ), but much more substantial differences between faecal samples from different study sites (*matK*: 19.8% of variance,  $p<10^{-6}$ ; *rbcL*: 18.6% of variance,  $p<10^{-6}$ ). However, no significant differences were observed between *Laverania* positive and negative faecal samples (*matK*: 1.2% of variance,  $p=0.18$ ; *rbcL*: 0.8% of variance,  $p=0.71$ ), suggesting that the lack of parasite detection was not associated with the abundance of certain plant phyla in the diet (Fig. 6a and b, Supplementary Fig. 5).

We also compiled a list of 466 African plant species (Supplementary Table 8), which have been reported to have potential antimalarial activity<sup>26,32,33</sup>, and looked for related *matK* and *rbcL* sequences in bonobo faecal samples from endemic and non-endemic field sites. Although a BLAST search identified 65 *matK* and 490 *rbcL* OTUs that shared >95% sequence identity with 3 and 17 of these putative antimalarial species, respectively, none was significantly more abundant at field sites where *Laverania* infections were absent (Supplementary Fig. 6). In addition, similar results were obtained when the remaining plant OTUs were compared between endemic and non-endemic bonobo field sites (all  $p>0.05$  after false discovery rate adjustment). Finally, no compositional differences were observed

in the plant content of *Laverania* positive and negative chimpanzee faecal samples (Fig. 6a and b). Although these analyses provide only a limited snapshot of bonobo and chimpanzee plant diet, they failed to identify an association between particular plant constituents and parasite detection in faecal samples.

**The faecal bacteriome does not predict *Laverania* infection.** *Plasmodium* infections have been reported to influence the bacterial communities in the gut, with certain parasites causing intestinal dysbiosis<sup>34</sup> and certain gut microbiota enhancing the host's anti-parasite immune responses<sup>35</sup>. To examine potential interactions between the faecal microbiome and *Laverania* infection in bonobos, we used the same samples selected for plant analyses for bacterial 16S rRNA sequencing (*Laverania* positive and negative chimpanzee samples again served as a control). Samples were sequenced to a mean depth of 65,132 reads, which were clustered into OTUs and assigned to taxonomic groups (Supplementary Fig. 7a). Examining Shannon diversity as a marker of dysbiotic outgrowth or loss of bacterial taxa, we failed to find significant differences in within-sample (alpha) diversity between specimens from *Laverania* positive and negative bonobos (or chimpanzees), or between specimens from endemic (TL2) and non-endemic (KR, IK, LG, LK) field sites (Supplementary Figure 8a). Using unweighted UniFrac distance to compare between-sample (beta) diversity<sup>31</sup>, we found that as previously reported<sup>36</sup> bonobo and chimpanzee faecal microbiomes differed in their bacterial composition (Fig. 6c, Supplementary Figs. 7b and 8b). In addition, samples from the same field site were often compositionally more similar to each other than to samples from other field sites (Supplementary Figs. 8b and c). Examining the sources of this variation, we found that ape species accounted for 7.4% ( $p < 10^{-6}$ ), study site for 19.3% ( $p < 10^{-6}$ ) and *Laverania* positivity for 1.2% of the variance ( $p = 0.043$ ), respectively. Considering only chimpanzee samples, study site accounted for 17.8% ( $p = 0.000018$ ) and *Laverania* positivity for 4.0% of variance ( $p = 0.25$ ). Comparing only samples from TL2 bonobos, differences among the three sample locations (Fig. 5b) accounted for 14.6% ( $p < 10^{-6}$ ) and *Laverania* infection for 4.5% of variance ( $p = 0.0023$ ). Thus, there was a small but significant compositional difference between the faecal microbiome of *Laverania* positive and negative bonobos at TL2 (the lack of significance in

chimpanzees maybe due to a smaller sample size).

Using Wilcoxon rank sum tests to look for OTUs that were driving these differences, we found one assigned to the family Ruminococcaceae that was significantly depleted, and two others assigned to family Lachnospiraceae and *Prevotella copri* that were significantly enriched in *Laverania* positive TL2 bonobo samples (Supplementary Fig. 9). However, comparing samples from TL2 to non-endemic field sites did not yield significantly higher UniFrac distance values than comparing samples between these non-endemic sites (Supplementary Fig. 8b). Thus, while the abundance of some bacterial taxa differed slightly between *Laverania* positive and negative bonobos at TL2, compositional differences between samples from TL2 and non-endemic sites were no greater than expected between any two random sites, thus failing to provide a microbial signature of *Laverania* infection for that site.

## Discussion

A complete account of *Plasmodium* infections in wild African apes, including their host species associations, prevalence, geographic distribution, and vector preferences, is critical for understanding the origins of human malaria and gauging future zoonotic risks. Previous studies documented numerous *Plasmodium* species in wild chimpanzees and gorillas, but failed to find evidence of similar infections in wild bonobos<sup>1,2</sup>. Here, we show that bonobos harbour a multitude of *Plasmodium* species, including a newly discovered *Laverania* parasite, although infection is limited to only a small part of their natural range east of the Lomami River. Analyses of climate data and parasite seasonality, as well as host characteristics, including bonobo population structure, plant consumption and faecal microbiome composition, failed to provide an explanation for this geographic restriction. Thus, it seems likely that ecological factors that impact parasite transmission are responsible for the uneven distribution of bonobo *Plasmodium* infections, although the possibility of a protective mutation that has not spread east of the Lomami River cannot be excluded.

Studies in southeast Asia have shown that both species richness and prevalence of primate malarias are closely linked to the habitat of forest-dwelling *Anopheles* of the *Leucosphyrus* group, rather than the distribution of the primates themselves<sup>10,12</sup>. Thus, factors that negatively impact the breeding

conditions, development and distribution of transmitting vectors may be responsible, at least in part, for the absence of *Plasmodium* infections at most bonobo field sites. Ecological factors may also influence bonobo density or other behaviours that affect vector exposure. For example, captive and semi-captive orangutans, which live in higher group densities than their wild counterparts, also have higher rates of *Plasmodium* infection<sup>11</sup>. Finally, it is conceivable that bonobos at the *Plasmodium* negative sites carry other infectious agents that induce cross-protective immune responses or compete for the same resources<sup>37</sup>. Bonobos are clearly susceptible to a variety of *Plasmodium* species. Thus, examining why neither *Laverania* nor non-*Laverania* infections are sustained throughout much of the bonobo range may identify new drivers of vector dynamics or other transmission risks that could aid malaria eradication efforts in humans.

The newly identified bonobo parasites prompt speculation about the causes and time-scale of *Laverania* diversification. When the only *Laverania* species characterised were *P. falciparum* and *P. reichenowi*, it was widely assumed that these two species had co-diverged with their hosts<sup>38,39</sup>, placing their common ancestor at the same time as the common ancestor of humans and chimpanzees around 6-7 Mya<sup>40</sup>. This hypothesis was undermined by the finding of additional *Laverania* species, in particular the discovery that *P. falciparum* was the result of a recent host switch of a gorilla parasite<sup>1</sup>. However, *P. praefalciparum* (the precursor of *P. falciparum*) and *P. reichenowi* could have co-diverged with the ancestors of gorillas and chimpanzees. The phylogenetic position (Figs. 2 and 3; Supplementary Figs. 1 and 2) of the newly described bonobo parasite, *P. lomamiensis* (B1), which is more closely related to *P. reichenowi* (C1) than to *P. praefalciparum* (G1), provides a triad of parasite species with the same relationships as their hosts. It is thus tempting to speculate that this clade arose through host-parasite co-divergence. Under this scenario, the common ancestor of *P. reichenowi* (C1) and *P. praefalciparum* (G1) would have existed approximately 8-9 Mya<sup>40</sup>, an estimate that is 2- to 4-times older than some have concluded from molecular clock analyses for the equivalent divergence of *P. reichenowi* and *P. falciparum*<sup>41,42</sup>. *P. reichenowi* (C1) and *P. lomamiensis* (B1) would have diverged around 2 Mya<sup>40</sup>. Molecular clocks for *Laverania* species may not be very precise: for example, *P. reichenowi* and *P. praefalciparum* are clearly not four times more divergent than *P. reichenowi* and

*P. lomamiensis* (Figs. 2 and 3). However, given that *P. reichenowi* and *P. gaboni* are about three times more divergent than *P. reichenowi* and *P. praefalciparum*<sup>9</sup>, it is possible that the common ancestor of the entire *Laverania* clade existed around 25-30 Mya.

The co-divergence scenario also predicts that the ancestor of current day bonobos was infected with the ancestor of *P. lomamiensis* (B1), which was subsequently lost from most bonobo populations. The Congo River, which forms the boundary between the ranges of chimpanzees and bonobos (Fig. 1), is thought to have existed since long before the divergences among African apes<sup>43</sup>; yet, somehow the ancestor of bonobos reached the southern (left) bank of the Congo. It has been suggested that this happened during one of several documented periods of relative aridity when river levels might have been low enough to permit the crossing at a point in the northeast of the current bonobo range, near Bayoma Falls<sup>43</sup>. Furthermore, it appears at least from mitochondrial DNA analyses that there may have been an early population split between the ancestors of bonobos now found on the two sides of the Lomami River<sup>44</sup>. Thus, the loss of *P. lomamiensis* from populations west of the Lomami River may have occurred early in bonobo history. It should be noted that the infection status of bonobos at sites other than TL2 east of the Lomami (e.g., BJ and BX; Fig. 1) remains unknown, because too few samples have been collected. However, bonobos immediately west of the Lomami at TL2 must have reacquired *P. lomamiensis*, indicating that the river is not a barrier to mosquitoes from the east, and that western bonobos as a whole do not share a genetically-based resistance to infection. The co-divergence scenario also implies that a related parasite was lost from the human lineage, which might have been due to an early human population bottleneck, an ancestral hunter-gatherer lifestyle<sup>45</sup> and/or the loss of the gene that synthesises N-Glycolylneuraminic acid (Neu5Gc), which may have affected the ability of the parasite to infect human erythrocytes<sup>46</sup>.

The extent of divergence (Figs. 2 and 3) between *P. gaboni* (C2) and *P. adleri* (G2) is similar to that between *P. reichenowi* (C1) and *P. praefalciparum* (G1), suggesting that the former pair may also have co-diverged with their hosts. Within the C2/G2 clade there is again no human parasite species, and the only bonobo parasites in this lineage clearly reflect recent transmissions of *P. gaboni* from eastern chimpanzees, rather than co-divergence. In this case, the loss of a putative B2 lineage from



bonobos is not surprising given the presumed loss of *P. lomamiensis* (B1) from most of the bonobo range. The lack of (known) close relatives of the other ape *Laverania* species, *P. billcollinsi* (C3) and *P. blacklocki* (G3) would also be indicative of past losses of parasite lineages from particular ape hosts. Although the processes that contributed to the emergence of today's *Laverania* lineages remain unknown, it seems clear that both co-divergence and cross-species transmission events shaped their evolutionary history, as has been observed for many other pathogens.

One characteristic feature of *Laverania* parasites infecting wild apes is their highly specific host tropism. This species-specificity is not shared by non-*Laverania* parasites, such as *P. vivax*, which infects bonobos as well as humans, chimpanzees and gorillas<sup>2,47</sup>. However, even within the *Laverania* subgenus, host specificity is not absolute. First, bonobos at TL2 are commonly infected with a chimpanzee parasite (*P. gaboni*), and phylogenetic analyses indicate that numerous *P. gaboni* parasites have crossed the Lualaba River (Fig. 2). Second, bonobos are susceptible to a second chimpanzee parasite, *P. reichenowi* (Supplementary Fig. 2d), while eastern chimpanzees appear susceptible to the bonobo parasite *P. lomamiensis* (Figs. 2 and 3), although both of these cross-species infections appear to reflect rare events that fail to result in more extensive transmission. Thus, on the one hand, *Laverania* species are extremely host specific, which implies strong barriers to cross-species transmission, while on the other hand there is evidence that on rare occasions these barriers can be overcome. Given the very close genetic relationship of chimpanzees and bonobos, examples of cross-species infection are perhaps not surprising. However, the finding that in captive settings bonobos can become infected with human *P. falciparum*<sup>17</sup>, while chimpanzees can harbour gorilla parasites and *vice versa*<sup>48</sup>, indicates that *Laverania* host-specificity is controlled by factors that extend beyond incompatibilities of receptor-ligand interactions during erythrocyte invasion<sup>49</sup>. While ape *Laverania* parasites have not yet been detected in humans<sup>8,50</sup>, it seems clear that the mechanisms governing host-specificity are complex and that some barriers are more readily surmountable than others. Given the new bonobo data, it will be critical to determine exactly how *P. praefalciparum* was able to jump the species barrier to humans to give rise to *P. falciparum*, in order to determine what might enable one of the other ape *Laverania* to do the same.



## Methods

**Ape samples.** Faecal samples from wild-living bonobos and eastern chimpanzees were obtained from existing specimen banks, or were newly collected at previously reported<sup>1-3</sup> as well as new study sites (LG, BX, MZ) in the DRC (Fig. 1). While all available bonobo samples (n=1,556) were analysed, eastern chimpanzee specimens (n=580) were selected from nine field sites most proximal to the bonobo range. All samples were obtained non-invasively from apes in remote forest areas, preserved (1:1 vol/vol) in RNA*later*, transported at ambient temperatures, and stored at -80 °C. Faecal DNA was extracted using the QIAamp Stool DNA mini kit (Qiagen, Valencia, CA) and all specimens were subjected to host mitochondrial DNA analysis to determine their species origin<sup>1-3</sup>. The latter analysis also gave an indication of sample quality, which confirmed that samples from *Laverania* negative field sites were not any more degraded than samples from TL2. For the KR, LK and TL2 field sites, the number of sampled individuals has previously been determined by microsatellite analyses<sup>2</sup>. All samples were obtained with approval from the Ministries of Scientific Research and Technology, the Department of Ecology and Management of Plant and Animal Resources of the University of Kisangani, the Ministries of Health and Environment, and the National Ethics Committee in the DRC, and shipped in compliance with Convention on International Trade in Endangered Species of Wild Fauna and Flora regulations and country specific import and export permits.

**Conventional and intensified PCR.** Bonobo and chimpanzee faecal samples were first screened for *Laverania* parasites by conventional (diagnostic) PCR, targeting a 956 bp mitochondrial *cytB* fragment using primers DW2 (5'-TAATGCCTAGACGTATTCCTGATTATCCAG-3') and DW4 (5'-TGTTTGCTTGGGAGCTGTAATCATAATGTG-3') in the first round, and Pfcytb1 (5'-CTCTATTAATTTAGTTAAAGCACA-3') and PLAS2a (5'-GTGGTAATTGACATCCWATCC-3') in the second round of PCR as previously described<sup>1</sup>. Since this approach tests only a single aliquot of each faecal DNA, we reasoned that parasites present in low concentrations may have been missed. To increase the sensitivity of parasite detection, we thus tested 8 to 10 aliquots of the same DNA using the same primers and amplification conditions. To guard against false positives, only samples that were

negative by conventional PCR were subjected to the intensified PCR screening. Intensified PCR was also used to screen 199 bonobo faecal samples from the TL2, KR, and LA field sites for non-*Laverania* infections using parasite specific primer sets. *P. vivax* primers targeted a 296 bp mitochondrial *cox1* fragment using Pv2768p (5'-GTATGGATCGAATCTTACTTATTC-3') and Pv3287n (5'-AATACCAGATACTAAAAGACCAACAATGATA -3') in the first round, and Pv2856p (5'-CTTATTACAAATTGCAATCATAAACTTTAGGT-3') and Pv3185n (5'-TCCTCCAAATTCTGCTGCTGTAGATAAAATG-3') in the second round of PCR as described<sup>8</sup>. *P. malariae* specific primers targeted a 600 bp mitochondrial *cytB* fragment using Pm4659p (5'-ATTTATTATCTTCAATTCCAGCACTT-3') and Pm5501n (5'-GCATGTTAACCTCGATAAATACTAA-3') in the first round, and Pm4740p (5'-ATTACATTTTATACTTCCATTTGTTGC-3') and Pm5369n (5'-TTCAGAAATATCGTCTTATCGTAGC-3') in the second round of PCR. *P. vivax* specific primers detected both *P. vivax* and *P. ovale*, while *P. malariae* specific primers amplified only positive control samples (one *P. malariae* positive sample was detected due to the cross-reactivity of regular *cytB* primers; Fig. 4a). All amplicons were sequenced directly without interim cloning.

**Single genome amplification.** To derive *Plasmodium* sequences devoid of PCR induced errors, all PCR positive bonobo and chimpanzee faecal samples were subjected to single genome amplification (SGA) as described<sup>1,2,18</sup>. According to a Poisson distribution, the DNA dilution that yields PCR products in no more than 30% of wells contains one amplifiable template per positive reaction more than 80% of the time. Faecal DNA was thus endpoint diluted in 96-well plates, and the dilution that yielded less than 30% positive wells was used to generate single template derived sequences. For *Laverania* positive bonobo samples, mitochondrial (*cytB*; 3.4kb and 3.3kb mitochondrial half genomes), apicoplast (*clpM*), and nuclear (*eba165*, *eba175* and *p47*) gene regions were amplified using previously reported primer sets and amplification conditions (Supplementary Table 2)<sup>1-3,8,49</sup>. For *Laverania* positive chimpanzee samples, only the 956 bp mitochondrial *cytB* fragment was amplified (Supplementary Table 4). One bonobo faecal sample (TL2.3874) positive for *P. ovale curtisi* by conventional PCR also yielded a *P. vivax* specific 574 bp apicoplast *clpM* fragment when subjected to SGA analysis.

**Phylogenetic analyses.** Sequences were aligned using CLUSTAL W (version 2.1), visually inspected, and regions that could not be unambiguously aligned were removed from subsequent analyses. Maximum likelihood phylogenetic trees and bootstrap support were estimated using PhyML (version 3.0)<sup>51</sup>, which infers evolutionary model parameters and phylograms concurrently. Evolutionary models were selected using jModelTest (version 2.1.4)<sup>52</sup>. Bayesian posterior probabilities were determined using MrBayes (version 3.2.4)<sup>53</sup> using two simultaneous independent analyses with a 25% burnin. Convergence was determined when the average deviation of split frequencies was <0.01.

**Climate model of ape *Laverania* infection.** To evaluate whether the absence or low prevalence of *Laverania* infection at most bonobo sampling sites could be explained by seasonal variation in parasite transmission, we developed a generalised linear mixed model with binomial fit and logit link function to infer the probability of parasite detection for each sample relative to the climatic variables observed at the time of specimen collection. Briefly, this model, which incorporates mean ambient temperature (AT), daily temperature variation (TV), and percent forest cover (FC), was parameterised using 2,436 chimpanzee faecal samples from 55 sampling sites across equatorial Africa<sup>7</sup> and found to be strongly predictive of *Laverania* infection in wild chimpanzees (Erik Scully, unpublished results). Assuming similar relationships between climatic variables and infection probability in chimpanzees and bonobos, and including only samples for which climate data were available, we inferred the predicted probability of *Laverania* infection for each bonobo sample using the equation:

$$\text{Predicted Probability} = \frac{1}{1 + e^{-(\text{intercept} + 0.355*AT - 0.164*AT^2 + 0.032*FC + 0.208*TV)}}$$

where *intercept* is -2.538 for samples screened using conventional PCR (i.e., one replicate) and -1.374 for those screened using intensive PCR (i.e., 8-10 replicates), and AT, TV, and FC are each corrected by subtracting the means of the chimpanzee dataset (23.4 for AT, 9.1 for TV, and 77.2 for FC. For each bonobo sample, we used MODerate Resolution Imaging Spectroradiometer (MODIS) and daytime and night-time Land Surface Temperature (LST) datasets<sup>54,55</sup> in one-day temporal resolution (MOD11A1)

after applying the minimum/maximum air temperature transformations as described<sup>21</sup> to derive (i) the mean ambient air temperature and (ii) the mean daily air temperature fluctuation. Each of the temperature variables was calculated as the average of LST measurements taken during the period 30 days prior to sample collection. Forest cover data were extracted from high resolution global maps as described<sup>56</sup>. For each sampling site, the mean and ranges of these ecological variables are summarised in Supplementary Table 6. Assuming that each specimen is independent and has a probability of detected infection as assigned by the climate model, the number of positives observed at a given site will be a sum of Bernoulli variables with varying probabilities and thus should follow the Poisson binomial distribution<sup>57</sup>. We calculated the cumulative probability of seeing less than or equal the observed number of positive samples<sup>57</sup> given the set of climate estimates for each site to generate p-values and used Bonferroni correction to account for multiple comparisons. A low p-value indicates that climatic variation is very unlikely to account for the observed scarcity of infection.

**Characterisation of faecal plant composition.** Chloroplast ribulose biphosphate carboxylase large chain (*rbcL*) and maturase K (*matK*) gene regions are widely used as bar codes for land plants<sup>27-29</sup> and were thus selected to characterise plant components in *Laverania* positive and negative bonobo (n=78) and chimpanzee (n=20) faecal samples (Supplementary Table 7). Faecal DNA was extracted using the PowerSoil-htp 96 Well Soil DNA Isolation Kit (MO BIO Laboratories, Carlsbad, CA). We modified *rbcL* primers previously reported to have high plant discriminatory ability<sup>29</sup> for MiSeq sequencing by adding an Illumina adapter (underlined). These included *rbcL*bF (5'-AGACCTWTTTGAAGAAGGTTCTWGT-3') and *rbcL*bR (5'-TCGGTYAGAGCRGGCATRTGCCA-3') for the first round of PCR, and R1\_*rbcL*634F (5'-TCGTCGGCAGCGTCAGATGTGTATAAAGAGACAGAT GCGTTGGAGAGACCGTTTC-3') and R2\_*rbcL*bR (5'-GTCTCGTGGGCTCGGAGATGTGTATAAAGAG ACAGTCGGTYAGAGCRGGCATRTGCCA-3') for the second round of PCR. We also modified *matK* primers recently improved to achieve high PCR success rates<sup>28</sup> in a similar fashion, using *matK*390F (5'-CGATCTATTCATTCAATATTTTC-3') and *matK*1326R (5'-TCTAGCACACGAAAGTCGAAGT-3') in the first round of PCR, and R1\_*matK*472F (5'-

TCGTCGGCAGCGTCAGATGTGTATAAGAGACAGCCCRTYCATCTGGAAATCTTGTTTC-3') and R2\_matK1248R (5'- GTCTCGTGGGCTCGGAGATGTGTATAAGAGACAGGCTRTRATAATGAGAAA GATTCTGC-3') in the second round of PCR.

Amplification for both *rbcL* and *matK* gene regions were performed using 2.5 µl of sample DNA in a 25 µl reaction volume containing 0.5 µl dNTPs (10mM of each dNTP), 10pmol of each first round primer, 2.5µl PCR buffer, 0.1 µl BSA solution (50µg/ml), and 0.25 µl Expand Long Template enzyme mix (Expand Long Template PCR System) for the first round of PCR. Cycling conditions included an initial denature step of 2 minutes at 94°C, followed by 15 cycles of denaturation (94°C, 10 sec), annealing (45°C, 30 sec), and elongation (68°C, 1 min), followed by 25 cycles of denaturation (94°C, 10 sec), annealing (48°C, 30 sec), and elongation (68°C, 1 min; with 10-sec increments for each successive cycle), followed by a final elongation step of 10 minutes at 68°C. For the second round PCR, 2µl of the first round product was used in 25µl reaction volume. Cycling conditions included an initial denature step of 2 minutes at 94°C, followed by 40 cycles of denaturation (94°C, 10 sec), annealing (52°C, 30 sec), and elongation (68°C, 1 min), followed by a final elongation step of 10 minutes at 68°C. For each faecal sample, *rbcL* and *matK* gene regions were amplified in duplicate, the products were pooled, purified using QIAquick Gel Extraction Kit, and sequenced using the Illumina Miseq v2 (500 cycle).

Sequence reads were separated by barcode, quality filtered for an expected number of errors <1 and an exact match to primer sequences, and the 5' and 3' reads of each pair were concatenated after trimming off primer sequences. Operational taxonomic units (OTUs) were formed using Swarm<sup>58</sup>, and OTUs containing only a single read discarded. Representative sequences of each OTU were aligned using MAFFT<sup>59</sup> and a phylogenetic tree was inferred using FastTree<sup>60</sup>. To create a database for taxonomic assignment, all reads matching the search terms "*matK*" or "*rbcL*" were downloaded from the European Nucleotide Archive and indexed in a BLAST database. This database was searched using a representative sequence from each OTU, and taxonomy was assigned as the most specific taxonomic rank shared by all BLAST hits with a total bit score within 98% of the best hit. Samples with fewer than 5,000 reads were removed from the analysis.

**Characterisation of faecal bacterial constituents.** The same faecal DNA samples used for plant analyses were also subjected to bacterial 16S rRNA gene sequencing (Supplementary Table 7). 16S rRNA gene amplification was performed as previously described<sup>61</sup>, using 5µl of faecal DNA, the AccuPrime Taq DNA Polymerase High Fidelity System (Thermo Fisher), and V1V2 region primers containing Illumina adapters, barcode, and linker regions. Each faecal sample was amplified in four independent reactions, with the products pooled and purified using AMPure XP beads (Beckman Coulter) before sequencing using Illumina MiSeq v2 (500 cycle). Sequences were separated by barcode, and paired reads were merged using bbmerge (<http://jgi.doe.gov/data-and-tools/bbtools/bb-tools-user-guide/bbmerge-guide/>). Reads were clustered into OTUs using a cutoff of 97% identity and taxonomically assigned using QIIME v1.9.1 and the Greengenes database<sup>62,63</sup>. OTUs formed from single reads were discarded. Samples with fewer than 15,000 sequences per sample were removed from the analysis.

**Statistical analyses.** All analyses were performed in R v3.3.3<sup>64</sup>. Within-sample (alpha) diversity was calculated using the Shannon diversity index<sup>65</sup>. Between-sample (beta) diversity of *matK* and *rbcL* data was calculated using unweighted UniFrac distances after rarefaction to 5,000 reads per sample<sup>31</sup>. Between-sample diversity of 16S rRNA data was also calculated using unweighted UniFrac, but after rarefaction to 15,000 reads per sample<sup>31</sup>. We opted to use unweighted distance values because they permit the examination of rare taxa that might be related to the phenotype examined; however, weighted UniFrac as well as weighted and unweighted Bray-Curtis dissimilarity values gave comparable results (*matk*: all Mantel tests  $r > 0.34$ ,  $p < 10^{-6}$ ; *rbcL*: all Mantel tests  $r > 0.68$ ,  $p < 10^{-6}$ ; 16S: all Mantel tests  $r > 0.77$ ,  $p < 10^{-6}$ ). Unweighted UniFrac distances were also used for principal coordinates analysis<sup>66</sup>, t-distributed stochastic neighbor embedding<sup>67</sup>, and permutational analysis of variance<sup>68,69</sup>. Analyses of 16S rRNA data revealed that TL2 bonobo samples formed three distinct clusters (Supplementary Figure 8c), corresponding to three different sampling locations west (TL2-W) and east (TL2-E and TL2-NE) of the Lomami River (Fig. 5b). To control for site-specific differences in faecal plant composition, we measured

depletion of *matK* and *rbcL* OTUs between samples from TL2-E, TL2-NE and TL2-W and three non-endemic LK, KR and IK field sites using Wilcoxon rank sum tests. The p-values from the nine pairwise comparisons were combined using Fisher's method with the test statistic and degrees of freedom divided by 3 to control for correlation between tests. Changes in bacterial OTU proportions between TL2 *Laverania* positive and negative samples were measured using Wilcoxon rank sum tests.

**Data availability.** Newly derived *Laverania* and non-*Laverania* parasite sequences as well as bonobo mtDNA haplotypes have been deposited in GenBank under accession numbers KY790455-KY790593 (also see Supplementary Tables 5 and 9). High throughput plant and microbiome sequences are archived in the NCBI Sequence Read Archive (SRA) under BioProject PRJNA389566.

**Code availability.** Analysis code is archived on Zenodo (<https://zenodo.org>) at doi:

## References

- 1 Liu, W. *et al.* Origin of the human malaria parasite *Plasmodium falciparum* in gorillas. *Nature* **467**, 420-425, doi:10.1038/nature09442 (2010).
- 2 Liu, W. *et al.* African origin of the malaria parasite *Plasmodium vivax*. *Nat. Commun.* **5**, 3346, doi:10.1038/ncomms4346 (2014).
- 3 Liu, W. *et al.* Multigenomic delineation of *Plasmodium* species of the *Laverania* subgenus infecting wild-living chimpanzees and gorillas. *Genome Biol. Evol.* **8**, 1929-1939, doi:10.1093/gbe/evw128 (2016).
- 4 Prugnolle, F. *et al.* African great apes are natural hosts of multiple related malaria species, including *Plasmodium falciparum*. *Proc. Natl. Acad. Sci. USA.* **107**, 1458-1463, doi:10.1073/pnas.0914440107 (2010).
- 5 Boundenga, L. *et al.* Diversity of malaria parasites in great apes in Gabon. *Malar. J.* **14**, 111, doi:10.1186/s12936-015-0622-6 (2015).



- 6 Kaiser, M. *et al.* Wild chimpanzees infected with 5 *Plasmodium* species. *Emerg. Infect. Dis.* **16**, 1956-1959, doi:10.3201/eid1612.100424 (2010).
- 7 Loy, D. E. *et al.* Out of Africa: origins and evolution of the human malaria parasites *Plasmodium falciparum* and *Plasmodium vivax*. *Int. J. Parasitol.* **47**, 87-97, doi:10.1016/j.ijpara.2016.05.008 (2017).
- 8 Sundararaman, S. A. *et al.* *Plasmodium falciparum*-like parasites infecting wild apes in southern Cameroon do not represent a recurrent source of human malaria. *Proc. Natl. Acad. Sci. USA.* **110**, 7020-7025 (2013).
- 9 Sundararaman, S. A. *et al.* Genomes of cryptic chimpanzee *Plasmodium* species reveal key evolutionary events leading to human malaria. *Nat. Commun.* **7**, 11078, doi:10.1038/ncomms11078 (2016).
- 10 Faust, C. & Dobson, A. P. Primate malarias: diversity, distribution and insights for zoonotic *Plasmodium*. *One Health* **1**, 66-75, doi:10.1016/j.onehlt.2015.10.001 (2015).
- 11 Wolfe, N. D. *et al.* The impact of ecological conditions on the prevalence of malaria among orangutans. *Vector Borne Zoonotic Dis.* **2**, 97-103, doi:10.1089/153036602321131896 (2002).
- 12 Collins, W. E. *Plasmodium knowlesi*: a malaria parasite of monkeys and humans. *Annu. Rev. Entomol.* **57**, 107-121, doi:10.1146/annurev-ento-121510-133540 (2012).
- 13 Fornace, K. M. *et al.* Association between landscape factors and spatial patterns of *Plasmodium knowlesi* infections in Sabah, Malaysia. *Emerg. Infect. Dis.* **22**, 201-208, doi:10.3201/eid2202.150656 (2016).
- 14 Paupy, C. *et al.* *Anopheles moucheti* and *Anopheles vinckei* are candidate vectors of ape *Plasmodium* parasites, including *Plasmodium praefalciparum* in Gabon. *PLoS One.* **8**, e57294, doi:10.1371/journal.pone.0057294 (2013).
- 15 Makanga, B. *et al.* Ape malaria transmission and potential for ape-to-human transfers in Africa. *Proc. Natl. Acad. Sci. USA.* **113**, 5329-5334, doi:10.1073/pnas.1603008113 (2016).
- 16 Sinka, M. E. in *Global distribution of the dominant vector species of malaria. Anopheles mosquitoes - New insights into malaria vectors* (ed Manguin, S.) 109-143 (InTech, 2013).



- 17 Krief, S. *et al.* On the diversity of malaria parasites in African apes and the origin of *Plasmodium falciparum* from bonobos. *PLoS Pathog.* **6**, e1000765, doi:10.1371/journal.ppat.1000765 (2010).
- 18 Liu, W. *et al.* Single genome amplification and direct amplicon sequencing of *Plasmodium* spp. DNA from ape faecal specimens. *Protocol Exchange.* (2010).
- 19 Eriksson, J., Hohmann, G., Boesch, C. & Vigilant, L. Rivers influence the population genetic structure of bonobos (*Pan paniscus*). *Mol. Ecol.* **13**, 3425-3435, doi:10.1111/j.1365-294X.2004.02332.x (2004).
- 20 Kawamoto, Y. *et al.* Genetic structure of wild bonobo populations: diversity of mitochondrial DNA and geographical distribution. *PLoS One.* **8**, e59660, doi:10.1371/journal.pone.0059660 (2013).
- 21 Weiss, D. J. *et al.* Air temperature suitability for *Plasmodium falciparum* malaria transmission in Africa 2000-2012: a high-resolution spatiotemporal prediction. *Malar. J.* **13**, 171, doi:10.1186/1475-2875-13-171 (2014).
- 22 Mordecai, E. A. *et al.* Optimal temperature for malaria transmission is dramatically lower than previously predicted. *Ecol. Lett.* **16**, 22-30, doi:10.1111/ele.12015 (2013).
- 23 Paaijmans, K. P. *et al.* Influence of climate on malaria transmission depends on daily temperature variation. *Proc. Natl. Acad. Sci. USA.* **107**, 15135-15139, doi:10.1073/pnas.1006422107 (2010).
- 24 Huffman, M. A. Animal self-medication and ethno-medicine: exploration and exploitation of the medicinal properties of plants. *Proc. Nutr. Soc.* **62**, 371-381 (2003).
- 25 Krief, S., Martin, M. T., Grellier, P., Kasenene, J. & Sevenet, T. Novel antimalarial compounds isolated in a survey of self-meditative behavior of wild chimpanzees in Uganda. *Antimicrob. Agents Chemother.* **48**, 3196-3199, doi:10.1128/AAC.48.8.3196-3199.2004 (2004).
- 26 Krief, S. *et al.* Bioactive properties of plant species ingested by chimpanzees (*Pan troglodytes schweinfurthii*) in the Kibale National Park, Uganda. *Am. J. Primatol.* **68**, 51-71, doi:10.1002/ajp.20206 (2006).

- 27 CBOL Plant Working Group: Hollingsworth, P.M. et al. A DNA barcode for land plants. *Proc. Natl. Acad. Sci. USA*. **106**, 12794-12797, doi:10.1073/pnas.0905845106 (2009).
- 28 Yu, J., Xue, J.-H. & Zhou, S.-L. New universal *matK* primers for DNA barcoding angiosperms *J. Syst. Evol.* **49**, 176-181 (2011).
- 29 Dong, W. et al. Discriminating plants using the DNA barcode *rbcLb*: an appraisal based on a large data set. *Mol. Ecol. Resour.* **14**, 336-343, doi:10.1111/1755-0998.12185 (2014).
- 30 Srivathsan, A., Sha, J. C., Vogler, A. P. & Meier, R. Comparing the effectiveness of metagenomics and metabarcoding for diet analysis of a leaf-feeding monkey (*Pygathrix nemaeus*). *Mol. Ecol. Resour.* **15**, 250-261, doi:10.1111/1755-0998.12302 (2015).
- 31 Lozupone, C. & Knight, R. UniFrac: a new phylogenetic method for comparing microbial communities. *Appl. Environ. Microbiol.* **71**, 8228-8235, doi:10.1128/AEM.71.12.8228-8235.2005 (2005).
- 32 Silva, J. R. et al. A review of antimalarial plants used in traditional medicine in communities in Portuguese-speaking countries: Brazil, Mozambique, Cape Verde, Guinea-Bissau, Sao Tome and Principe and Angola. *Mem. Inst. Oswaldo Cruz* **106 Suppl 1**, 142-158 (2011).
- 33 Lawal, B. et al. Potential antimalarials from African natural products: A review. *J. Intercult. Ethnopharmacol.* **4**, 318-343, doi:10.5455/jice.20150928102856 (2015).
- 34 Taniguchi, T. et al. *Plasmodium berghei* ANKA causes intestinal malaria associated with dysbiosis. *Sci. Rep.* **5**, 15699, doi:10.1038/srep15699 (2015).
- 35 Yilmaz, B. et al. Gut microbiota elicits a protective immune response against malaria transmission. *Cell* **159**, 1277-1289, doi:10.1016/j.cell.2014.10.053 (2014).
- 36 Ochman, H. et al. Evolutionary relationships of wild hominids recapitulated by gut microbial communities. *PLoS Biol.* **8**, e1000546, doi:10.1371/journal.pbio.1000546 (2010).
- 37 Springer, A., Fichtel, C., Calvignac-Spencer, S., Leendertz, F. H. & Kappeler, P. M. Hemoparasites in a wild primate: Infection patterns suggest interaction of *Plasmodium* and *Babesia* in a lemur species. *Int. J. Parasitol. Parasites Wildl.* **4**, 385-395, doi:10.1016/j.ijppaw.2015.10.006 (2015).

- 38 Escalante, A. A. & Ayala, F. J. Phylogeny of the malarial genus *Plasmodium*, derived from rRNA gene sequences. *Proc Natl Acad Sci USA*. **91**, 11373-11377 (1994).
- 39 Silva, J. C. *et al.* Genome sequences reveal divergence times of malaria parasite lineages. *Parasitology* **138**, 1737-1749, doi:10.1017/S0031182010001575 (2011).
- 40 Perelman, P. *et al.* A molecular phylogeny of living primates. *PLoS Genet.* **7**, e1001342, doi:10.1371/journal.pgen.1001342 (2011).
- 41 Ricklefs, R. E. & Outlaw, D. C. A molecular clock for malaria parasites. *Science* **329**, 226-229, doi:10.1126/science.1188954 (2010).
- 42 Silva, J. C., Egan, A., Arze, C., Spouge, J. L. & Harris, D. G. A new method for estimating species age supports the coexistence of malaria parasites and their Mammalian hosts. *Mol. Biol. Evol.* **32**, 1354-1364, doi:10.1093/molbev/msv005 (2015).
- 43 Takemoto, H., Kawamoto, Y. & Furuichi, T. How did bonobos come to range south of the congo river? Reconsideration of the divergence of *Pan paniscus* from other *Pan* populations. *Evol. Anthropol.* **24**, 170-184, doi:10.1002/evan.21456 (2015).
- 44 Takemoto, H. *et al.* The mitochondrial ancestor of bonobos and the origin of their major haplogroups. *PLoS One*. **12**, e0174851, doi:10.1371/journal.pone.0174851 (2017).
- 45 Carter, R. & Mendis, K. N. Evolutionary and historical aspects of the burden of malaria. *Clin. Microbiol. Rev.* **15**, 564-594, doi:10.1128/cmr.15.4.564-594.2002 (2002).
- 46 Martin, M. J., Rayner, J. C., Gagneux, P., Barnwell, J. W. & Varki, A. Evolution of human-chimpanzee differences in malaria susceptibility: relationship to human genetic loss of N-glycolylneuraminic acid. *Proc. Natl. Acad. Sci. USA*. **102**, 12819-12824, doi:10.1073/pnas.0503819102 (2005).
- 47 Prugnolle, F. *et al.* Diversity, host switching and evolution of *Plasmodium vivax* infecting African great apes. *Proc. Natl. Acad. Sci. USA*. **110**, 8123-8128 (2013).
- 48 Ngoubangoye, B. *et al.* The host specificity of ape malaria parasites can be broken in confined environments. *Int. J. Parasitol.* **46**, 737-744, doi:10.1016/j.ijpara.2016.06.004 (2016).

- 49 Wanaguru, M., Liu, W., Hahn, B. H., Rayner, J. C. & Wright, G. J. RH5-Basigin interaction plays a major role in the host tropism of *Plasmodium falciparum*. *Proc. Natl. Acad. Sci. USA*. **110**, 20735-20740, doi:10.1073/pnas.1320771110 (2013).
- 50 Delicat-Loembet, L. *et al.* No evidence for ape *Plasmodium* infections in humans in Gabon. *PLoS One*. **10**, e0126933, doi:10.1371/journal.pone.0126933 (2015).
- 51 Guindon, S. *et al.* New algorithms and methods to estimate maximum-likelihood phylogenies: assessing the performance of PhyML 3.0. *Syst. Biol.* **59**, 307-321, doi:10.1093/sysbio/syq010 (2010).
- 52 Darriba, D., Taboada, G. L., Doallo, R. & Posada, D. jModelTest 2: more models, new heuristics and parallel computing. *Nat. Methods*. **9**, 772, doi:10.1038/nmeth.2109 (2012).
- 53 Huelsenbeck, J. P. & Ronquist, F. MRBAYES: Bayesian inference of phylogenetic trees. *Bioinformatics* **17**, 754-755 (2001).
- 54 National Aeronautics and Space Administration: MODIS. Available at: <http://modis.gsfc.nasa.gov/> (accessed 1st May 2016).
- 55 Tatem, A. J., Goetz, S. J. & Hay, S. I. Terra and Aqua: new data for epidemiology and public health. *Int. J. Appl. Earth Obs. Geoinf.* **6**, 33-46 (2004).
- 56 Hansen, M. C. *et al.* High-resolution global maps of 21st-century forest cover change. *Science* **342**, 850-853, doi:10.1126/science.1244693 (2013).
- 57 Hong, Y. On computing the distribution function for the Poisson binomial distribution. *Computational Statistics & Data Analysis*. **59**, 41-51, doi:<http://dx.doi.org/10.1016/j.csda.2012.10.006> (2013).
- 58 Mahe, F., Rognes, T., Quince, C., de Vargas, C. & Dunthorn, M. Swarm v2: highly-scalable and high-resolution amplicon clustering. *PeerJ*. **3**, e1420, doi:10.7717/peerj.1420 (2015).
- 59 Katoh, K., Misawa, K., Kuma, K. & Miyata, T. MAFFT: a novel method for rapid multiple sequence alignment based on fast Fourier transform. *Nucleic Acids Res.* **30**, 3059-3066 (2002).
- 60 Price, M. N., Dehal, P. S. & Arkin, A. P. FastTree 2--approximately maximum-likelihood trees for large alignments. *PLoS One*. **5**, e9490, doi:10.1371/journal.pone.0009490 (2010).

- 61 Lauder, A. P. *et al.* Comparison of placenta samples with contamination controls does not provide evidence for a distinct placenta microbiota. *Microbiome*. **4**, 29, doi:10.1186/s40168-016-0172-3 (2016).
- 62 Caporaso, J. G. *et al.* QIIME allows analysis of high-throughput community sequencing data. *Nat. Methods*. **7**, 335-336, doi:10.1038/nmeth.f.303 (2010).
- 63 DeSantis, T. Z. *et al.* Greengenes, a chimera-checked 16S rRNA gene database and workbench compatible with ARB. *Appl. Environ. Microbiol.* **72**, 5069-5072, doi:10.1128/AEM.03006-05 (2006).
- 64 R Core Team. R: A language and environment for statistical computing. R Foundation for Statistical Computing, Vienna, Austria. ISBN 3-900051-07-0, URL <http://www.r-project.org/>. (2013).
- 65 Shannon, C. A mathematical theory of communication *SIGMOBILE Mobile Computing Communications Review* 5:3–55. (2001).
- 66 Paradis, E., Claude, J. & Strimmer, K. APE: Analyses of Phylogenetics and Evolution in R language. *Bioinformatics* **20**, 289-290 (2004).
- 67 van der Maaten, L. & Hinton, G. Visualizing Data using t-SNE. *J Machine Learning Research*. **9**, 2579-2605 (2008).
- 68 McArdle, B. H. & Anderson, M. J. Fitting multivariate models to community data: a comment on distance - based redundancy analysis. *Ecology* **82**, 290-297 (2001).
- 69 Oksanen, J. *et al.* Ordination methods, diversity analysis and other functions for community and vegetation ecologists. *vegan: Community Ecology Package*. <https://cran.r-project.org/package=vegan> (2017).
- 70 Li, Y. *et al.* Eastern chimpanzees, but not bonobos, represent a simian immunodeficiency virus reservoir. *J. Virol.* **86**, 10776-10791, doi:10.1128/JVI.01498-12 (2012).

## End Notes

**Acknowledgements** We thank the staff of the TL2 site, the Institut National de Recherches Biomédicales (INRB, Kinshasa, DRC), and the Bonobo Conservation Initiative for field work in the DRC; Richard Carter for helpful discussions; the Ministry of Scientific Research and Technology, the Department of Ecology and Management of Plant and Animal Resources of the University of Kisangani, the Ministries of Health and Environment, and the National Ethics Committee for permission to collect samples in the DRC. This work was supported by grants from the National Institutes of Health (R01 AI 091595, R01 AI 058715, R01 AI 120810, R37 AI 050529, T32 AI 007532, T32 AI 007632, P30 AI 045008), the Agence Nationale de Recherche sur le Sida (ANRS 12125/12182/12255), the Agence Nationale de Recherche (Programme Blanc, Sciences de la Vie, de la Santé et des Ecosystèmes and ANR 11 BSV3 021 01, Projet PRIMAL), Harvard University, and the Arthur L. Greene Fund.

**Author contributions** All authors contributed to the acquisition, analysis, and interpretation of the data; W.L., S.S.-M., G.M.S., P.M.S., and B.H.H. conceived, planned and executed the study; J.-B.N.N., A.V.G., S.A.-M., M.P., P.B., J.D., C.G., J.A.H. and T.B.H conducted or supervised fieldwork; W.L., Y.L., D.E.L, A.N.A., and S.A.S. performed non-invasive ape *Plasmodium* testing; W.L. and A.P.L. performed faecal plant and microbiome analyses; E.J.S. developed a climate model predictive of ape *Laverania* infection; S.S.-M. performed statistical and bioinformatic analyses; G.H.L., L.J.P. and P.M.S. performed phylogenetic analyses; W.L., S.S.-M., G.M.S., P.M.S, and B.H.H. coordinated the contributions of all authors and wrote the manuscript.

**Competing financial interests:** The authors declare no competing financial interests.

### **Additional Information**

Supplementary information is available for this paper.

Correspondence and requests for materials should be addressed to Beatrice H. Hahn ([bhahn@upenn.edu](mailto:bhahn@upenn.edu))

## Figure Legends

**Figure 1 *Plasmodium* infections of wild-living bonobos.** Ape study sites are shown in relation to the ranges of the bonobo (*P. paniscus*, hatched red) and the eastern chimpanzee (*P. t. schweinfurthii*, hatched blue), with white dots indicating sites where no *Plasmodium* infection was found (see Table 1 and Supplementary Table 3 for a list of all field sites and their code designation). The Tshuapa-Lomami-Lualaba (TL2) site where bonobos are endemically infected with multiple *Plasmodium* species, including a newly discovered *Laverania* species (B1), is shown in red with two dots indicating sampling on both sides of the Lomami River. Eastern chimpanzee field sites with endemic *P. reichenowi*, *P. gaboni*, and/or *P. billcollinsi* infections are shown in yellow. A red circle highlights one bonobo (KR) and one chimpanzee (PA) field site where B1 parasite sequences were detected in a single faecal sample. Forested areas are shown in dark green, while arid or semiarid areas are depicted in brown. Major lakes and rivers are shown in blue. Dashed yellow lines indicate national boundaries. The scale bar indicates 200 kilometers.

**Figure 2 Relationship of bonobo parasites to ape *Laverania* species.** A maximum likelihood tree of mitochondrial cytochrome B (*cytB*) sequences (956 bp) depicting the phylogenetic position of newly derived bonobo parasite sequences (magenta) is shown. Only distinct *cytB* haplotypes are depicted (the full set of SGA-derived bonobo parasite sequences is shown in Supplementary Figure 1). Sequences are colour-coded, with capital letters indicating their field site of origin (see Fig. 1 for location of field sites) and lower case letters denoting their host species and subspecies origin (ptt: *P. t. troglodytes*, red; pte: *P. t. ellioti*, orange; pts: *P. t. schweinfurthii*, blue; ggg: *G. g. gorilla*, green; pp: *Pan paniscus*, magenta). C1, C2 and C3 represent the chimpanzee parasites *P. reichenowi*, *P. gaboni*, and *P. billcollinsi*; G1, G2 and G3 represent the gorilla parasites *P. praefalciparum*, *P. adleri*, and *P. blacklocki* (the *P. falciparum* 3D7 reference sequence is shown in black). *P. reichenowi* (C1) and *P. gaboni* (C2) mitochondrial sequences are known to segregate into two geographically defined subclades according to their collection site in “western” (W) or “eastern” (E) Africa<sup>3</sup>. Bonobo parasite



sequences (magenta) cluster with *P. gaboni* from eastern chimpanzees (C2E), but also form a new clade, termed B1. The tree was constructed using PhyML<sup>51</sup> with TIM2+I+G as the evolutionary model. Bootstrap values are shown for major nodes only (the scale bar represents 0.01 substitutions per site).

**Figure 3 A new *Laverania* species specific for bonobos.** (a, b) Maximum likelihood phylogenetic trees are shown for nuclear gene fragments of the (a) erythrocyte-binding antigen 165 (*eba165*; 790 bp) and (b) the gametocyte surface protein P47 (*p47*; 800 bp) of *Laverania* parasites. Sequences are labeled and coloured as in Fig. 2 (identical sequences from different samples are shown; identical sequences from the same sample are excluded). C1, C2 and C3 represent the chimpanzee parasites *P. reichenowi*, *P. gaboni*, and *P. billcollinsi*; G1, G2 and G3 represent the gorilla parasites *P. praefalciparum*, *P. adleri*, and *P. blacklocki* (PrCDC and Pf3D7 reference sequences are shown in black). Bonobo parasite sequences cluster within *P. gaboni* (C2) or form a new distinct clade (B1), indicating a new *Laverania* species (see text for information on the single *eba165* B1 sequence from an eastern chimpanzee). The trees were constructed using PhyML<sup>51</sup> with TPM3uf+G (a) and GTR+G (b) as evolutionary models. Bootstrap values are shown for major nodes only (the scale bar represents 0.01 substitutions per site).

**Figure 4 Bonobo infections with non-*Laverania* parasites.** Maximum likelihood phylogenetic trees are shown for mitochondrial and apicoplast gene sequences of non-*Laverania* parasites. Ape derived (a) *cytB* (956 bp), (b) *clpM* (327 bp), (c) *cox1* (296 bp) and (d) *clpM* (574 bp) sequences are labeled and coloured as in Fig. 2 (identical sequences from different samples are shown; identical sequences from the same sample are excluded). Human and monkey parasite reference sequences from the database are labeled by black squares and circles, respectively. Brackets indicate non-*Laverania* species, including *P. malariae*, *P. vivax*, *P. ovale curtisi*, and *P. ovale wallikeri* (available sequences are too short to differentiate ape and human specific lineages) as well as the monkey parasites *P. inui* and *P. hylobati*. Newly identified bonobo parasite sequences are indicated by arrows, all of which are from



the TL2 site. One TL2 *cytB* sequence clusters with a previously reported parasite sequence from a chimpanzee sample (DGptt540), forming a well-supported lineage that is only distantly related to human and ape *P. malariae*, and thus likely represents a new *P. malariae*-related species. The trees were constructed using PhyML<sup>51</sup> with GTR+G (a), TRN+I (b, d) and TIM2+I (c) as evolutionary models. Bootstrap values  $\geq 70\%$  are shown for major nodes only (the scale bar represents 0.01 substitutions per site).

**Figure 5 The Lomami River is not a barrier to *Laverania* parasite transmission.** (a) Maximum likelihood phylogenetic tree of bonobo mitochondrial (D-loop) sequences. Haplotypes are labeled by field site (see Fig. 1 and refs. 7, 19, 20, and 70 for their geographic location and code designation), with those identified at multiple field sites indicated (e.g. C/Wamba/KR/BN/IK/LA). Newly derived haplotypes from the TL2 site are shown in blue (previously reported mtDNA sequences are shown in black)<sup>19,20,70</sup>. Brackets highlight two clades that are exclusively comprised of mtDNA sequences from bonobos sampled east of the Lomami River. TL2 haplotypes that do not fall within these clades (denoted by arrows) were all sampled west of the Lomami River (TL2-W). The tree was constructed using PhyML<sup>51</sup> with HKY+G as the evolutionary model. Bayesian posterior probability values  $\geq 0.6$  are shown (the scale bar represents 0.01 substitutions per site). (b) Locations of individual bonobo faecal samples collected at the TL2 site. Sampling locations west (TL2-W) and east (TL2-E and TL2-NE) of the Lomami River were plotted using GPS coordinates, with red and white dots indicating *Laverania* parasite positive and negative specimens, respectively. Samples that contained *P. reichenowi*, *P. malariae*-like, *P. vivax*-like, and *P. ovale*-like parasites are also indicated. Forested areas are shown in green, while savannas are depicted in brown. The Lomami River is shown in blue. Local villages are denoted by black squares. The scale bar indicates 2 kilometers.

**Figure 6. *Laverania* infection of bonobos is not associated with particular faecal plant and microbiome constituents.** A principal component analysis of unweighted UniFrac distances was used to visualise compositional differences of (a, b) plant (*matK* and *rbcL*) and (c) bacterial (16S rRNA)

constituents in *Laverania* positive (dark border) and negative (light border) faecal samples from bonobos (blue) and chimpanzees (pink). The sample positions (shown for the first two components) do not indicate separate clustering of *Laverania* positive and negative samples.

## Supplementary Information

### **Geographically restricted malaria infections of wild bonobos include a new *Laverania* species**

Weimin Liu<sup>1#</sup>, Scott Sherrill-Mix<sup>1,2#</sup>, Gerald H. Learn<sup>1</sup>, Erik J. Scully<sup>3,4</sup>, Yingying Li<sup>1</sup>, Alexa N. Avitto<sup>1</sup>, Dorothy E. Loy<sup>1,2</sup>, Abigail P. Lauder<sup>2</sup>, Sesh A. Sundararaman<sup>1,2</sup>, Lindsey J. Plenderleith<sup>5</sup>, Jean-Bosco N. Ndjango<sup>6</sup>, Alexander V. Georgiev<sup>7,8</sup>, Steve Ahuka-Mundeke<sup>9</sup>, Martine Peeters<sup>10</sup>, Paco Bertolani<sup>11</sup>, Jef Dupain<sup>12</sup>, Cintia Garai<sup>13</sup>, John A. Hart<sup>13</sup>, Terese B. Hart<sup>13</sup>, George M. Shaw<sup>1,2</sup>, Paul M. Sharp<sup>5</sup> and Beatrice H. Hahn<sup>1,2\*</sup>



C1E

B1

G1

C3

G3

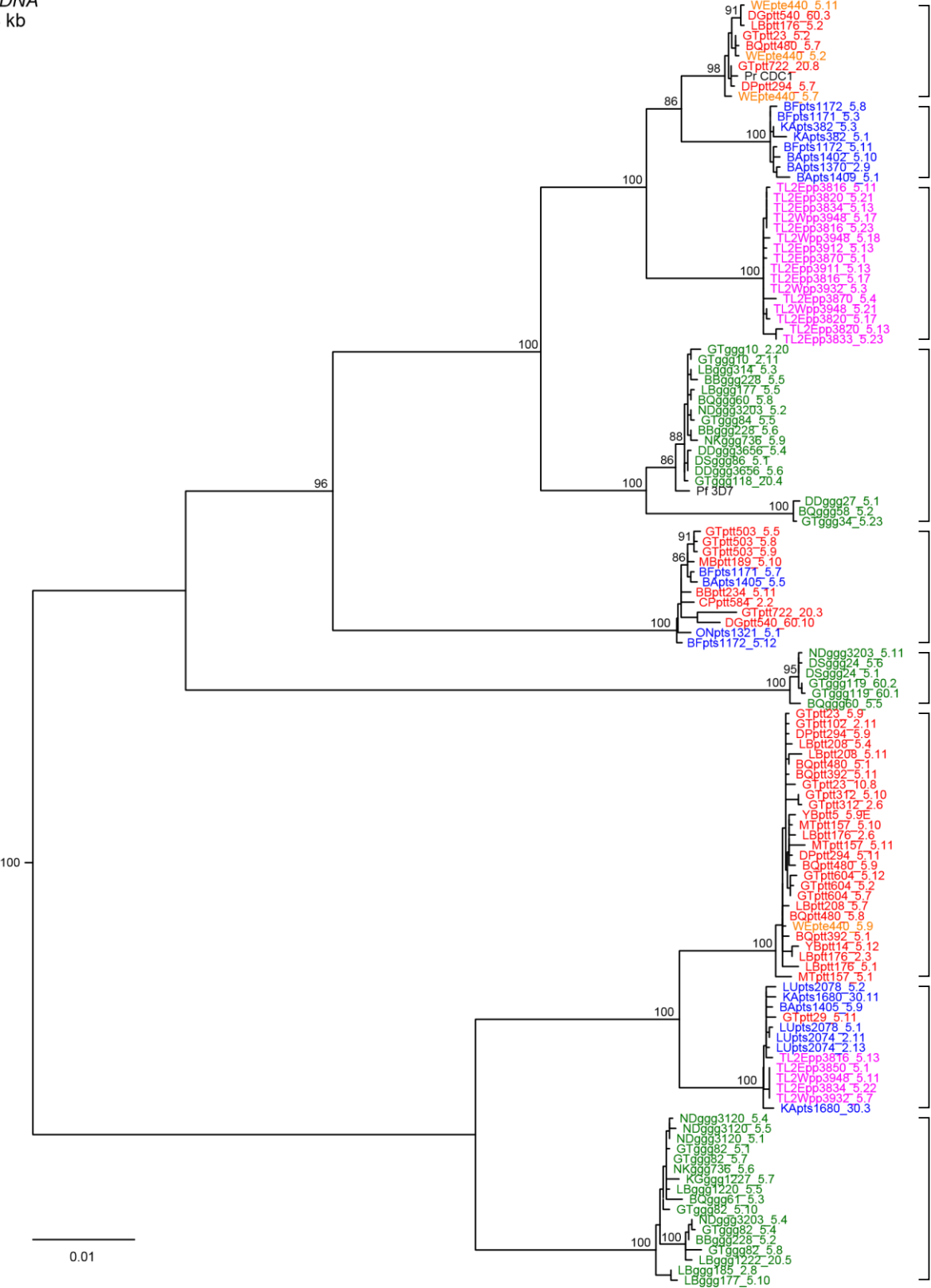
C2W

C2E

G2

**Supplementary Figure 1 Evolutionary relationships of *Laverania* mitochondrial sequences.** A maximum likelihood tree of cytochrome B (*cytB*) sequences (956 bp) from chimpanzee, gorilla, and bonobo *Laverania* parasites is shown. Sequences are colour-coded, with capital letters indicating their field site of origin (see Fig. 1 and ref. 1 for their location) and lower case letters denoting their host species and subspecies origin (pp: *Pan paniscus*, magenta; ptt: *P. t. troglodytes*, red; pte: *P. t. ellioti*, orange; pts: *P. t. schweinfurthii*, blue; ggg: *G. g. gorilla*, green). Asterisks indicate sequences derived by intensified PCR, all of which were confirmed to be single template derived (PApts1059\_1.7 represents an intensified PCR derived sequence amplified from the undiluted PApts1059 faecal DNA and identified at position 7 in a plate of multiple PCR replicates). The remaining faecal derived ape parasite sequences were generated by single genome amplification (SGA) (e.g., GTptt312\_5.8 represents an SGA derived sequence amplified from a 1:5 dilution of GTptt312 faecal DNA and identified at position 8 in a plate of multiple PCR reactions). Brackets indicate six previously defined *Laverania* species, with C1, C2 and C3 denoting the chimpanzee parasites *Plasmodium reichenowi*, *P. gaboni*, and *P. billcollinsi*, and G1, G2 and G3 the gorilla parasites *P. praefalciparum*, *P. adleri*, and *P. blacklocki*, respectively. Sequences from *P. reichenowi* and *P. gaboni* segregate into geographic (“western”, W; “eastern”, E) subclades. Newly derived bonobo parasite sequences (n=77) fall into two *Laverania* lineages, including *P. gaboni* from eastern chimpanzees (C2E) and a new distinct clade (B1) that appears to be host-specific (see text for a description of the single B1 *cytB* sequence from an eastern chimpanzee sample PApts368). Identical sequences from different samples are shown (identical sequences from the same sample are excluded). The human *P. falciparum* reference sequence 3D7 is shown in black. Arrows indicate parasite sequences newly generated (n=147) from faecal DNA of eastern chimpanzees collected at field sites close to the bonobo range (Fig. 1), all of which cluster within *P. reichenowi* (C1E), *P. gaboni* (C2E) or *P. billcollinsi* (C3). The tree was constructed using PhyML<sup>2</sup> with HKY+I+G as the evolutionary model. Bootstrap support values ≥ 70% are shown for major nodes only (the scale bar represents 0.01 substitutions per site).

mtDNA  
3.4 kb



C1W

C1E

**B1**

**G1**

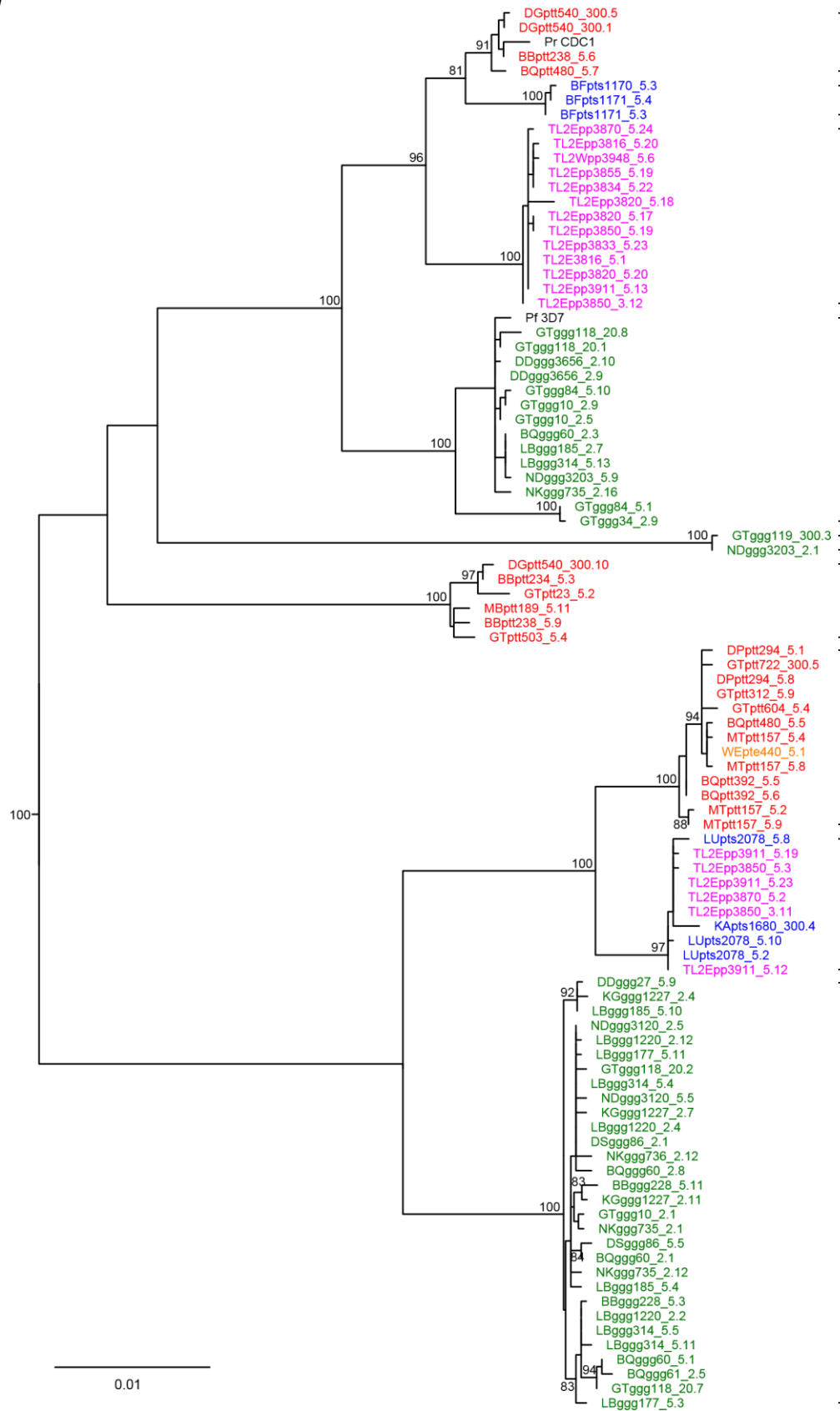
**C3**

**G3**

**C2W**

**C2E**

*mtDNA*  
3.3 kb





**C1E**

**B1**

**G1**

**G3**

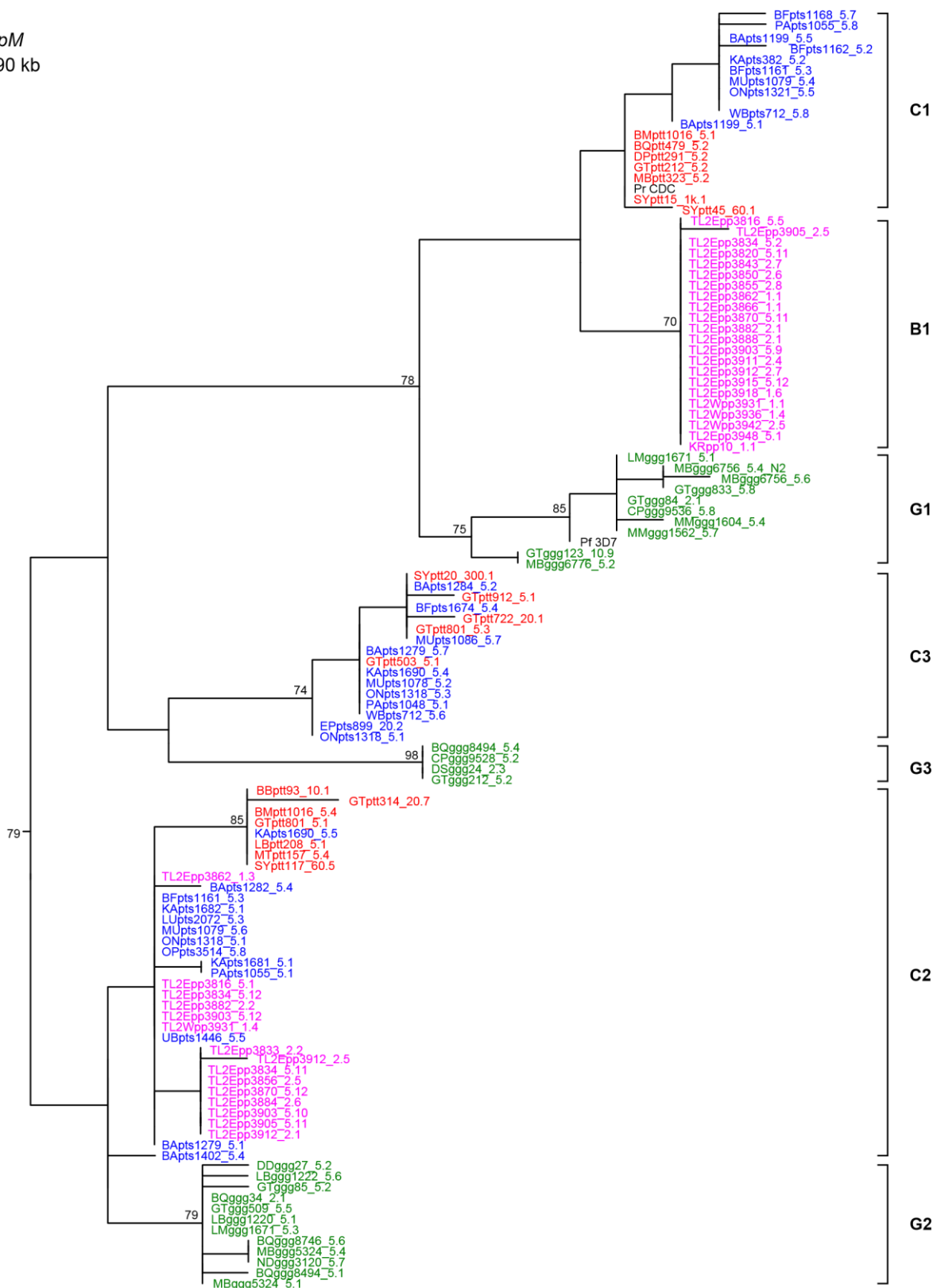
**C3**

**C2W**

**C2E**

**G2**

**c**  
*clpM*  
 390 kb



PApts369\_5.5

*eba175*  
394 kb

Phylogenetic tree showing the relationships between 100 *Plasmodium falciparum* sequences. The tree is rooted on the left and branches out to the right. Bootstrap values are indicated at the nodes. The sequences are color-coded: red for clinical isolates, blue for laboratory isolates, green for reference strains, and purple for other isolates. The tree shows several distinct clusters, including a large cluster of clinical isolates (red) and a cluster of laboratory isolates (blue). A scale bar of 0.01 is shown at the bottom left.

**C1**

B1

G1

C3

G3

C2

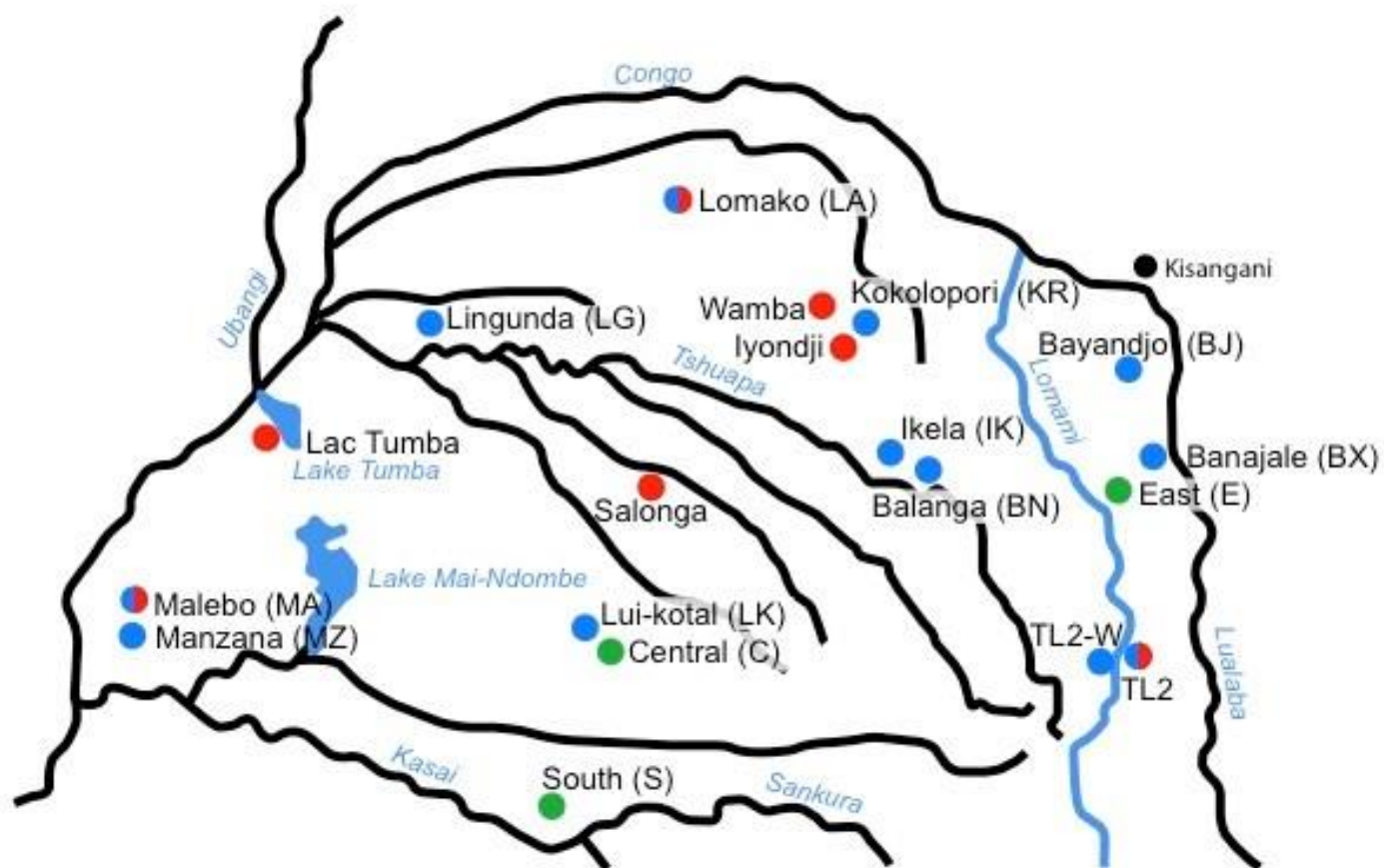
G2

**Supplementary Figure 2 Wild-living bonobos harbour two *Laverania* species.** Maximum likelihood trees depicting the phylogenetic relationships of (a, b) mitochondrial (3.4 and 3.3 kb half genomes), (c) apicoplast (*clpM* gene; 390 bp), and (d) nuclear (erythrocyte binding antigen 175; 394 bp) gene sequences of *Laverania* parasites are shown. Sequences are colour-coded to indicate the host species (pp: *Pan paniscus*, magenta; ptt: *P. t. troglodytes*, red; pte: *P. t. ellioti*, orange; pts: *P. t. schweinfurthii*, blue; ggg: *G. g. gorilla*, green) and are otherwise labeled as in Supplementary Fig. 1. Identical sequences from different samples are shown (identical sequences from the same sample are excluded). Brackets identify six previously defined *Laverania* species, with C1, C2 and C3 denoting the chimpanzee parasites *Plasmodium reichenowi*, *P. gaboni*, and *P. billcollinsi*, and G1, G2 and G3 the gorilla parasites *P. praefalciparum*, *P. adleri*, and *P. blacklocki*, respectively (mitochondrial sequences from *P. reichenowi* and *P. gaboni* segregate into “western” (W) and “eastern” (E) subclades). In all genomic regions, the newly derived bonobo parasite sequences either cluster with *P. gaboni* from

eastern chimpanzees or form a new clade (B1) that appears to be host-specific. Reference sequences for *P. falciparum* (Pf 3D7) and *P. reichenowi* (Pr CDC1) are shown in black. The trees were constructed using PhyML<sup>2</sup> with TIM2+I+G (**a**), TIM3+I+G (**b**) HKY+G (**c**) and TPM3uf+G (**d**) as evolutionary models. Bootstrap values  $\geq 70\%$  are shown for major nodes only (the scale bar represents 0.01 substitutions per site).

[illegible]

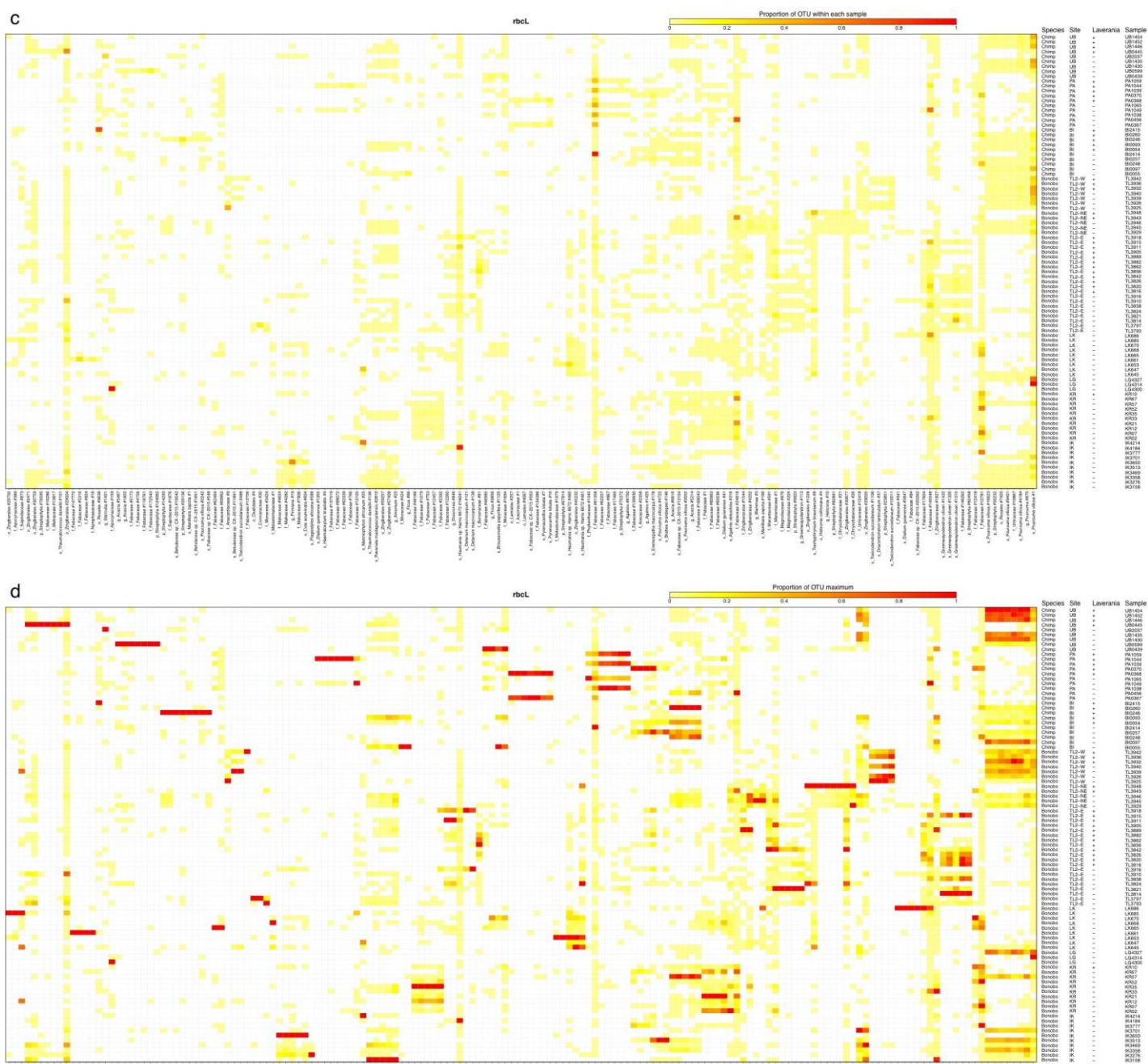
b



**Supplementary Figure 3 The Lomami River represents a barrier to bonobo gene flow. (a)** A maximum likelihood tree of previously reported<sup>3-5</sup> and newly generated (n=165) bonobo mitochondrial haplotypes with known sampling location is shown. Sequences are labeled by field site and GenBank accession code, with colours indicating results from three different groups: Sequences from Eriksson and colleagues are shown in green<sup>3</sup>; sequences from Kawamoto and colleagues are shown in red<sup>4</sup>; and sequencing from Li and colleagues<sup>5</sup> and the current study are shown in blue. Identical sequences from different collection sites are shown (identical sequences from the same location are excluded). All haplotypes from bonobos sampled east of the Lomami River (brackets) fall into two separate clades, confirming limited gene flow across this riverine barrier. The four TL2 haplotypes that do not fall within these two clades were all sampled west of the Lomami River and are indicated by an arrow. The tree was constructed using PhyML<sup>2</sup> with HKY+G as the evolutionary model. Bayesian posterior probability values  $\geq 0.6$  are shown (the scale bar represents 0.01 substitutions per site). **(b)** Geographic locations of faecal collection sites from which the bonobo mitochondrial haplotypes shown in **(a)** were derived. The full names of the field sites are listed, with haplotype abbreviations shown in parentheses. Bonobo sampling sites are colour coded to match the haplotypes shown in **(a)**, with sites/haplotypes described by Eriksson and colleagues shown in green<sup>3</sup>; by Kawamoto and colleagues shown in red<sup>4</sup>; and by Li and colleagues and the current study shown in blue<sup>5</sup>. Field sites where bonobos were independently sampled by two groups of investigators (Lomako, Malebo, TL2) are also denoted. The Lomami River is highlighted in blue; other rivers are shown in black.

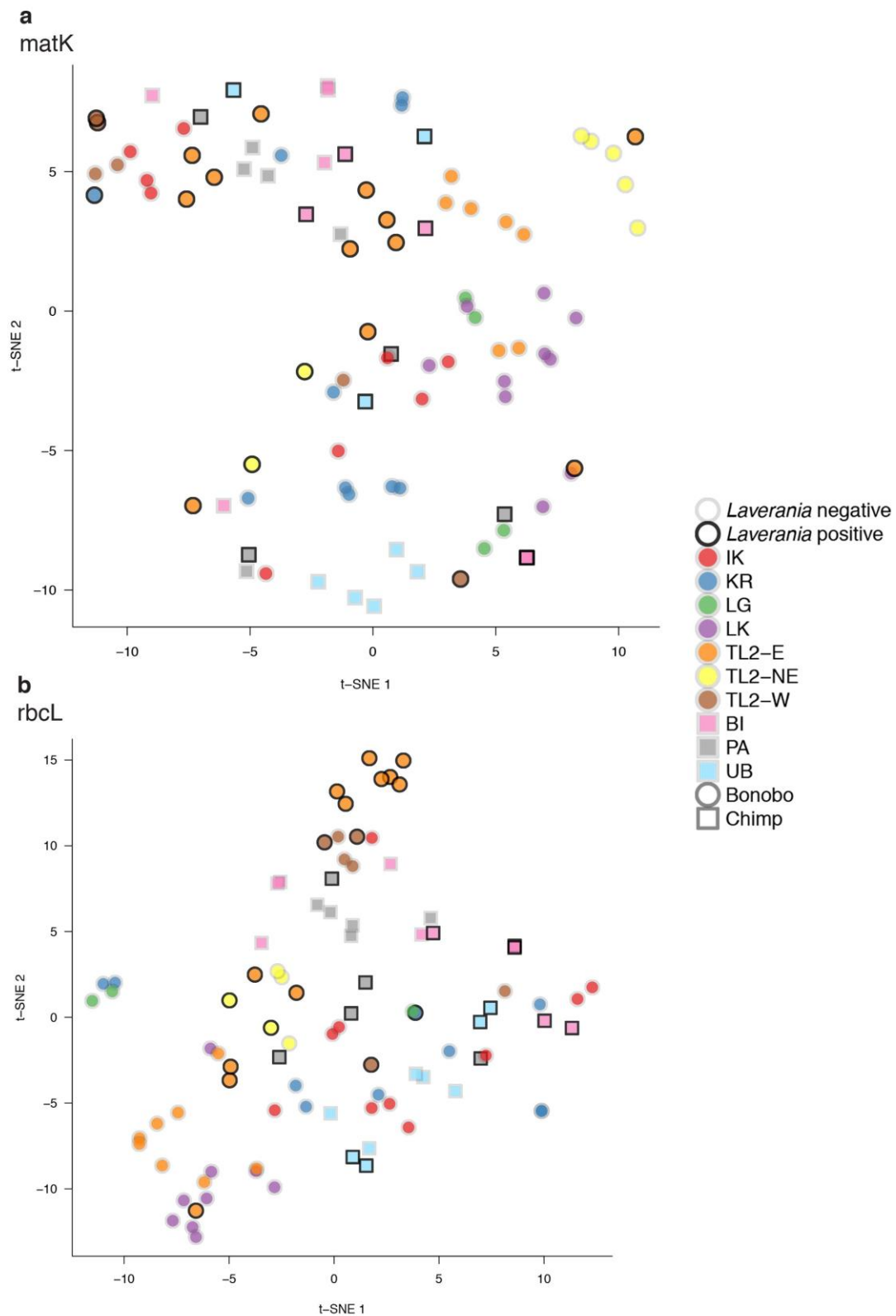






**Supplementary Figure 4 Relative abundance of major plant phyla in *Laverania* positive and negative ape faecal samples. (a) Heatmap of operational taxonomic units (OTUs) as determined**

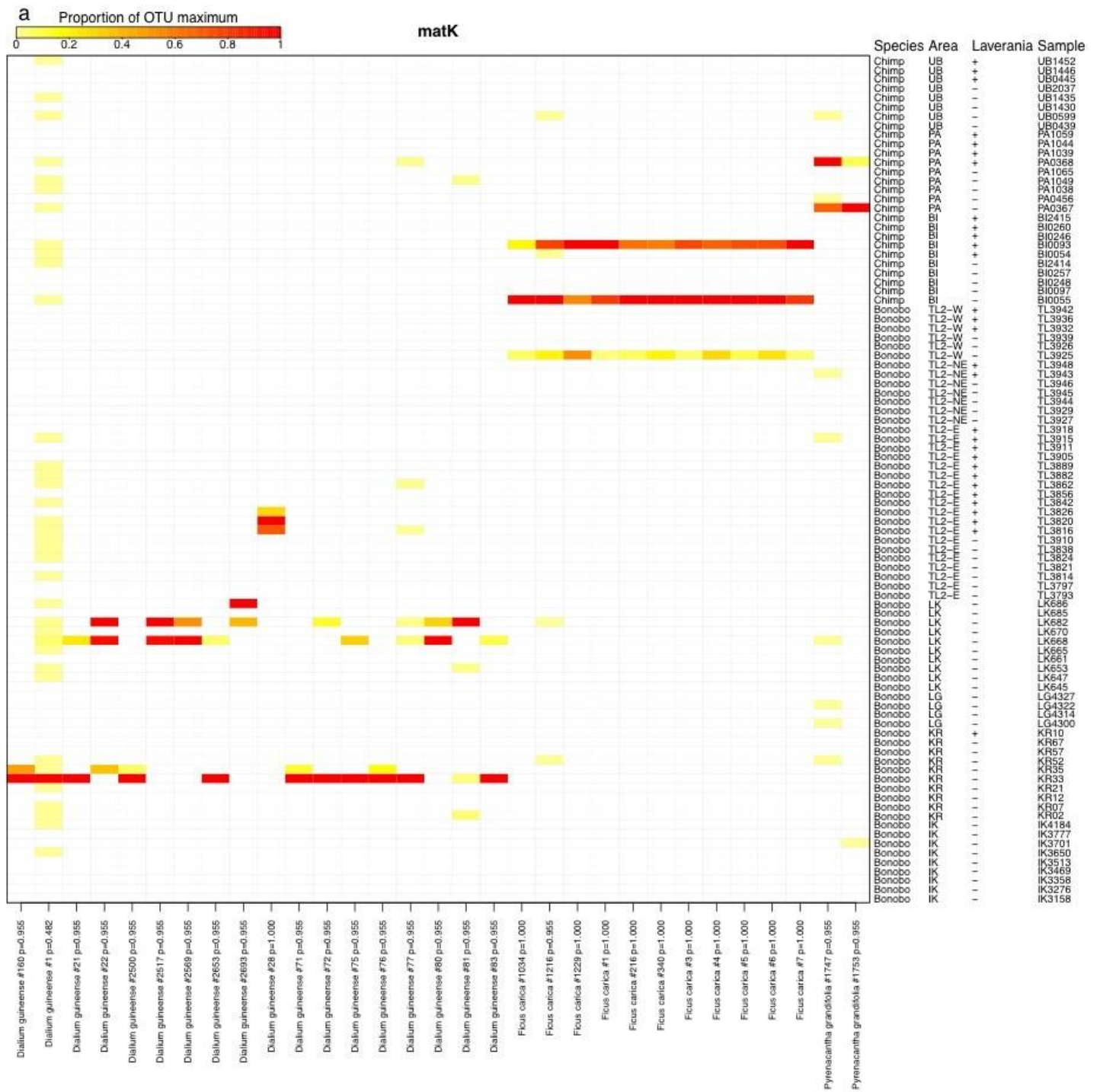
by *matK* gene sequencing. Each grid entry represents the relative abundance of an OTU (column) within each sample (row). Only OTUs with an abundance of greater than 2% in at least one sample are shown. OTUs are ordered by co-occurrence to emphasise patterns in the data. Samples are labeled by ape species (chimpanzee and bonobo), field site (see Fig. 5b for the location of TL2-W, TL2-E and TL2-NE samples), as well as with a + and – prefix to indicate *Laverania* positive and negative status, respectively (see Supplementary Table 7 for a description of all samples). OTUs are labeled according to their most specific assigned taxonomic rank, with letters indicating order (o), family (f), genus (g), and species (s), followed by an arbitrary ID number. Plant taxa that could not be classified are labeled “Unknown”. **(b)** Heatmap of OTUs as in **(a)** but with OTU abundance measured relative to the maximum proportion within that OTU (red cells indicate samples with the highest proportional abundance of the corresponding OTU). **(c)** Heatmap of OTUs as in **(a)** but for *rbcL* gene sequences. **(d)** Heatmap of OTUs as in **(b)** but for *rbcL* gene sequences.

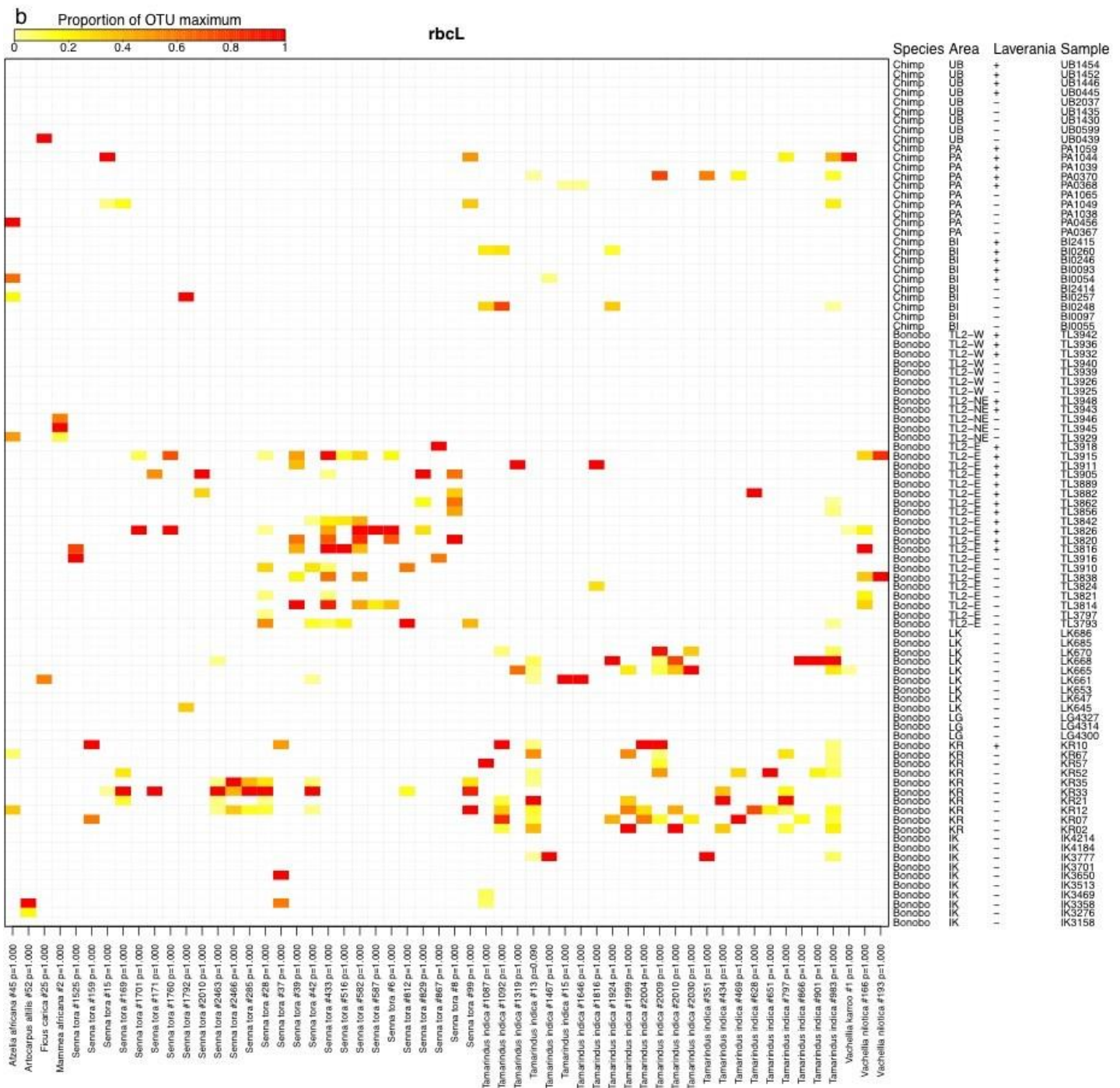


**Supplementary Figure 5 Plant composition in *Laverania* positive and negative bonobo and chimpanzee faecal samples across study sites.** A two dimensional representation of a



tdistributed stochastic neighbor embedding (t-SNE) analysis of unweighted Unifrac distances is shown for **(a)** chloroplast *matK* and **(b)** *rbcL* sequences, comparing faecal plant composition of bonobos (circles) and chimpanzees (squares) from various study sites (indicated by colour). *Laverania* positive faecal samples are highlighted by a dark outline. Note that during dimensional reduction, t-SNE attempts to preserve local differences so that similar samples cluster together, but the distance between samples with large differences is not necessarily preserved.





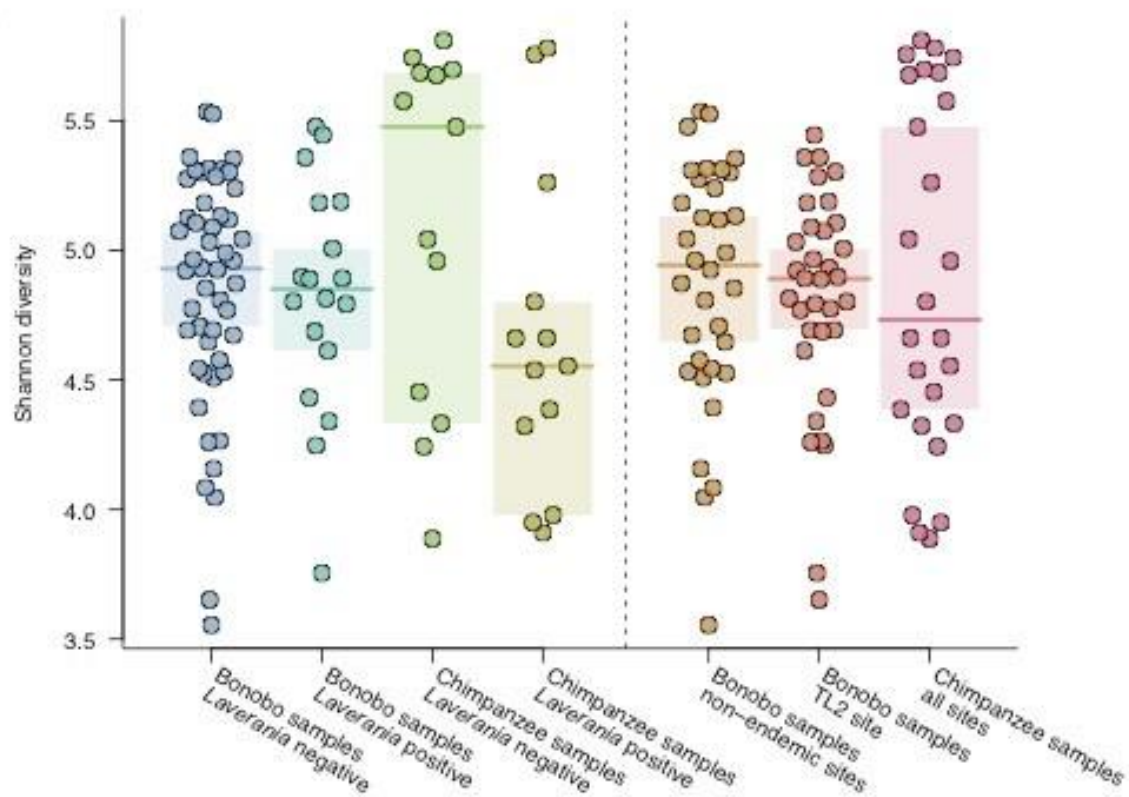
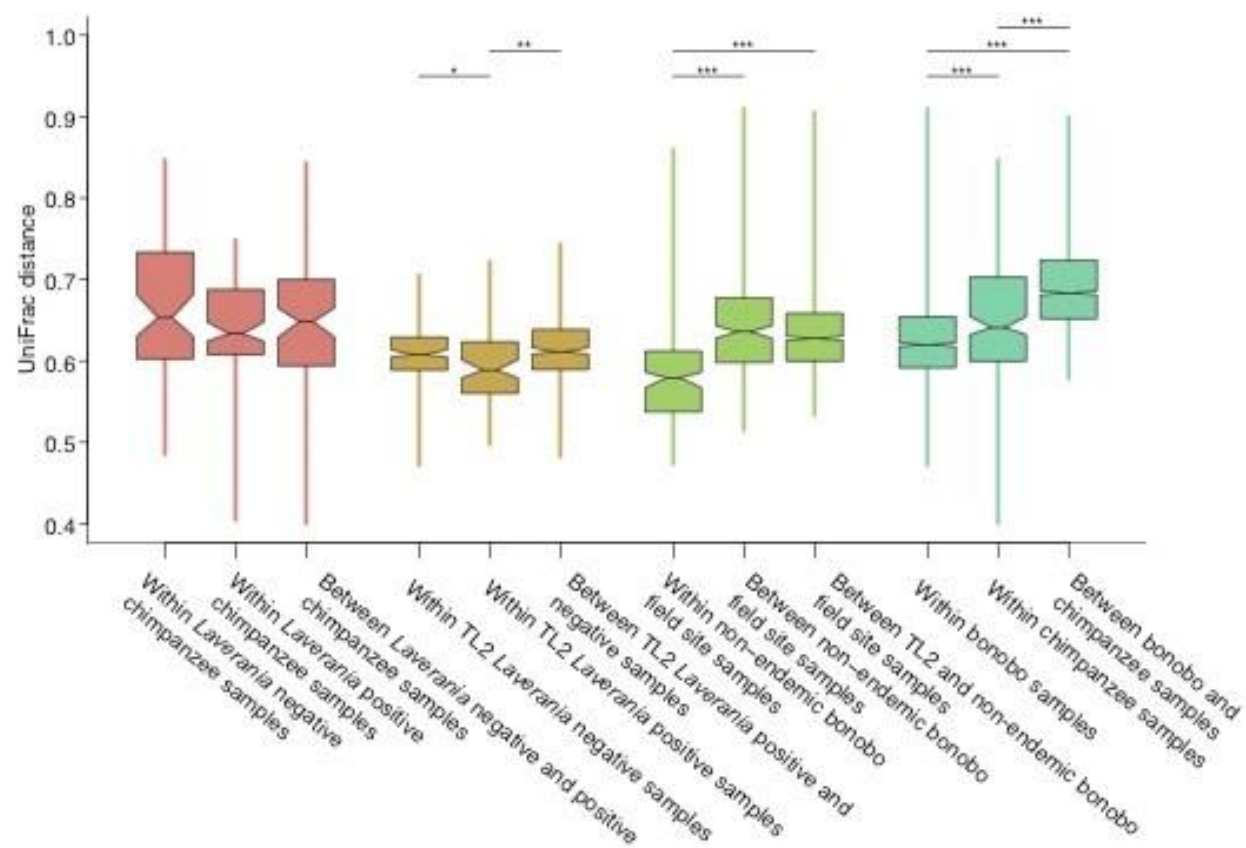
**Supplementary Figure 6 Relative abundance of potentially antimalarial plants in ape faecal samples. (a)** A heatmap of operational taxonomic units (OTUs) as determined by faecal *matK* sequencing is shown. Each grid entry represents the abundance of an OTU (column) within a

sample (row) relative to the maximum proportional abundance for that OTU. Only OTUs that matched a putative antimalarial plant (Supplementary Table 8) with >95% sequence identity and were found in more than one sample are shown. Samples are labeled by ape species (chimpanzee and bonobo), field site (see Fig. 5b for the location of TL2-W, TL2-E and TL2-NE samples), as well as with a + and – prefix to indicate *Laverania* positive and negative status. OTUs are labeled according to their assigned taxonomy followed by an arbitrary ID number and the false discovery rate (FDR) corrected p-value for a comparison between the endemic and nonendemic bonobo field sites. **(b)** Heatmap of OTUs as in **(a)** but for *rbcL* sequences.



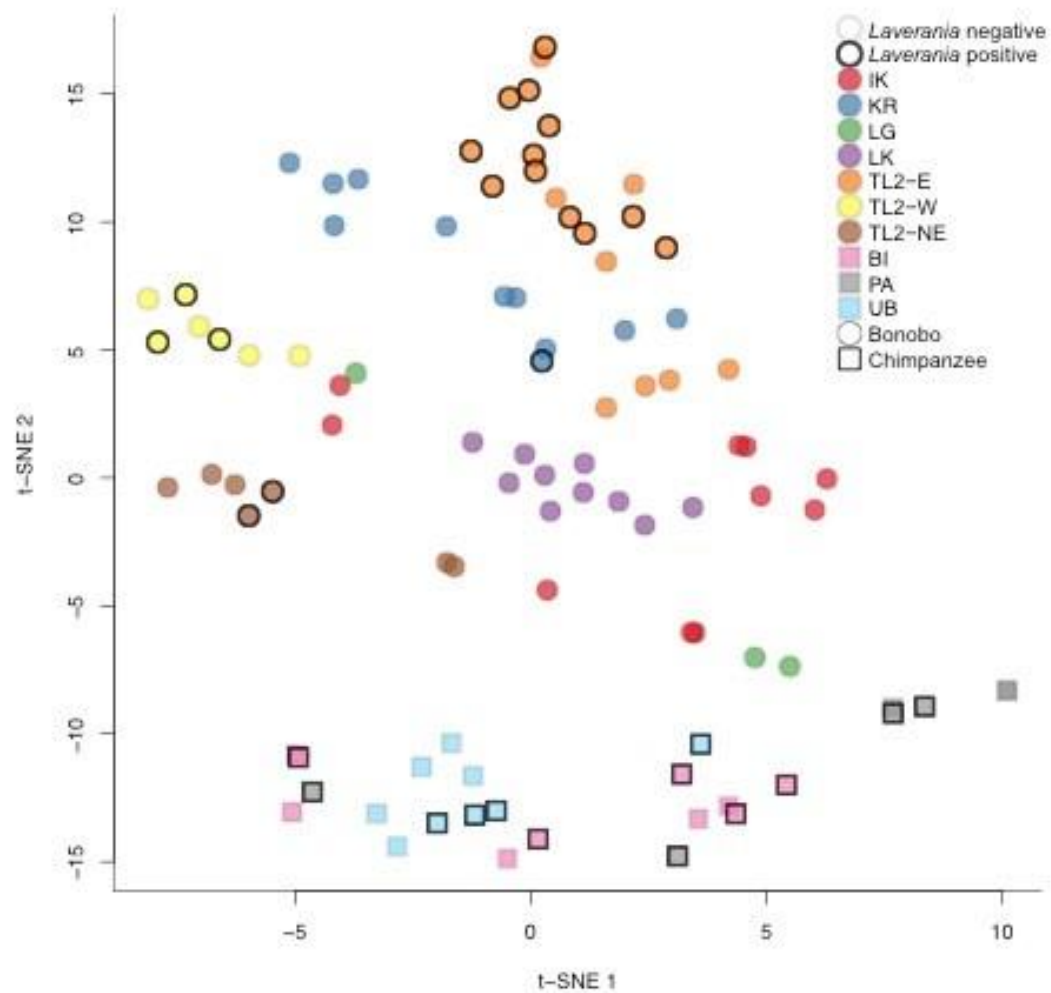


**Supplementary Figure 7 Relative abundance of major bacterial phyla in *Laverania* positive and negative ape faecal samples.** **(a)** A heatmap of operational taxonomic units (OTUs) as determined by 16S rRNA gene sequencing is shown. Each grid entry represents the relative abundance of an OTU (column) within each sample (row). Only OTUs with an abundance of greater than 2% in at least one sample are shown. OTUs are ordered by co-occurrence to emphasise patterns in the data. Samples are labeled by ape species (chimpanzee and bonobo), field site (see Fig. 5b for the location of TL2-W, TL2-E and TL2-NE samples), as well as with a + and – prefix to indicate *Laverania* positive and negative status, respectively (see Supplementary Table 7 for a description of all samples). OTUs are labeled according to the most specific taxonomic rank assigned, with letters indicating order (o), family (f), genus (g), and species (s), followed by an arbitrary ID number. Bacterial taxa that could not be classified are labeled “Unknown”. **(b)** Heatmap of OTUs as in **(a)** but with taxon abundance measured relative to the maximum proportion observed within that OTU (red cells indicate samples with the highest proportional abundance of the corresponding OTU).

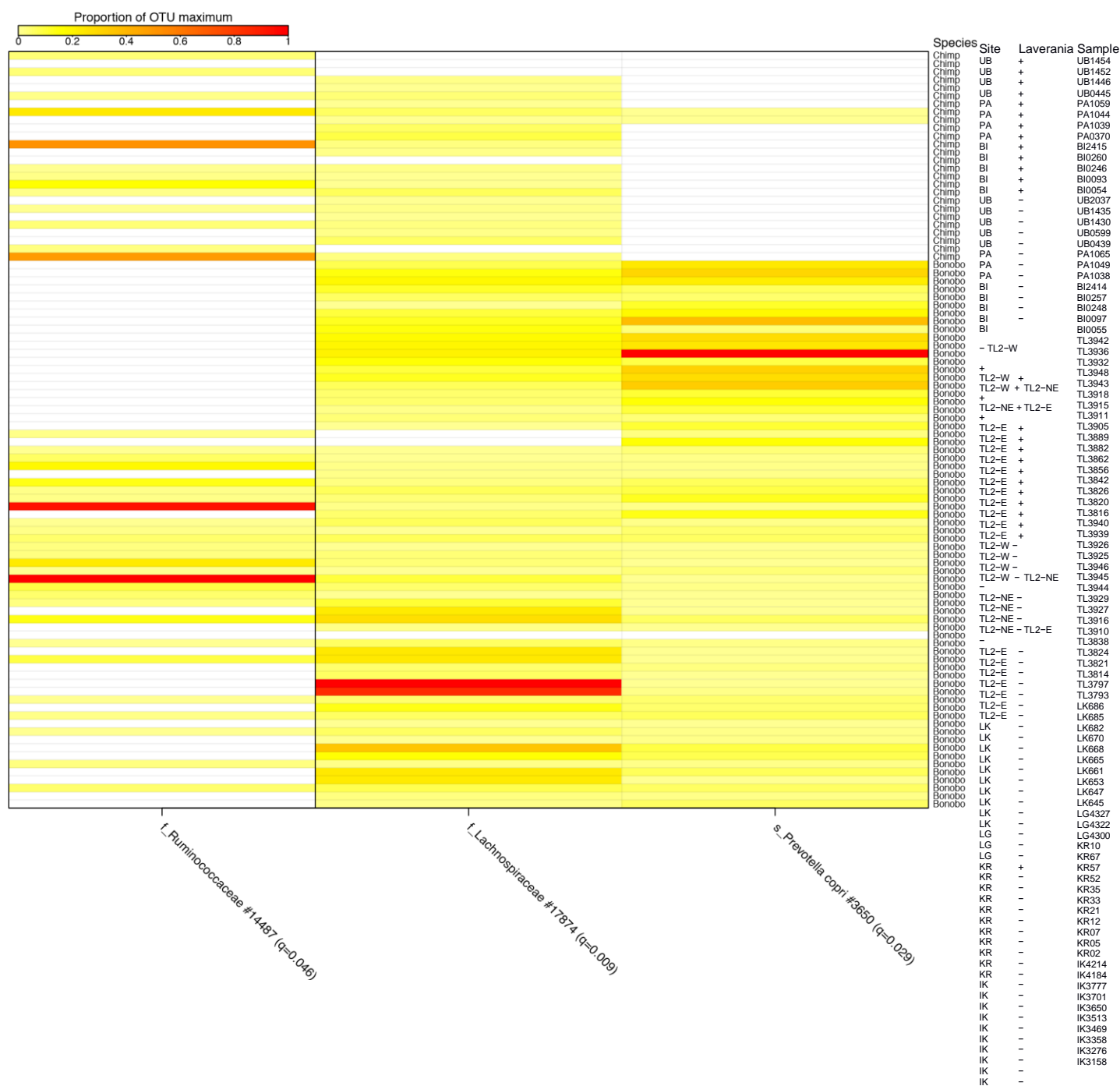
**a****b**



c



**Supplementary Figure 8 Compositional analysis of the faecal microbiome in *Laverania* positive and negative bonobos and chimpanzees.** (a) Analysis of alpha diversity. A comparison of the Shannon diversity for *Laverania* positive and negative faecal samples from bonobos and chimpanzees (left of dashed line), as well as *Laverania* endemic (TL2) and nonendemic (IK, KR, LG, LK) bonobo field sites, and all chimpanzee sites (right of dashed line) is shown. Each point indicates a faecal sample. Horizontal lines indicate the median within each grouping and shaded regions the 95% confidence interval of the median. Note that each sample is shown once to the left and again to the right of the dashed line (see Supplementary Table 7 for a description of all samples). There were no significant differences between the Shannon diversity medians for any of the groups shown. (b) Analysis of beta diversity. The distribution of rarefied unweighted UniFrac distances within and between faecal microbiomes of various groupings of apes is shown ("within non-endemic field sites" shows only comparisons between samples from the same field site, while "between non-endemic field sites" shows comparisons between samples from different non-endemic field sites). Boxes indicate the interquartile range of UniFrac distances for that grouping, and whiskers extend to minimum and maximum values. Horizontal lines indicate the median and notches show the 95% confidence interval of the median. Asterisks indicate Wilcoxon rank-sum test p-values <0.01 (\*), p<0.0001 (\*\*) and p<0.000001 (\*\*\*). For comparisons of within- to between-group beta diversity (comparisons between the first and second box in each subset to the third box), a one-sided Wilcoxon test was used to search for larger between-group than within-group diversity. (c) A two-dimensional representation of the unweighted UniFrac distances generated using a t-distributed stochastic neighbor embedding (t-SNE), comparing faecal bacteriomes of bonobos (circles) and chimpanzees (squares) from various study sites (indicated by colour). Faecal samples that tested positive for *Laverania* DNA are circled. The sampling location of groups of TL2 samples labeled TL2-E, TL2-NE and TL2-W are shown in Fig. 5b (sample GPS coordinates are listed in Supplementary Tables 2 and 7).



**Supplementary Figure 9 Enrichment and depletion of bacterial taxa in *Laverania* positive faecal samples from TL2 bonobos.** The abundances of all OTUs with a Benjamini-Hochberg corrected p-value less than 0.05 for a Wilcoxon rank sum test between *Laverania* positive and negative faecal samples of TL2 bonobos are shown. Each grid entry represents the abundance of an OTU (column) within a sample (row) measured relative to the maximum proportional abundance observed within that OTU. Wilcoxon rank sum tests were performed only for samples from TL2, but all other bonobo and chimpanzee samples are shown for comparison. Samples are labeled by ape species (chimpanzee and bonobo), field site (see Fig. 5b for the location of TL2W, TL2-E and TL2-NE samples), as well as with a + and – prefix to indicate *Laverania* positive and negative status (see Supplementary Table 7 for a description of all samples). OTU names are assigned as their most specific taxonomic classification, with a letter representing taxonomic rank (f, family; s, species) and an arbitrary ID number. The false discovery rate (FDR)-corrected p-value for each OTU is shown in parenthesis.

**Supplementary Table 1. Intensified PCR of bonobo and chimpanzee faecal samples**

Sample <sup>a</sup>	Host	Date (m/d/y)	Number of replicates	Intensified <i>cytB</i> PCR	
				Number of positives	Distinguishable <i>cytB</i> haplotypes
TL2.3888 (ID04)	<i>P. paniscus</i>	12/12/12	8	1	1
TL2.3843 (ID05)	<i>P. paniscus</i>	11/26/12	8	1	1
TL2.3812 (ID06)	<i>P. paniscus</i>	11/19/12	8	3	1
TL2.3846 (ID15)	<i>P. paniscus</i>	11/26/12	10	3	1
TL2.3882 (ID15)	<i>P. paniscus</i>	12/12/12	8	2	1
TL2.3826 (ID18)	<i>P. paniscus</i>	11/19/12	8	1	1
TL2.3866 (ID18)	<i>P. paniscus</i>	11/28/12	8	1	1
TL2.3874 (ID18)	<i>P. paniscus</i>	11/28/12	8	1	1
TL2.3873 (ID20)	<i>P. paniscus</i>	11/28/12	8	1	1
TL2.3842 (ID27)	<i>P. paniscus</i>	11/26/12	8	5	2
TL2.3856 (ID43)	<i>P. paniscus</i>	11/28/12	8	2	2
TL2.3862 (ID46)	<i>P. paniscus</i>	11/28/12	10	2	1
TL2.3943 (ID49)	<i>P. paniscus</i>	02/13/13	8	1	1
TL2.3918 (ID50)	<i>P. paniscus</i>	01/11/13	8	2	1
TL2.3931 (ID60)	<i>P. paniscus</i>	02/15/13	10	1	1
TL2.3936 (ID61)	<i>P. paniscus</i>	02/15/13	8	1	1
TL2.3942 (ID63)	<i>P. paniscus</i>	02/15/13	8	1	1
KRpp10 (ID28)	<i>P. paniscus</i>	10/21/06	8	1	1
Blpts54	<i>P. t. schweinfurthii</i>	03/15/03	8	2	2
Blpts67	<i>P. t. schweinfurthii</i>	n/a	8	4	2
Blpts93	<i>P. t. schweinfurthii</i>	03/15/03	8	3	2
Blpts260	<i>P. t. schweinfurthii</i>	07/25/05	8	2	2
ENpts4388	<i>P. t. schweinfurthii</i>	03/18/16	8	1	1
KSpts201	<i>P. t. schweinfurthii</i>	12/15/04	8	2	2
LUpts2029	<i>P. t. schweinfurthii</i>	06/30/07	8	1	1
LUpts2084	<i>P. t. schweinfurthii</i>	08/20/07	8	2	2
PApts75	<i>P. t. schweinfurthii</i>	05/27/03	8	1	1
PApts1039	<i>P. t. schweinfurthii</i>	09/12/06	8	1	1
PApts1040	<i>P. t. schweinfurthii</i>	09/12/06	8	1	1
PApts1041	<i>P. t. schweinfurthii</i>	09/12/06	8	2	2
PApts1042	<i>P. t. schweinfurthii</i>	09/12/06	8	2	2
PApts1044	<i>P. t. schweinfurthii</i>	09/12/06	8	2	2
PApts1053	<i>P. t. schweinfurthii</i>	09/15/06	8	1	1
PApts1054	<i>P. t. schweinfurthii</i>	09/15/06	8	4	1
PApts1056	<i>P. t. schweinfurthii</i>	09/15/06	8	2	2
PApts1058	<i>P. t. schweinfurthii</i>	12/02/06	8	1	1
PApts1059	<i>P. t. schweinfurthii</i>	12/02/06	8	2	2
PApts1060	<i>P. t. schweinfurthii</i>	12/02/06	8	1	1
PApts1061	<i>P. t. schweinfurthii</i>	12/02/06	8	1	1
PApts1062	<i>P. t. schweinfurthii</i>	12/02/06	8	1	1
PApts1064	<i>P. t. schweinfurthii</i>	12/06/06	8	1	1
WApts01	<i>P. t. schweinfurthii</i>	02/22/03	8	6	1
WApts07	<i>P. t. schweinfurthii</i>	n/a	8	1	1
WApts41	<i>P. t. schweinfurthii</i>	03/03	8	2	2
WApts394	<i>P. t. schweinfurthii</i>	12/24/05	8	2	1
WApts396	<i>P. t. schweinfurthii</i>	12/24/05	8	1	1
WApts397	<i>P. t. schweinfurthii</i>	12/04/05	8	6	4
WApts467	<i>P. t. schweinfurthii</i>	03/03/06	8	1	1
WApts469	<i>P. t. schweinfurthii</i>	03/04/06	8	1	1
WApts520	<i>P. t. schweinfurthii</i>	03/19/06	8	1	1
WApts522	<i>P. t. schweinfurthii</i>	03/20/06	8	1	1
WApts527	<i>P. t. schweinfurthii</i>	03/21/06	8	2	2
WApts529	<i>P. t. schweinfurthii</i>	03/24/06	8	1	1
WApts530	<i>P. t. schweinfurthii</i>	03/24/06	8	1	1
WApts531	<i>P. t. schweinfurthii</i>	03/24/06	8	2	2
WApts548	<i>P. t. schweinfurthii</i>	03/29/06	8	2	2
WApts555	<i>P. t. schweinfurthii</i>	03/30/06	8	1	1
WApts561	<i>P. t. schweinfurthii</i>	03/30/06	8	1	1
WLpts99	<i>P. t. schweinfurthii</i>	02/27/04	8	1	1
WLpts103	<i>P. t. schweinfurthii</i>	03/01/04	8	2	2
WLpts104	<i>P. t. schweinfurthii</i>	03/03/04	8	1	1
WLpts120	<i>P. t. schweinfurthii</i>	04/26/04	8	4	1
WLpts125	<i>P. t. schweinfurthii</i>	04/29/04	8	1	1
WLpts128	<i>P. t. schweinfurthii</i>	04/29/04	8	1	1



<sup>a</sup>Only samples that were found negative by conventional *cytB* PCR were subjected to intensified PCR, which entailed testing 810 aliquots of the same DNA preparation.

Sample <sup>a</sup>	Date (m/d/y)	Collection location	<i>cytB</i> <sup>b</sup>		3.4kb <sup>b</sup>		3.3kb <sup>b</sup>		<i>eba165</i> <sup>b</sup>		<i>eba175</i> <sup>b</sup>		<i>p47</i> <sup>b</sup>		<i>clpM</i> <sup>b</sup>		int PCR <i>cox1</i> <sup>c</sup>		
			No. (hap) <sup>d</sup>	<i>P.</i> <i>spp.</i> <sup>e</sup>	No. (hap) <sup>d</sup>	<i>P.</i> <i>spp.</i> <sup>e</sup>	No. (hap) <sup>d</sup>	<i>P.</i> <i>spp.</i> <sup>e</sup>	No. (hap) <sup>d</sup>	<i>P.</i> <i>spp.</i> <sup>e</sup>	No. (hap) <sup>d</sup>	<i>P.</i> <i>spp.</i> <sup>e</sup>	No. (hap) <sup>d</sup>	<i>P.</i> <i>spp.</i> <sup>e</sup>	No. (hap) <sup>d</sup>	<i>P.</i> <i>spp.</i> <sup>e</sup>	No (hap) <sup>d</sup>	<i>P.</i> <i>spp.</i> <sup>e</sup>	
TL2.3888 (ID04)*	12/12/12	TL2-E	5 (2)	B1, C2												1 (1)	B1		
TL2.3843 (ID05)*	11/26/12	TL2-E	7 (4)	B1, C2												1 (1)	B1		
TL2.3812 (ID06)*	11/19/12	TL2-E	3 (1)	B1												1 (1)	Pv-like	1 (1)	Pv-like
TL2.3905 (ID06)	11/26/12	TL2-E	3 (2)	B1, C2							1 (1)	B1				1 (1)	C2		
TL2.3911 (ID07)	01/08/13	TL2-E	9 (3)	B1, C2	1 (1)	B1	4 (4)	B1, C2	4 (4)	B1, C2	13 (9)	C1, B1, C2	1 (1)	B1		2 (2)	B1, C2		
TL2.3912 (ID07)	01/08/13	TL2-E	2 (1)	B1	1 (1)	B1			2 (2)	B1, C2						3 (3)	B1, C2		
TL2.3870 (ID13)	11/28/12	TL2-E	14 (8)	B1, C2	2 (2)	B1	2 (2)	B1, C2	1 (1)	B1						2 (2)	B1, C2		
TL2.3846 (ID15)*	11/26/12	TL2-E	3 (1)	B1															
TL2.3882 (ID15)*	12/12/12	TL2-E	2 (1)	B1												3 (2)	B1, C2		
TL2.3826 (ID18)*	11/19/12	TL2-E	3 (2)	B1, C2															
TL2.3866 (ID18)*	11/28/12	TL2-E	3 (2)	B1, C2												1 (1)	B1		
TL2.3874 (ID18)*	11/28/12	TL2-E	1 (1)	B1												1 (1) <sup>f</sup>	Pv-like	1 (1)	Po-like
TL2.3853 (ID20)	11/21/12	TL2-E																1 (1)	Pv-like
TL2.3873 (ID20)*	11/28/12	TL2-E	2 (2)	B1, C2															
TL2.3816 (ID24)	11/19/12	TL2-E	10 (3)	B1, C2	4 (4)	B1, C2	3 (2)	B1	2 (2)	B1	2 (1)	B1				3 (2)	B1, C2		
TL2.3834 (ID24)	11/26/12	TL2-E	8 (4)	B1, C2	3 (2)	B1, C2	1 (1)	B1			3 (3)	B1, C2				3 (3)	B1, C2		
TL2.3850 (ID24)	12/12/12	TL2-E	7 (3)	B1, C2	2 (1)	C2	5 (4)	B1, C2								1 (1)	B1		
TL2.3948 (ID25)	02/13/13	TL2-NE	7 (2)	B1, C2	7 (4)	B1, C2	1 (1)	B1								5 (1)	B1		
TL2.3842 (ID27)*	11/26/12	TL2-E	9 (2)	B1, C2												1 (1)	Pv-like		
TL2.3889 (ID33)	12/12/12	TL2-E	1 (1)	B1										2 (2)	B1				
TL2.3884 (ID37)	11/26/12	TL2-E	5 (1)	C2							1 (1)	C2				1 (1)	C2		
TL2.3833 (ID39)	11/19/12	TL2-E	2 (2)	C2	1 (1)	B1	1 (1)	B1								1 (1)	C2		
TL2.3915 (ID41)	01/08/13	TL2-E	4 (2)	B1, C2					2 (2)	B1				1 (1)	C2	1 (1)	C2		
TL2.3856 (ID43)*	11/28/12	TL2-E	2 (2)	B1, C2												1 (1)	C2		
TL2.3820 (ID45)	11/19/12	TL2-E	12 (7)	B1, C2	6 (3)	B1	5 (3)	B1						1 (1)	B1	1 (1)	B1		
TL2.3903 (ID45)	12/13/12	TL2-E	2 (1)	C2												3 (3)	B1, C2		
TL2.3862 (ID46)*	11/28/12	TL2-E	10 (4)	B1, C2, Pm-related															

TL2.3918 (ID50)*	01/11/13	TL2-E	4 (2)	B1				1 (1)	B1
TL2.3931 (ID60)*	02/15/13	TL2-W	3 (2)	B1, C2				3 (2)	B1, C2
TL2.3932 (ID60)	02/15/13	TL2-W	5 (2)	B1, C2	2 (2)	B1, C2			
TL2.3936 (ID61)*	02/15/13	TL2-W	2 (2)	B1, C2				1 (1)	B1
TL2.3942 (ID63)*	02/15/13	TL2-W	6 (2)	B1, C2				1 (1)	B1
KRpp10 (ID28)*	10/21/06	KR	3 (1)	B1				2 (1)	B1

<sup>a</sup> Samples are labeled to indicate their field site of origin (TL2 and KR; see Figs. 1 and 5b for location) followed by an individual (ID) number as determined by microsatellite analysis at 8 polymorphic loci . Asterisks indicate *Laverania* positive samples that were identified by intensified PCR.

<sup>b</sup> Single genome amplified loci of *Plasmodium* mitochondrial (*cytB*, 3.4 kb, 3.3 kb), nuclear (*eba165*, *eba175* and *p47*) and apicoplast (*clpM*) genes. For samples TL2.3812, TL2.3846, TL2.3856, TL2.3873, TL2.3874, TL2.3882 and TL2.3943, *cytB* sequences were derived from the intensified PCR screen. All of the respective sequences lacked double peaks, indicating that they were single template-derived.

<sup>c</sup> int PCR, intensified PCR targeting a 296 bp mitochondrial *cox1* fragment using *P. vivax*-specific primers.

<sup>d</sup> No., number of single template derived sequences (SGA or intensified PCR), with brackets indicating the number of distinguishable haplotypes (hap). See Supplementary Table 9 for GenBank accession numbers.

<sup>e</sup> *Plasmodium* species present in the faecal sample: B1, *P. lomamiensis*; C1, *P. reichenowi*; C2, *P. gaboni*; Pm-related, *P. malariae*-related; Po-like, *P. ovale*-like; Pv-like, *P. vivax*-like.

<sup>f</sup> Obtained using *P. vivax*-specific *clpM* primers as previously described .

**Supplementary Table 3. Faecal based screening of eastern chimpanzees for *Laverania* infections**

Field Sites <sup>b</sup>	Conventional <i>cytB</i> screen			Intensified <i>cytB</i> screen <sup>a</sup>			Combined
	Samples	Samples	Detection rate (%)	Samples	Samples	Detection rate (%)	tested <sup>c</sup> positive <sup>d</sup> rate (%)
Amunyala (AM)	37	0	0	23 <sup>e</sup>	0	0	0
Azunu (AZ)	31	0	0	31	0	0	0
Babingi (BI)	96	7	7.3	89	4	4.5	11.5
Engali (EN)	26	0	0.0	26	1	3.8	3.8
Kisangani (KS)	11	0	0.0	11	1	9.1	9.1
Lubutu (LU)	131	10	7.6	117 <sup>e</sup>	2	1.7	9.4
Parisi (PA)	77	10	13.0	67	15	22.4	32.5
Wanie-rukula (WA)	134	13	9.7	121	17	14.0	22.4
Walengola (WL)	37	5	13.5	32	6	18.8	29.7

<sup>a</sup> Samples initially negative in the conventional (diagnostic) *cytB* screen were subsequently tested by intensified PCR, performing 8 to 10 independent amplification reactions per faecal DNA (see Supplementary Table 1 for details). <sup>b</sup> Field sites are designated by a two-letter code (their location is shown in Fig. 1).

<sup>c</sup> The host species origin of all faecal samples was confirmed by mitochondrial DNA (D loop) analysis; for most of these sites, regular *cytB* screening results have previously been reported<sup>7</sup>. <sup>d</sup> All amplification products were sequence confirmed to represent *Laverania* parasites (see Supplementary Table 4).

<sup>e</sup> Only a subset of the originally screened AM and LU samples was available for intensified PCR.

**Supplementary Table 4. *Laverania* species in eastern chimpanzee faecal samples collected most proximal to the bonobo range**

No.	Sample		Collection		<i>P. t. schweinfurthii</i>		<i>cytB</i> PCR <sup>d</sup>	
	code <sup>a</sup>		date <sup>b</sup>		mtDNA haplotype <sup>c</sup>		No. (hap) <sup>e</sup>	<i>P. spp.</i> <sup>f</sup>
1	Blpts54	03/15/03		DQ370342	2 (2)*	C2		
2	Blpts67	n/a		DQ370345	4 (2)*	C2		
3	Blpts93	03/15/03		DQ370346	2 (2)*	C2		
4	Blpts244	05/16/05		DQ370333	1 (1)	C2		
5	Blpts245	05/17/05		DQ370333	1 (1)	C2		
6	Blpts246	05/19/05		DQ370333	1 (1)	C2		
7	Blpts253	07/10/05		JQ866111	1 (1)	C2		
8	Blpts260	07/25/05		JQ866111	2 (2)*	C2		
9	Blpts266	07/27/05		JQ866111	1 (1)	C2		
10	Blpts2415		04/21/07	EU527448	2 (2)	C2		
11	Blpts2416		04/21/07	EU527448	1 (1)	C2		
12	ENpts4388		03/18/16	JQ866157	1 (1)*	C1		
13	KSpts201	12/15/04		JQ866156	2 (2)*	C2		
14	LUpts2029		06/30/07	JQ866180	1 (1)*	C1		
15	LUpts2067		08/09/07	JQ866096	1 (1)	C2		
16	LUpts2069		08/09/07	DQ370340	1 (1)	C2		
17	LUpts2070		08/09/07	DQ370342	1 (1)	C2		
18	LUpts2071		08/13/07	DQ370342	7 (4)	C2		
19	LUpts2072		08/13/07	DQ370342	1 (1)	C2		
20	LUpts2073		08/13/07	JQ866096	7 (3)	C1, C2		
21	LUpts2074		08/15/07	JQ866096	1 (1)	C2		
22	LUpts2078		08/15/07	DQ370342	1 (1)	C2		
23	LUpts2079		08/15/07	JQ866096	1 (1)	C2		
24	LUpts2084		08/20/07	DQ370332	2 (2)*	C1, C2		
25	LUpts2089		08/20/07	DQ370332	1 (1)	C3		
26	PApts75	05/27/03		DQ370340	1 (1)*	C1		
27	PApts369	01/04/06		JQ866214	1 (1)	C1		
28	PApts370	01/04/06		JQ866214	4 (2)	C1, C2		
29	PApts1039		09/12/06	JQ866206	1 (1)*	C3		
30	PApts1040		09/12/06	JQ866206	1 (1)*	C2		
31	PApts1041		09/12/06	JQ866206	2 (2)*	C1, C3		
32	PApts1042		09/12/06	JQ866206	2 (2)*	C1, C3		
33	PApts1043		09/12/06	JQ866206	1 (1)	C1		
34	PApts1044		09/12/06	JQ866205	2 (2)*	C2, C3		
35	PApts1046		09/15/06	JQ866205	3 (3)	C2, C3		
36	PApts1047		09/15/06	JQ866205	3 (3)	C2, C3		
37	PApts1048		09/15/06	JQ866205	2 (2)	C3		
38	PApts1052		09/15/06	JQ866205	4 (3)	C2, C3		
39	PApts1053		09/15/06	JQ866205	1 (1)*	C1		
40	PApts1054		09/15/06	JQ866205	3 (1)*	C2		
41	PApts1056		09/15/06	JQ866205	2 (2)*	C1, C2		
42	PApts1058		12/02/06	JQ866206	1 (1)*	C1		
43	PApts1059		12/02/06	JQ866206	2 (2)*	C1, C2		
44	PApts1060		12/02/06	JQ866206	1 (1)*	C3		
45	PApts1061		12/02/06	JQ866206	1 (1)*	C3		
46	PApts1062		12/02/06	JQ866206	1 (1)*	C1		
47	PApts1063		12/02/06	JQ866206	2 (2)	C2		
48	PApts1064		12/06/06	JQ866206	1 (1)*	C3		
49	PApts3143		12/12/10	JQ866211	1 (1)	C2		

50	PApts3146	12/13/10	JQ866211	4 (4)	C1, C2
51	WApts1	02/22/03	DQ370332	5 (1)*	C3
52	WApts2	02/22/03	DQ370332	5 (2)	C2, C3
53	WApts7	n/a	DQ370334	1 (1)*	C1
54	WApts21	n/a	DQ370342	3 (3)	C2
55	WApts22	n/a	DQ370342	2 (2)	C1, C2
56	WApts41	03/03	EU527448	2 (2)*	C3
57	WApts392	12/24/05	JQ866254	6 (3)	C2
58	WApts393	12/24/05	JQ866254	6 (3)	C2
59	WApts394	12/24/05	JQ866247	1 (1)*	C2
60	WApts395	12/24/05	JQ866247	1 (1)	C2
61	WApts396	12/24/05	JQ866247	1 (1)*	C2
62	WApts397	12/04/05	JQ866254	5 (4)*	C2
63	WApts398	12/04/05	JQ866247	1 (1)	C1
64	WApts399	12/04/05	JQ866247	5 (2)	C2
65	WApts467	03/03/06	UE527409	1 (1)*	C2
66	WApts469	03/04/06	UE527409	1 (1)*	C2
67	WApts513	03/17/06	DQ370336	2 (2)	C1, C2
68	WApts519	03/19/06	DQ370342	2 (2)	C1, C3
69	WApts520	03/19/06	DQ370342	1 (1)*	C1
70	WApts522	03/20/06	DQ370342	1 (1)*	C3
71	WApts523	03/20/06	DQ370342	1 (1)	C3
72	WApts525	03/21/06	DQ370342	2 (1)	C1
73	WApts527	03/21/06	DQ370342	2 (2)*	C1
74	WApts529	03/24/06	DQ370342	1 (1)*	C3
75	WApts530	03/24/06	DQ370342	1 (1)*	C1
76	WApts531	03/24/06	DQ370342	2 (2)*	C1
77	WApts548	03/29/06	JQ866255	2 (2)*	C1, C2
78	WApts555	03/30/06	JQ866257	1 (1)*	C1
79	WApts561	03/30/06	JQ866255	1 (1)*	C1
80	WApts563	03/30/06	JQ866257	1 (1)	C1
81	WLpts99	02/27/04	JQ866203	1 (1)*	C1
82	WLpts101	03/01/04	EU527447	5 (4)	C1, C3
83	WLpts103	03/01/04	EU527450	2 (2)*	C1, C2
84	WLpts104	03/03/04	EU527451	1 (1)*	C3
85	WLpts111	04/16/04	EU527455	2 (1)	C1
86	WLpts113	04/22/04	EU527455	5 (1)	C1
87	WLpts120	04/26/04	EU527455	5 (1)	C1
88	WLpts125	04/29/04	EU527455	1 (1)*	C1
89	WLpts128	04/29/04	EU527455	1 (1)*	C1
90	WLpts131	04/29/04	EU527455	5 (2)	C1, C2
91	WLpts132	04/29/04	EU527455	5 (4)	C1, C2

<sup>a</sup>Samples are labeled to indicate their field site (Fig. 1) and chimpanzee subspecies of origin (pts, *P. t. schweinfurthii*), followed by a number.

<sup>b</sup>Collection dates are listed by month, day and year (m/d/y); n/a, not available.

<sup>c</sup>Faecal samples were subjected to mitochondrial DNA analysis to confirm their host species and subspecies origin.

<sup>d</sup>*cytB* sequences were derived by single genome amplification or intensified PCR. Only single template derived sequences lacking double peaks in sequence chromatograms were included; see Supplementary Table 1 for additional detail.

<sup>e</sup>No., number of SGA or intensified PCR derived sequences (indicated by asterisks), with brackets indicating the number of distinguishable haplotypes (hap); see Supplementary Table 9 for GenBank accession numbers.

<sup>f</sup>Ape *Laverania* species present in the sample: C1, *P. reichenowi*; C2, *P. gaboni*; C3, *P. billcollinsi*.

**Supplementary Table 5. Bonobo mitochondrial haplotypes derived from different collection sites**

Field site <sup>a</sup>	Samples collected	Samples with intact D loop sequence	Number of distinct mtDNA haplotypes	Haplotype designation	GenBank Accession Number
-------------------------	-------------------	-------------------------------------	-------------------------------------	-----------------------	--------------------------

BJ	2	2	1	BJ688	JQ866273
BN	85	84	7	BN3014	JQ866276
				BN3015	JQ866278
				BN3016	JQ866274
				BN3019	JQ866279
				BN3024	JQ866275
				BN3026	JQ866284
				BN3028	JQ866282
BX	1	1	1	BX4799	KY790543 <sup>b</sup>
IK	465	465	8	IK2876	JQ866274
				IK2879	JQ866275
				IK2885	JQ866276
				IK2891	JQ866279
				IK3150	JQ866278
				IK3166	JQ866282
				IK3187	JQ866280
				IK3244	JQ866284
KR	69	69	11	KR01	JQ866274
				KR02	JQ866277
				KR03	JQ866278
				KR05	JQ866282
				KR06	JQ866284
				KR10	JQ866279
				KR23	JQ866280
				KR37	JQ866292
				KR48	JQ866281
				KR66	JQ866283
				KR73	JQ866285
LA	328	307	9	LA4819	KY790544 <sup>b</sup>
				LA4820	JQ866279
				LA4823	KY790545 <sup>b</sup>
				LA4829	KY790546 <sup>b</sup>
				LA4851	KY790547 <sup>b</sup>
				LA7795	JQ866280
				LA7799	JQ866292
				LA7807	KY790548 <sup>b</sup>
				LA8196	JQ866278
LG	25	25	2	LG4300	JQ866292
				LG4314	JQ866280
LK	38	38	8	LK645	JQ866286
				LK646	JQ866287
				LK647	JQ866288
				LK648	JQ866289
				LK650	JQ866290
				LK652	JQ866291
				LK664	JQ866292
				LK673	JQ866293
ML	262	262	6	ML5472	JQ866288
				ML5473	JQ866293
				ML5475	JQ866287

MZ	165	165	3	ML5487	JQ866294
				ML5490	JQ866295
				ML5505	JQ866296
				MZ11574	JQ866293
				MZ11576	JQ866296
TL2	138	138	16	MZ11578	KY790549 <sup>b</sup>
				TL3793	JQ866273
				TL3795	KY790550 <sup>b</sup>
				TL3796	KY790551 <sup>b</sup>
				TL3798	KY790552 <sup>b</sup>
				TL3803	KY790553 <sup>b</sup>
				TL3814	KY790554 <sup>b</sup>
				TL3821	KY790555 <sup>b</sup>
				TL3846	KY790556 <sup>b</sup>
				TL3876	KY790557 <sup>b</sup>
				TL3878	KY790558 <sup>b</sup>
				TL3883	KY790559 <sup>b</sup>
				TL3886	KY790560 <sup>b</sup>
				TL3924	KY790561 <sup>b</sup>
				TL3926	KY790562 <sup>b</sup>
				TL3931	KY790563 <sup>b</sup>
				TL3940	KY790564 <sup>b</sup>

<sup>a</sup>Field sites are labelled by a two- or three-letter code and their location is shown in Fig. 1. <sup>b</sup>New haplotypes derived in this study.





**Supplementary Table 6. Ecological variables at bonobo sampling sites**

Site <sup>a</sup>	<sup>b</sup>			<sup>b</sup>			Forest <sup>c</sup>	<sup>d</sup>		
	Ambient temperature			Daily temperature variation				Rainfall (mm/day)		
	Min	Max	Mean	Min	Max	Mean		Min	Max	Mean
BN	24.5°C	25.9°C	25.2°C	8.1°C	8.6°C	8.4°C	100%	3.0	5.7	4.1
BX	25.1°C	25.1°C	25.1°C	8.9°C	8.9°C	8.9°C	100%	7.1	7.1	7.1
BJ	24.1°C	24.1°C	24.1°C	8.7°C	8.7°C	8.7°C	98%	3.2	3.2	3.2
IK	23.9°C	26.3°C	25.0°C	6.8°C	9.2°C	8.4°C	100%	3.4	6.8	5.1
KR	23.3°C	24.5°C	24.2°C	8.8°C	9.5°C	9.2°C	100%	1.3	7.0	4.4
LG	23.5°C	25.4°C	24.2°C	6.3°C	9.3°C	8.5°C	90%	5.8	5.8	5.8
LA	23.9°C	26.3°C	25.3°C	7.1°C	9.3°C	8.3°C	93%	5.7	8.8	6.7
LK	24.8°C	25.9°C	25.3°C	9.2°C	9.6°C	9.3°C	100%	3.2	5.7	3.8
ML	25.0°C	26.3°C	25.7°C	9.0°C	9.8°C	9.2°C	47%	2.4	6.9	4.3
MZ	24.6°C	25.7°C	24.9°C	8.4°C	10.0°C	9.5°C	55%	0.7	7.0	3.0
TL2	22.2°C	25.0°C	23.8°C	8.3°C	10.3°C	8.7°C	100%	4.5	8.6	7.4

<sup>a</sup>Field sites are designated by a two-letter code (their location is shown in Fig. 1).

<sup>b</sup>

Mean ambient temperature and daily temperature fluctuation were derived from MODIS LST datasets after applying minimum and maximum air temperature transformations<sup>10</sup>. Each metric was calculated as the average of temperature estimates recorded during the 30 days prior to sample collection.

<sup>c</sup>

Forest cover was derived from high resolution maps of global forest cover .

<sup>d</sup>

Rainfall measurements were derived from the Global Precipitation Climatology Project (GPCP V2.3) at monthly temporal resolution. We used rainfall estimates corresponding to the month during which each sample was collected.

8,9

11

12

Supplementary Table 7. Analysis of plant and microbiome constituents in *Laverania* positive and negative ape faecal samples

Collection			mtDNA		GPS Coordinates									
date								<i>matK</i>		<i>rbcL</i>		16S rRNA		<i>Laverania</i>
No.	Sample	mm/dd/yy	Species	Haplotype <sup>a</sup>	Latitude	Longitude	Filtered <sup>b</sup>	Filtered <sup>b</sup>	Filtered <sup>b</sup>	<i>cytB</i> code	reads	reads	reads	
1	TL2.3793	10/09/12	<i>P. p.</i>	JQ866273	S2.71434°	E025.13563°	7947	15360	20998	neg				
2	TL2.3797	10/09/12	<i>P. p.</i>	JQ866273	S2.71464°	E025.13543°	5722	20919	94860	neg				
3	TL2.3814	11/19/12	<i>P. p.</i>	KY790554	S2.73634°	E025.11536°	23741	23378	119333	neg				
4	TL2.3816	11/19/12	<i>P. p.</i>	KY790552	S2.73634°	E025.11536°	22541	18222	76728	pos				
5	TL2.3820	11/19/12	<i>P. p.</i>	KY790554	S2.69626°	E025.13756°	15980	12506	62538	pos	6	TL2.3821		
		11/19/12	<i>P. p.</i>	KY790555	S2.69672°	E025.13752°	10483	18662	45145	neg				

7	<b>TL2.3824</b>	11/19/12	<i>P. p.</i>	KY790552	S2.69673°	E025.13754°	14012	24745	54876	neg
8	<b>TL2.3826</b>	11/19/12	<i>P. p.</i>	KY790552	S2.69610°	E025.13711°	27873	17856	44839	<b>pos</b>
9	<b>TL2.3838</b>	11/26/12	<i>P. p.</i>	KY790555	S2.69751°	E025.13761°	17244	20513	79467	neg
10	<b>TL2.3842</b>	11/26/12	<i>P. p.</i>	KY790555	S2.69776°	E025.13740°	16785	25140	73647	<b>pos</b>
11	<b>TL2.3856</b>	11/28/12	<i>P. p.</i>	KY790554	S2.69353°	E025.13725°	17809	26893	51001	<b>pos</b>
12	<b>TL2.3862</b>	11/28/12	<i>P. p.</i>	KY790554	S2.69321°	E025.13744°	16211	29616	47867	<b>pos</b>
13	<b>TL2.3882</b>	12/12/12	<i>P. p.</i>	KY790556	S2.67151°	E025.14455°	8264	18803	85344	<b>pos</b>
14	<b>TL2.3889</b>	12/12/12	<i>P. p.</i>	KY790553	S2.67129°	E025.14424°	17953	15526	78724	<b>pos</b>
15	<b>TL2.3905</b>	11/26/12	<i>P. p.</i>	JQ866273	S2.69218°	E025.13.760°	9894	19656	61606	<b>pos</b> 16 <b>TL2.3910</b>
	10/09/12	<i>P. p.</i>	JQ866273	S2.71429°	E025.13545°	8892	20340	52017	neg	
17	<b>TL2.3911</b>	01/08/13	<i>P. p.</i>	JQ866273	S 2.71764°	E25.13718°	6004	20126	47547	<b>pos</b>
18	<b>TL2.3915</b>	01/08/13	<i>P. p.</i>	KY790554	S 2.71777°	E25.13698°	12350	24011	98946	<b>pos</b> 19 <b>TL2.3916</b>
	01/11/13	<i>P. p.</i>	KY790550	S 2.73126°	E25.14773°	4	14324	75531	neg	
20	<b>TL2.3918</b>	01/11/13	<i>P. p.</i>	KY790557	S 2.73117°	E25.14776°	5461	6455	97977	<b>pos</b> 21 <b>TL2.3925</b> 02/14/13 <i>P. p.</i> KY790561 S2.73794° E25.08592° 17959
	13637	60840	neg							
22	<b>TL2.3926</b>	02/14/13	<i>P. p.</i>	KY790562	S2.73790°	E25.08533°	14300	17784	52793	neg
23	<b>TL2.3927</b>	02/13/13	<i>P. p.</i>	JQ866273	S2.46740°	E25.10224°	7431	4185	31964	neg
24	<b>TL2.3929</b>	02/13/13	<i>P. p.</i>	KY790558	S2.46748°	E25.10211°	9298	8936	43821	neg
25	<b>TL2.3932</b>	02/15/13	<i>P. p.</i>	KY790563	S2.73758°	E25.08219°	103020	16768	85037	<b>pos</b>
26	<b>TL2.3936</b>	02/15/13	<i>P. p.</i>	KY790563	S2.73733°	E25.08259°	8064	5543	58927	<b>pos</b>
27	<b>TL2.3939</b>	02/15/13	<i>P. p.</i>	KY790563	S2.73741°	E25.08270°	8503	21353	60304	neg
28	<b>TL2.3940</b>	02/15/13	<i>P. p.</i>	KY790564	S2.73773°	E25.08260°	4968	15543	62308	neg
29	<b>TL2.3942</b>	02/15/13	<i>P. p.</i>	KY790564	S2.73769°	E25.08246°	38565	13599	61839	<b>pos</b>
30	<b>TL2.3943</b>	02/13/13	<i>P. p.</i>	KY790557	S2.46743°	E25.10205°	27889	14550	72265	<b>pos</b>
31	<b>TL2.3944</b>	02/13/13	<i>P. p.</i>	KY790556	S2.46740°	E25.10197°	27335	2675	76918	neg
32	<b>TL2.3945</b>	02/13/13	<i>P. p.</i>	KY790560	S2.46741°	E25.10191°	29458	11265	42629	neg
33	<b>TL2.3946</b>	02/13/13	<i>P. p.</i>	KY790560	S2.46726°	E25.10183°	19068	8706	42537	neg
34	<b>TL2.3948</b>	02/13/13	<i>P. p.</i>	KY790555	S2.47118°	E25.08098°	28899	9829	46888	<b>pos</b>
35	<b>KR02</b>	09/28/06	<i>P. p.</i>	JQ866277	n/a	n/a	14646	21960	83123	neg
36	<b>KR05</b>	09/29/06	<i>P. p.</i>	JQ866282	n/a	n/a	4771	2036	81899	neg
37	<b>KR07</b>	10/21/06	<i>P. p.</i>	JQ866278	n/a	n/a	26741	33636	115307	neg 38 <b>KR10</b> 10/21/06 <i>P. p.</i> JQ866279 n/a n/a 21173 20332 59075 <b>pos</b>
39	<b>KR12</b>	10/28/06	<i>P. p.</i>	JQ866278	n/a	n/a	9687	25001	89109	neg
40	<b>KR21</b>	11/07/06	<i>P. p.</i>	JQ866274	n/a	n/a	15947	22351	54062	neg
41	<b>KR33</b>	12/06/06	<i>P. p.</i>	JQ866274	n/a	n/a	17148	20767	50734	neg
42	<b>KR35</b>	12/07/06	<i>P. p.</i>	JQ866282	n/a	n/a	23884	25620	76542	neg
43	<b>KR52</b>	12/19/06	<i>P. p.</i>	JQ866280	n/a	n/a	27954	12586	64347	neg

44	<b>KR57</b>	12/19/06	<i>P. p.</i>	JQ866278	n/a	n/a	7079	12881	24998	neg	
45	<b>KR67</b>	01/04/07	<i>P. p.</i>	JQ866279	n/a	n/a	9515	39674	126801	neg	
46	<b>IK3158</b>	03/21/11	<i>P. p.</i>	JQ866275	S01°11.200'	E023°44.790'	13214	28956	44740	neg	
47	<b>IK3276</b>	03/21/11	<i>P. p.</i>	JQ866282	S01°06'41.2"	E023°36'55.4"	31517	26904	50873	neg	
48	<b>IK3358</b>	04/11/11	<i>P. p.</i>	JQ866275	S01°07'47"	E023°37'25"	13822	33260	42949	neg	
49	<b>IK3469</b>	07/07/11	<i>P. p.</i>	JQ866278	S01°07.724	E023°41.576	22060	26309	114142	neg	
50	<b>IK3513</b>	07/09/11	<i>P. p.</i>	JQ866279	S01°07'03.4"	E023°38'34.4	23806	34224	74192	neg	
51	<b>IK3650</b>	12/14/11	<i>P. p.</i>	JQ866276	S01°07'38.3"	E023°37'30.6"	23584	20059	43577	neg	
52	<b>IK3701</b>	12/20/11	<i>P. p.</i>	JQ866274	S01°08.677'	E023°41.501'	33665	37953	127273	neg	
53	<b>IK3777</b>	01/05/12	<i>P. p.</i>	JQ866280	S01°07.390"	E023°37.308	11927	35568	36793	neg	
54	<b>IK4184</b>	10/18/14	<i>P. p.</i>	JQ866282	S01°07'43.7"	E023°39'49.9"	13565	18817	38340	neg	55 <b>IK4214</b> 11/27/14 <i>P. p.</i> JQ866282 S01°09'19.7" E023°37'10.2" 394 12082 116207 neg
56	<b>LG4300</b>	12/14/15	<i>P. p.</i>	JQ866292	N 00°33'21.4"	E20°45'39.2"	15492	19342	28653	neg	
57	<b>LG4314</b>	12/15/15	<i>P. p.</i>	JQ866280	N 00°33'21.4" "	E20°45'39.2"	14440	41723	2035	neg	
58	<b>LG4322</b>	12/20/15	<i>P. p.</i>	JQ866292	N 00°34'50.7"	E20°47'51.2"	16035	233	74266	neg	
59	<b>LG4327</b>	01/08/16	<i>P. p.</i>	JQ866280	N 00°34'50.7"	E20°47'51.2"	22440	40332	61003	neg	
60	<b>LK645</b>	03/24/06	<i>P. p.</i>	JQ866286	n/a	n/a	16112	24076	85344	neg	
61	<b>LK647</b>	03/28/06	<i>P. p.</i>	JQ866288	n/a	n/a	24322	17476	101494	neg	
62	<b>LK653</b>	04/06/06	<i>P. p.</i>	JQ866287	n/a	n/a	23559	29513	96049	neg	
63	<b>LK661</b>	05/05/06	<i>P. p.</i>	JQ866290	n/a	n/a	12913	39493	109686	neg	
64	<b>LK665</b>	05/11/06	<i>P. p.</i>	JQ866291	n/a	n/a	30148	31452	47672	neg	
65	<b>LK668</b>	05/11/06	<i>P. p.</i>	JQ866292	n/a	n/a	17831	28287	36821	neg	
66	<b>LK670</b>	05/11/06	<i>P. p.</i>	JQ866286	n/a	n/a	23314	23285	104503	neg	
67	<b>LK682</b>	05/19/06	<i>P. p.</i>	JQ866289	n/a	n/a	17084	3631	72794	neg	68 <b>LK685</b> 05/19/06 <i>P. p.</i>
		JQ866287	n/a	n/a	6461	5684	54426	neg			
69	<b>LK686</b>	05/24/06	<i>P. p.</i>	JQ866289	n/a	n/a	6786	6640	72085	neg	
70	<b>BI0054</b>	03/15/03	<i>P. t. s.</i>	DQ370342	n/a	n/a	20681	47084	68351	pos	71 <b>BI0055</b> 03/15/03
		<i>P. t. s.</i>	DQ370346	n/a	n/a	16785	8170	63608	neg	72 <b>BI0093</b> 03/15/03 <i>P. t. s.</i> DQ370346	
		n/a	n/a	6138	24965	69915	pos	73 <b>BI0097</b> 04/25/03	<i>P. t. s.</i>	DQ370347	n/a n/a 18241
		19367	42972	neg	74 <b>BI0246</b> 05/19/05	<i>P. t. s.</i>	DQ370333	n/a	n/a	14555	43796 17592 pos
75	<b>BI0248</b>	07/08/05	<i>P. t. s.</i>	JQ866111	n/a	n/a	22069	27501	47217	neg	
76	<b>BI0257</b>	07/14/05	<i>P. t. s.</i>	EU527455	n/a n/a 25117	24624 80433	neg	77 <b>BI0260</b> 07/25/05 <i>P. t. s.</i> JQ866111	n/a n/a 11974	37047 62062 pos	78 <b>BI2414</b> 04/21/07 <i>P. t. s.</i> JQ866093
		<i>P. t. s.</i>	JQ866093	n/a n/a 22075	34955 79300	neg	79 <b>BI2415</b> 04/21/07 <i>P. t. s.</i> EU527448	n/a n/a 10745	42345 44487 pos	80 <b>UB0439</b> 01/15/06 <i>P. t. s.</i> JQ866237	
		<i>P. t. s.</i>	JQ866237	n/a n/a 14645	23095 86804	neg	81 <b>UB0445</b> 01/18/06 <i>P. t. s.</i> JQ866239	n/a n/a 6465	13292 83467 pos		
82	<b>UB0599</b>	02/12/06	<i>P. t. s.</i>	JQ866242	n/a	n/a	18716	5956	129171	neg	

83	<b>UB1430</b>	01/09/07	<i>P. t. s.</i>	JQ866226	N03° 38'36	E022° 26'03	20021	50333	56542	neg
84	<b>UB1435</b>	02/14/07	<i>P. t. s.</i>	JQ866224	N03° 38'36	E022° 26'03	28602	17081	119248	neg
85	<b>UB1446</b>	02/22/07	<i>P. t. s.</i>	JQ866224	N03° 24'15	E022° 10'17	10862	52110	47583	<b>pos</b>
86	<b>UB1452</b>	02/22/07	<i>P. t. s.</i>	JQ866238	n/a	n/a	16446	13066	35664	<b>pos</b>
87	<b>UB1454</b>	02/22/07	<i>P. t. s.</i>	JQ866224	N03° 24'15	E022° 10'17	4718	14353	55044	<b>pos</b>
88	<b>UB2037</b>	04/05/07	<i>P. t. s.</i>	JQ866230	N03°38'36	E022°26'03	15020	23895	56189	neg
89	<b>PA0367</b>	12/15/05	<i>P. t. s.</i>	JQ866213	n/a	n/a	8961	12530	4527	neg
90	<b>PA0368</b>	12/15/05	<i>P. t. s.</i>	JQ866213	n/a	n/a	6949	32878	5549	<b>pos</b>
91	<b>PA0370</b>	01/04/06	<i>P. t. s.</i>	JQ866214	n/a	n/a	2121	19918	87786	<b>pos</b>
92	<b>PA0456</b>	01/30/06	<i>P. t. s.</i>	JQ866215	n/a	n/a	6184	10997	19	neg
93	<b>PA1038</b>	09/12/06	<i>P. t. s.</i>	JQ866206	n/a	n/a	12362	35343	46648	neg
94	<b>PA1039</b>	09/12/06	<i>P. t. s.</i>	JQ866206	n/a	n/a	12770	38723	54476	<b>pos</b>
95	<b>PA1044</b>	09/12/06	<i>P. t. s.</i>	JQ866205	n/a	n/a	29407	12171	111292	<b>pos</b>
	<b>PA1049</b>	09/15/06	<i>P. t. s.</i>	JQ866205	n/a	n/a	27144	18356	87174	neg
	<b>PA1059</b>	12/02/06	<i>P. t. s.</i>	JQ866206	n/a	n/a	17838	36066	57812	<b>pos</b>
98	<b>PA1065</b>	12/06/06	<i>P. t. s.</i>	JQ866206	n/a	n/a	15533	36026	52100	neg

<sup>a</sup>

GenBank accession numbers of mtDNA haplotypes

<sup>b</sup>

reads remaining after filtering expected errors to <1 and removing singleton OTUs

**Supplementary Table 8.** African plant species reported to have potential antimalarial activity.

No.	Plant	Family	Country/Region	References
1	<i>Abrus precatorius</i>	Fabaceae	Nigeria/South Africa	Lawal et al, 2015
2	<i>Abuta grandifolia</i>	Menispermaceae	Brazil	Silva et al, 2011
3	<i>Acacia karroo</i>	Fabaceae	Mozambique	Lawal et al, 2015
4	<i>Acacia erioloba</i>	Fabaceae	South Africa	Lawal et al, 2015
5	<i>Acacia nilotica</i>	Fabaceae	South Africa/Sudan	Lawal et al, 2015
6	<i>Acacia tortilis</i>	Fabaceae	South Africa	Lawal et al, 2015
7	<i>Acanthospermum australe</i>	Asteraceae	Brazil	Silva et al, 2011
8	<i>Acanthospermum hispidum</i>	Asteraceae	Benin/Ivory Coast/Sudan	Lawal et al, 2015
9	<i>Anchomanes difformis</i>	Araceae	Cameroon/Benin	Lawal et al, 2015
10	<i>Achyranthes aspera</i>	Amaranthaceae	South Africa	Lawal et al, 2015
11	<i>Acokanthera oppositifolia</i>	Apocynaceae	Kenya	Lawal et al, 2015
12	<i>Acokanthera schimperi</i>	Apocynaceae	Kenya	Lawal et al, 2015
13	<i>Adenia cissampeloides</i>	Passifloraceae	Ghana	Lawal et al, 2015
14	<i>Adenia rumicifolia</i>	Passifloraceae	Ghana	Lawal et al, 2015
15	<i>Aerva javanica</i>	Amaranthaceae	Sudan	Lawal et al, 2015
16	<i>Afzelia africana</i>	Fabaceae	Nigeria	Lawal et al, 2015
17	<i>Agathosma apiculata</i>	Rutaceae	South Africa	Lawal et al, 2015
18	<i>Agathosma puberula</i>	Rutaceae	South Africa	Lawal et al, 2015
19	<i>Ageratum conyzoides</i>	Asteraceae	São Tomé/South Africa	Lawal et al, 2015, Silva et al, 2011
20	<i>Alangium chinense</i>	Alangiaceae	Kenya	Lawal et al, 2015
21	<i>Albizia ferruginea</i>	Fabaceae	Ivory Coast	Lawal et al, 2015
22	<i>Albizia versicolour</i>	Fabaceae	South Africa	Lawal et al, 2015
23	<i>Albizia zygia</i>	Mimosaceae	Cameroon	Lawal et al, 2015
24	<i>Alchornea cordifolia</i>	Euphorbiaceae	Congo/Ivory Coast	Lawal et al, 2015
25	<i>Alchornea floribunda</i>	Euphorbiaceae	Congo	Lawal et al, 2015
26	<i>Alepidea amatymbica</i>	Apiaceae	South Africa	Lawal et al, 2015
27	<i>Alhagi graecorum</i>	Papilionaceae	Egypt	Lawal et al, 2015
28	<i>Aloe ferox</i>	Asphodelaceae	South Africa	Lawal et al, 2015
29	<i>Aloe maculata</i>	Asphodelaceae	South Africa	Lawal et al, 2015
30	<i>Aloe marlothii</i>	Asphodelaceae	South Africa	Lawal et al, 2015
31	<i>Aloe parvibracteata</i>	Aloaceae	Mozambique	Lawal et al, 2015
32	<i>Alstonia boonei</i>	Apocynaceae	Congo/Ivory Coast	Lawal et al, 2015
33	<i>Alternanthera pungens</i>	Amaranthaceae	Nigeria	Lawal et al, 2015
34	<i>Amaranthus lividus</i>	Amaranthaceae	Egypt	Lawal et al, 2015
35	<i>Ambrosia maritime</i>	Asteraceae	Sudan	Lawal et al, 2015
36	<i>Ampelozizyphus amazonicus</i>	Rhamanaceae	Brazil	Silva et al, 2011
37	<i>Anacardium occidentale</i>	Anacardiaceae	Ivory Coast	Lawal et al, 2015
38	<i>Anastatica hierochuntica</i>	Cruciferae	Egypt	Lawal et al, 2015
39	<i>Andira inermis</i>	Fabaceae	Brazil	Silva et al, 2011
40	<i>Anisopappus chinensis</i>	Asteraceae	Congo	Lawal et al, 2015
41	<i>Annona muricata</i>	Annonaceae	Cameroon	Lawal et al, 2015
42	<i>Annona senegalensis</i>	Annonaceae	South Africa	Lawal et al, 2015
43	<i>Anogeissus leiocarpa</i>	Combrataceae	Nigeria	Lawal et al, 2015
44	<i>Anonidium mannii</i>	Annonaceae	Congo	Lawal et al, 2015
45	<i>Anthocleista djalensis</i>	Loganiaceae	Ivory Coast	Lawal et al, 2015
46	<i>Anthocleista grandiflora</i>	Gentianaceae	South Africa	Lawal et al, 2015

47	<i>Anthocleista nobilis</i>	Loganiaceae	Burkina Faso	Lawal et al, 2015
48	<i>Anthonotha macrophylla</i>	Caesalpiniaceae	Ivory Coast	Lawal et al, 2015
49	<i>Aristolochia bracteolata</i>	Aristolochiaceae	Sudan	Lawal et al, 2015
50	<i>Aristolochia elegans</i>	Aristolochiaceae	Rwanda	Lawal et al, 2015
51	<i>Artabotrys brachypetalus</i>	Annonaceae	South Africa	Lawal et al, 2015
52	<i>Artabotrys monteiroae</i>	Annonaceae	South Africa	Lawal et al, 2015
53	<i>Artemisia absinthium</i>	Asteraceae	Egypt	Lawal et al, 2015
54	<i>Artemisia afra</i>	Asteraceae	South Africa	Lawal et al, 2015
55	<i>Artemisia annua</i>	Asteraceae	Asia	Artemesinin
56	<i>Artemisia gorgonum</i>	Asteraceae	Cape Verde	Silva et al, 2011
57	<i>Artocarpus communis</i>	Moraceae	Cameroon	Lawal et al, 2015
58	<i>Asparagus virgatus</i>	Asparagaceae	South Africa	Lawal et al, 2015
59	<i>Aspidosperma desmanthum</i>	Apocynaceae	Brazil	Silva et al, 2011
60	<i>Aspidosperma vargasii</i>	Apocynaceae	Brazil	Silva et al, 2011
61	<i>Aspilia africana</i>	Asteraceae	Nigeria	Lawal et al, 2015
62	<i>Aster squamatus</i>	Compositae	Egypt	Lawal et al, 2015
63	<i>Asystasia gangetica</i>	Acanthaceae	South Africa	Lawal et al, 2015
64	<i>Autranella congolensis</i>	Sapotaceae	Congo	Lawal et al, 2015
65	<i>Azadirachta indica</i>	Meliaceae	Nigeria	Lawal et al, 2015
66	<i>Baillonella toxisperma</i>	Sapotaceae	Benin	Lawal et al, 2015
67	<i>Balanites aegyptiaca</i>	Balanitaceae	Sudan/Togo	Lawal et al, 2015
68	<i>Barringtonia racemosa</i>	Lecythidaceae	South Africa	Lawal et al, 2015
69	<i>Bersama abyssinica</i>	Meliantaceae	Ivory Coast	Lawal et al, 2015
70	<i>Berula erecta</i>	Apiaceae	South Africa	Lawal et al, 2015
71	<i>Beta vulgaris</i>	Chenopodiaceae	Egypt	Lawal et al, 2015
72	<i>Bidens engleri</i>	Asteraceae	Burkina Faso	Lawal et al, 2015
73	<i>Bidens pilosa</i>	Asteraceae	South Africa/Brazil	Lawal et al, 2015; Silva et al, 2011
74	<i>Boscia angustifolia</i>	Capparaceae	Mali	Lawal et al, 2015
75	<i>Boswellia dalzielii</i>	Burceraceae	Benin/Nigeria	Lawal et al, 2015
76	<i>Bridelia cathartica</i>	Euphorbiaceae	Mozambique	Silva et al, 2011
77	<i>Bridelia ferruginea</i>	Euphorbiaceae	Angola	Silva et al, 2011
78	<i>Bridelia micrantha</i>	Euphorbiaceae	Mozambique/South Africa	Lawal et al, 2015
79	<i>Bridelia mollis</i>	Phyllanthaceae	South Africa	Lawal et al, 2015
80	<i>Bruguiera gymnorhiza</i>	Rhizophoraceae	South Africa	Lawal et al, 2015
81	<i>Burchellia bubalina</i>	Rubiaceae	South Africa	Lawal et al, 2015
82	<i>Byrsocarpus coccineus</i>	Connaraceae	Benin	Lawal et al, 2015
83	<i>Cadaba farinosa</i>	Capparaceae	Kenya	Lawal et al, 2015
84	<i>Caesalpinia bonduc</i>	Caesalpiniaceae	Ghana	Lawal et al, 2015
85	<i>Calycobolus sp.</i>	Convolvulaceae	Congo	Lawal et al, 2015
86	<i>Camellia sinensis</i>	Theaceae	Egypt	Lawal et al, 2015
87	<i>Capparis tomentosa</i>	Capparaceae	South Africa	Lawal et al, 2015
88	<i>Caralluma tuberculata</i>	Asclepiadaceae	Congo	Lawal et al, 2015
89	<i>Cardiospermum halicacabum</i>	Sapindaceae	South Africa	Lawal et al, 2015
90	<i>Carica papaya</i>	Caricaceae	Nigeria	Lawal et al, 2015



91	<i>Carissa edulis</i>	Apocynaceae	Kenya/South Africa	Lawal et al, 2015
92	<i>Carpolobia lutea</i>	Polygalaceae	Benin	Lawal et al, 2015
93	<i>Carapichea ipecacuanha</i>	Rubiaceae	Egypt	Lawal et al, 2015
94	<i>Casearia sylvestris</i>	Salicaceae	Brazil	Silva et al, 2011
95	<i>Cassia abbreviata</i>	Fabaceae	Mozambique	Lawal et al, 2015
96	<i>Cassia alata</i>	Caesalpiniaceae	Ivory Coast	Lawal et al, 2015
97	<i>Cassia arereh</i>	Fabaceae	Sudan	Lawal et al, 2015
98	<i>Cassia occidentalis</i>	Caesalpiniaceae	Congo/Ivory Coast/ Ghana/Mozambique	Lawal et al, 2015
99	<i>Cassia podocarpa</i>	Caesalpiniaceae	Burkina Faso	Lawal et al, 2015
100	<i>Cassia sieberiana</i>	Fabaceae	Nigeria	Lawal et al, 2015
101	<i>Cassia singueana</i>	Fabaceae	Nigeria	Lawal et al, 2015
102	<i>Cassia tora</i>	Caesalpiniaceae	Sudan	Lawal et al, 2015
103	<i>Catha edulis</i>	Celastraceae	South Africa	Lawal et al, 2015
104	<i>Cecropia pachystachya</i>	Urticaceae	Brazil	Silva et al, 2011
105	<i>Cedrela odorata</i>	Meliaceae	Brazil/São Tomé	Silva et al, 2011
106	<i>Celtis integrifolia</i>	Ulmaceae	Burkina Faso	Lawal et al, 2015
107	<i>Centella asiatica</i>	Apiaceae	South Africa	Lawal et al, 2015
108	<i>Cephalanthus natalensis</i>	Rubiaceae	South Africa	Lawal et al, 2015
109	<i>Cestrum laevigatum</i>	Solanaceae	São Tomé	Silva et al, 2011
110	<i>Chenopodium murale</i>	Chenopodiaceae	Egypt	Lawal et al, 2015
111	<i>Cichorium endivia</i>	Asteraceae	Egypt	Lawal et al, 2015
112	<i>Cichorium intybus</i>	Asteraceae	Egypt	Lawal et al, 2015
113	<i>Cinchona calisaya</i>	Rubiaceae	South America	Quinine
114	<i>Cinnamomum cassia</i>	Lauraceae	Egypt	Lawal et al, 2015
115	<i>Cissus populnea</i>	Amplidaceae	Nigeria	Lawal et al, 2015
116	<i>Cissus quadrangularis</i>	Vitaceae	Mali	Lawal et al, 2015
117	<i>Citrullus colocynthis</i>	Cucurbitaceae	Sudan	Lawal et al, 2015
118	<i>Citrus aurantifolia</i>	Rutaceae	Ghana	Lawal et al, 2015
119	<i>Citrus limon</i>	Rutaceae	Nigeria	Lawal et al, 2015
120	<i>Citrus reticulata</i>	Rutaceae	Egypt	Lawal et al, 2015
121	<i>Clausena anisata</i>	Rutaceae	South Africa	Lawal et al, 2015
122	<i>Cleistopholis patens</i>	Annonaceae	Ghana	Lawal et al, 2015
123	<i>Clematis brachiata</i>	Ranunculaceae	South Africa	Lawal et al, 2015
124	<i>Cleome rutidosperma</i>	Cleomaceae	Cameroon	Lawal et al, 2015
125	<i>Clerodendrum glabrum</i>	Verbenaceae	South Africa	Lawal et al, 2015
126	<i>Clutia hirsuta</i>	Euphorbiaceae	South Africa	Lawal et al, 2015
127	<i>Clutia pulchella</i>	Euphorbiaceae	South Africa	Lawal et al, 2015
128	<i>Cnestis ferruginia</i>	Connaraceae	Ghana	Lawal et al, 2015
129	<i>Cochlospermum tinctorium</i>	Cochlospermaceae	Guinea-Bissau	Silva et al, 2011
130	<i>Cocos nucifera</i>	Arecaceae	Nigeria	Lawal et al, 2015
131	<i>Combretum collinum</i>	Combretaceae	Burkina Faso	Lawal et al, 2015
132	<i>Combretum glutinosum</i>	Combretaceae	Burkina Faso	Lawal et al, 2015
133	<i>Combretum molle</i>	Combretaceae	Burkina Faso	Lawal et al, 2015

134	<i>Combretum sericeum</i>	Combretaceae	Burkina Faso	Lawal et al, 2015
135	<i>Combretum zeyheri</i>	Combretaceae	South Africa	Lawal et al, 2015
136	<i>Commiphora kerstingii</i>	Burseraceae	Nigeria	Lawal et al, 2015
137	<i>Conyza aegyptiaca</i>	Asteraceae	Rwanda	Lawal et al, 2015
138	<i>Conyza albida</i>	Asteraceae	South Africa	Lawal et al, 2015
139	<i>Conyza dioscoridis</i>	Compositae	Egypt	Lawal et al, 2015
140	<i>Conyza podocephala</i>	Asteraceae	South Africa	Lawal et al, 2015
141	<i>Conyza scabrida</i>	Asteraceae	South Africa	Lawal et al, 2015
142	<i>Copaifera religiosa</i>	Fabaceae	Gabon	Lawal et al, 2015
143	<i>Corchorus olitorius</i>	Tiliaceae	Egypt	Lawal et al, 2015
144	<i>Crateva religiosa</i>	Capparidaceae	Benin	Lawal et al, 2015
145	<i>Crinum macowanii</i>	Amaryllidaceae	South Africa	Lawal et al, 2015
146	<i>Crossopteryx febrifuga</i>	Rubiaceae	Mozambique	Lawal et al, 2015; Silva et al, 2011
147	<i>Crotalaria burkeana</i>	Fabaceae	South Africa	Lawal et al, 2015
148	<i>Croton gratissimus</i>	Euphorbiaceae	South Africa	Lawal et al, 2015
149	<i>Croton menyharthii</i>	Euphorbiaceae	South Africa	Lawal et al, 2015
150	<i>Croton zambesicus</i>	Euphorbiaceae	Sudan	Lawal et al, 2015
151	<i>Cryptolepis sanguinolenta</i>	Apocynaceae	Guinea-Bissau	Silva et al, 2011
152	<i>Cucumis meohuliferus</i>	Curcubitaceae	Burkina Faso	Lawal et al, 2015
153	<i>Cucurbita maxima</i>	Cucurbitaceae	Brazil	Silva et al, 2011
154	<i>Curcuma aromatic</i>	Zingiberaceae	Egypt	Lawal et al, 2015
155	<i>Cussonia spicata</i>	Araliaceae	South Africa	Lawal et al, 2015
156	<i>Cymbopogon citratus</i>	Poaceae	Cameroon/Nigeria	Lawal et al, 2015
157	<i>Cymbopogon giganteus</i>	Poaceae	Benin	Lawal et al, 2015
158	<i>Cymbopogon nardus</i>	Poaceae	Benin	Lawal et al, 2015
159	<i>Cymbopogon proximus</i>	Poaceae	Egypt	Lawal et al, 2015
160	<i>Cymbopogon schoenanthus</i>	Poaceae	Benin/Sudan	Lawal et al, 2015
161	<i>Cymbopogon validus</i>	Poaceae	South Africa	Lawal et al, 2015
162	<i>Cyperus alopecuroides</i>	Cyperaceae	Egypt	Lawal et al, 2015
163	<i>Cyperus rotundus</i>	Cyperaceae	Egypt	Lawal et al, 2015
164	<i>Dalhousiea africana</i>	Leguminosae	Congo	Lawal et al, 2015
165	<i>Daniellia oliveri</i>	Fabaceae	Nigeria	Lawal et al, 2015
166	<i>Daucus carota</i>	Apiaceae	Egypt	Lawal et al, 2015
167	<i>Desmodium velutinum</i>	Fabaceae	Burkina Faso	Lawal et al, 2015
168	<i>Desmostachya bipinnata</i>	Poaceae	Egypt	Lawal et al, 2015
169	<i>Dialium guineense</i>	Leguminosae	Benin	Lawal et al, 2015
170	<i>Dicerocaryum eriocarpum</i>	Pedaliaceae	Namibia	Lawal et al, 2015
171	<i>Dichrostachys cinerea</i>	Fabaceae	South Africa	Lawal et al, 2015
172	<i>Diosma sp.</i>	Rutaceae	South Africa	Lawal et al, 2015
173	<i>Diospyros abyssinica</i>	Ebenaceae	Uganda	Krief et al, 2006
174	<i>Diospyros mespiliformis</i>	Ebenaceae	South Africa	Lawal et al, 2015
175	<i>Diplorhynchus condylocarpon</i>	Apocynaceae	South Africa	Lawal et al, 2015
176	<i>Dodonaea viscosa</i>	Sapindaceae	South Africa	Lawal et al, 2015
177	<i>Drypetes gerrardii</i>	Meliaceae	South Africa	Lawal et al, 2015
178	<i>Drypetes gossweileri</i>	Euphorbiaceae	Congo	Lawal et al, 2015

179	<i>Ekebergia capensis</i>	Meliaceae	South Africa	Lawal et al, 2015
180	<i>Elaeis guineensis</i>	Palmaceae	Ghana	Lawal et al, 2015
181	<i>Elephantorrhiza elephantina</i>	Fabaceae	South Africa	Lawal et al, 2015
182	<i>Emblica officinalis</i>	Phyllanthaceae	Egypt	Lawal et al, 2015
183	<i>Enantia chlorantha</i>	Annonaceae	Congo	Lawal et al, 2015
184	<i>Entada africana</i>	Fabaceae	Togo	Lawal et al, 2015
185	<i>Entandrophragma angolense</i>	Meliaceae	Cameroon	Lawal et al, 2015
186	<i>Entandrophragma palustre</i>	Meliaceae	Congo	Lawal et al, 2015
187	<i>Erigeron floribundus</i>	Asteraceae	Ivory Coast	Lawal et al, 2015
188	<i>Eruca sativa</i>	Brassicaceae	Egypt	Lawal et al, 2015
189	<i>Erythrina senegalensis</i>	Fabaceae	Nigeria/Ivory Coast	Lawal et al, 2015
190	<i>Esenbeckia febrifuga</i>	Rutaceae	Brazil	Silva et al, 2011
191	<i>Euclea natalensis</i>	Ebenaceae	South Africa	Lawal et al, 2015
192	<i>Eucomis autumnalis</i>	Asparagaceae	South Africa	Lawal et al, 2015
193	<i>Euphorbia heterophylla</i>	Euphorbiaceae	South Africa	Lawal et al, 2015
194	<i>Euphorbia hirta</i>	Euphorbiaceae	Congo/Nigeria/Ivory Coast/Angola	Lawal et al, 2015
195	<i>Euphorbia tirucalli</i>	Euphorbiaceae	South Africa	Lawal et al, 2015
196	<i>Zanthoxylum gillettii</i>	Rutaceae	Ivory Coast	Lawal et al, 2015
197	<i>Zanthoxylum zanthoxyloides</i>	Rutaceae	Nigeria	Lawal et al, 2015
198	<i>Ficus capensis</i>	Moraceae	Ivory Coast	Lawal et al, 2015
199	<i>Ficus capreifolia</i>	Moraceae	Burkina Faso	Lawal et al, 2015
200	<i>Ficus carica</i>	Moraceae	Egypt	Lawal et al, 2015
201	<i>Ficus platyphylla</i>	Moraceae	Nigeria	Lawal et al, 2015
202	<i>Ficus thonningii</i>	Moraceae	Nigeria	Lawal et al, 2015
203	<i>Flacourtia indica</i>	Flacourtiaceae	South Africa	Lawal et al, 2015
204	<i>Flueggea virosa</i>	Euphorbiaceae	South Africa	Lawal et al, 2015
205	<i>Afrostryax lepidophyllus</i>	Huaceae	Congo	Lawal et al, 2015
206	<i>Fuerstia africana</i>	Lamiaceae	Rwanda	Lawal et al, 2015
207	<i>Funtumia elastica</i>	Apocynaceae	Ivory Coast	Lawal et al, 2015
208	<i>Garcinia kola</i>	Clusiaceae	Congo	Lawal et al, 2015
209	<i>Garcinia punctata</i>	Clusiaceae	Congo	Lawal et al, 2015
210	<i>Gardenia jovis tonatis</i>	Rubiaceae	Sudan	Lawal et al, 2015
211	<i>Gardenia lutea</i>	Rubiaceae	Sudan	Lawal et al, 2015
212	<i>Geissospermum sericeum</i>	Apocynaceae	Brazil	Silva et al, 2011
213	<i>Gloriosa superba</i>	Colchicaceae	South Africa	Lawal et al, 2015
214	<i>Glycyrrhiza glabra</i>	Fabaceae	Egypt	Lawal et al, 2015
215	<i>Gnidia cuneata</i>	Thymelaeaceae	South Africa	Lawal et al, 2015
216	<i>Gnidia kraussiana</i>	Thymelaeaceae	South Africa	Lawal et al, 2015
217	<i>Gomphocarpus fruticosus</i>	Apocynaceae	South Africa	Lawal et al, 2015
218	<i>Guiera senegalensis</i>	Combretaceae	Nigeria/Guinea-Bissau	Silva et al, 2011
219	<i>Harungana madagascariensis</i>	Hypnaceae	Congo/Guinea-Bissau/Nigeria	Lawal et al, 2015; Silva et al, 2011
220	<i>Helianthus annuus</i>	Poaceae	Sudan	Lawal et al, 2015
221	<i>Helichrysum nudifolium</i>	Asteraceae	South Africa	Lawal et al, 2015
222	<i>Helichrysum pedunculatum</i>	Asteraceae	South Africa	Lawal et al, 2015
223	<i>Heliotropium indicum</i>	Boraginaceae	Benin	Lawal et al, 2015

224	<i>Hermannia depressa</i>	Sterculiaceae	South Africa	Lawal et al, 2015
225	<i>Hexalobus crispiflorus</i>	Annonaceae	Angola	Silva et al, 2011
226	<i>Hibiscus sabdariffa</i>	Malvaceae	Egypt	Lawal et al, 2015
227	<i>Hippobromus pauciflorus</i>	Sapindaceae	South Africa	Lawal et al, 2015
228	<i>Hypericum aethiopicum</i>	Hypericaceae	South Africa	Lawal et al, 2015
229	<i>Hyphaene thebaica</i>	Arecaceae	Egypt	Lawal et al, 2015
230	<i>Hypoxis colchicifolia</i>	Hypoxidaceae	South Africa	Lawal et al, 2015
231	<i>Hyptis pectinata</i>	Lamiaceae	South Africa	Lawal et al, 2015
232	<i>Hyptis spicigera</i>	Lamiaceae	Burkina Faso	Lawal et al, 2015
233	<i>Irvingia gabonensis</i>	Simaroubaceae	Ivory Coast	Lawal et al, 2015
234	<i>Isolona hexaloba</i>	Annonaceae	Congo	Lawal et al, 2015
235	<i>Jatropha curcas</i>	Euphorbiaceae	Congo/Nigeria	Lawal et al, 2015
236	<i>Jatropha tanjorensis</i>	Euphorbiaceae	Nigeria	Lawal et al, 2015
237	<i>Justicia flava</i>	Acanthaceae	South Africa	Lawal et al, 2015
238	<i>Keetia leucantha</i>	Rubiaceae	Benin	Lawal et al, 2015
239	<i>Khaya grandifoliola</i>	Maliaceae	Nigeria	Lawal et al, 2015
240	<i>Khaya senegalensis</i>	Maliaceae	Benin	Lawal et al, 2015
241	<i>Kigelia africana</i>	Bignoniaceae	Kenya/South Africa	Lawal et al, 2015
242	<i>Kirkia wilmsii</i>	Kirkiaceae	South Africa	Lawal et al, 2015
243	<i>Lannea discolor</i>	Anacardiaceae	South Africa	Lawal et al, 2015
244	<i>Lawsonia inermis</i>	Lythraceae	Egypt	Lawal et al, 2015
245	<i>Leonotis leonurus</i>	Lamiaceae	Mozambique/ South Africa	Lawal et al, 2015
246	<i>Leonotis nepetifolia</i>	Lamiaceae	South Africa	Lawal et al, 2015
247	<i>Leonotis ocyimifolia</i>	Lamiaceae	South Africa	Lawal et al, 2015
248	<i>Leucas martinicensis</i>	Lamiaceae	South Africa	Lawal et al, 2015
249	<i>Lippia javanica</i>	Verbenaceae	Kenya/South Africa	Lawal et al, 2015
250	<i>Lonchocarpus cyanescens</i>	Fabaceae	Nigeria	Lawal et al, 2015
251	<i>Lophira alata</i>	Ochnaceae	Nigeria	Lawal et al, 2015
252	<i>Lophira lanceolata</i>	Ochnaceae	Burkina Faso	Lawal et al, 2015
253	<i>Lupinus termis</i>	Fabaceae	Egypt	Lawal et al, 2015
254	<i>Macrostylis squarrosa</i>	Rutaceae	South Africa	Lawal et al, 2015
255	<i>Maesa lanceolata</i>	Maesaceae	South Africa	Lawal et al, 2015
256	<i>Malva parviflora</i>	Malvaceae	Egypt	Lawal et al, 2015
257	<i>Mammea africana</i>	Clusiaceae	Congo	Lawal et al, 2015
258	<i>Mangifera indica</i>	Anacardiaceae	Cameron/Ivory Coast	Lawal et al, 2015
259	<i>Manniophyton fulvum</i>	Euphorbiaceae	Congo	Lawal et al, 2015
260	<i>Mareya micrantha</i>	Euphorbiaceae	Ivory Coast	Lawal et al, 2015
261	<i>Markhamia lutea</i>	Bignoniaceae	Rwanda	Lawal et al, 2015
262	<i>Massularia acuminata</i>	Rubiaceae	Congo	Lawal et al, 2015
263	<i>Maytenus heterophylla</i>	Celastraceae	Kenya	Lawal et al, 2015
264	<i>Maytenus senegalensis</i>	Celastraceae	South Africa	Lawal et al, 2015
265	<i>Maytenus undata</i>	Celastraceae	South Africa	Lawal et al, 2015
266	<i>Melanthera scandens</i>	Asteraceae	Ivory Coast	Lawal et al, 2015
267	<i>Melia azedarach</i>	Meliaceae	Congo	Lawal et al, 2015
268	<i>Mallotus oppositifolius</i>	Euphorbiaceae	Cameroon	Lawal et al, 2015
269	<i>Mentha longifolia</i>	Labiatae	Egypt	Lawal et al, 2015
270	<i>Microdesmis keayana</i>	Pandaceae	Ivory Coast	Lawal et al, 2015

271	<i>Microglossa pyrifolia</i>	Asteraceae	Ivory Coast/Rwanda /Kenya	Lawal et al, 2015
272	<i>Millettia zechiana</i>	Fabaceae	Ivory Coast	Lawal et al, 2015
273	<i>Mimusops caffra</i>	Sapotaceae	South Africa	Lawal et al, 2015
274	<i>Mimusops obtusifolia</i>	Sapotaceae	South Africa	Lawal et al, 2015
275	<i>Mitragyna stipulosa</i>	Rubiaceae	Nigeria	Lawal et al, 2015
276	<i>Mitragyna rubrostipulata</i>	Rubiaceae	Rwanda	Lawal et al, 2015
277	<i>Momordica balsamina</i>	Cucurbitaceae	Mozambique/Nigera/ South Africa	Lawal et al, 2015, Silva et al, 2011
278	<i>Momordica cissoides</i>	Cucurbitaceae	Ghana	Lawal et al, 2015
279	<i>Morinda lucida</i>	Rubiaceae	Nigeria	Lawal et al, 2015
280	<i>Morinda morindoides</i>	Rubiaceae	Congo/Ghana/Ivory Coast	Lawal et al, 2015
281	<i>Moringa oleifera</i>	Moringaceae	Nigeria	Lawal et al, 2015
282	<i>Morus alba</i>	Moraceae	Egypt	Lawal et al, 2015
283	<i>Musanga cecropioides</i>	Cecropiaceae	Congo	Lawal et al, 2015
284	<i>Napoleona vogelii</i>	Lecythidaceae	Congo	Lawal et al, 2015
285	<i>Nauclea latifolia</i>	Rubiaceae	Ivory Coast/Nigeria	Lawal et al, 2015
286	<i>Nicolasia costata</i>	Asteraceae	Namibia	Lawal et al, 2015
287	<i>Nigella sativa</i>	Ranunculaceae	Sudan	Lawal et al, 2015
288	<i>Ocimum americanum</i>	Lamiaceae	South Africa	Lawal et al, 2015
289	<i>Ocimum gratissimum</i>	Lamiaceae	Congo/Brazil/ Nigeria/Benin	Lawal et al, 2015; Silva et al, 2011
290	<i>Oedera genistifolia</i>	Asteraceae	South Africa	Lawal et al, 2015
291	<i>Olea europaea</i>	Olacaceae	South Africa	Lawal et al, 2015
292	<i>Oncoba spinosa</i>	Flacourtiaceae	Ghana	Lawal et al, 2015
293	<i>Opilia celtidifolia</i>	Opiliaceae	Burkina Faso/Togo	Lawal et al, 2015
294	<i>Opuntia ficus-indica</i>	Cactaceae	Egypt	Lawal et al, 2015
295	<i>Origanum majorana</i>	Lamiaceae	Egypt	Lawal et al, 2015
296	<i>Osteospermum imbricatum</i>	Asteraceae	South Africa	Lawal et al, 2015
297	<i>Ozoroa sphaerocarpa</i>	Anacardiaceae	South Africa	Lawal et al, 2015
298	<i>Pachypodantium confine</i>	Annonaceae	Angola	Silva et al, 2011
299	<i>Pappea capensis</i>	Sapindaceae	South Africa	Lawal et al, 2015
300	<i>Parinari curatellifolia</i>	Chrysobalanaceae	South Africa/Togo	Lawal et al, 2015
301	<i>Parkia biglobosa</i>	Leguminosae	Nigeria	Lawal et al, 2015
302	<i>Parkinsonia aculeata</i>	Fabaceae	Mozambique/ South Africa	Lawal et al, 2015
303	<i>Parquetina nigrescens</i>	Asclepiadaceae	Ivory Coast	Lawal et al, 2015
304	<i>Pavetta corymbosa</i>	Rubiaceae	Togo	Lawal et al, 2015
305	<i>Peganum harmal</i>	Nitrariaceae	Egypt	Lawal et al, 2015
306	<i>Pelargonium alchemilloides</i>	Gentianaceae	South Africa	Lawal et al, 2015
307	<i>Penianthus longifolius</i>	Menispermaceae	Congo	Lawal et al, 2015
308	<i>Pentzia globosa</i>	Asteraceae	South Africa	Lawal et al, 2015
309	<i>Periploca linearifolia</i>	Asclepiadaceae	Kenya	Lawal et al, 2015
310	<i>Tabernaemontana hystrix</i>	Apocynaceae	Brazil	Silva et al, 2011
311	<i>Phaseolus vulgaris</i>	Papilionaceae	Egypt	Lawal et al, 2015
312	<i>Phragmites communis</i>	Poaceae	Egypt	Lawal et al, 2015
313	<i>Phyllanthus amarus</i>	Euphorbiaceae	Nigeria	Lawal et al, 2015
314	<i>Phyllanthus muellerianus</i>	Euphorbiaceae	Ivory Coast	Lawal et al, 2015
315	<i>Physalis angulata</i>	Solanaceae	Congo/Ivory Coast	Lawal et al, 2015



316	<i>Picralima nitida</i>	Apocynaceae	Congo/Ivory Coast	Lawal et al, 2015
317	<i>Picrolemma sprucei</i>	Simaroubaceae	Brazil	Silva et al, 2011
318	<i>Piliostigma thonningii</i>	Fabaceae	Nigeria/South Africa	Lawal et al, 2015
319	<i>Pimpinella anisum</i>	Umbelliferae	Egypt	Lawal et al, 2015
320	<i>Piper guineense</i>	Piperaceae	Congo	Lawal et al, 2015
321	<i>Piper sp.</i>	Piperaceae	Angola/Brazil	Silva et al, 2011
322	<i>Piper umbellatum</i>	Piperaceae	Cameroon	Lawal et al, 2015
323	<i>Piptadeniastrum africanum</i>	Leguminosae	Congo	Lawal et al, 2015
324	<i>Pittosporum tobira</i>	Pittosporaceae	Mozambique	Lawal et al, 2015
325	<i>Pittosporum viridiflorum</i>	Pittosporaceae	South Africa	Lawal et al, 2015
326	<i>Plantago major</i>	Plantaginaceae	South Africa	Lawal et al, 2015
327	<i>Pleiocarpa mutica</i>	Apocynaceae	Ghana	Lawal et al, 2015
328	<i>Plumbago auriculata</i>	Plumbaginaceae	Mozambique	Lawal et al, 2015
329	<i>Plumbago zeylanica</i>	Plumbaginaceae	South Africa	Lawal et al, 2015
330	<i>Polygonum glabrum</i>	Polgonaceae	Sudan	Lawal et al, 2015
331	<i>Pollichia campestris</i>	Illecebraceae	South Africa	Lawal et al, 2015
332	<i>Polyalthia oliveri</i>	Annonaceae	Congo	Lawal et al, 2015
333	<i>Polyalthia suaveolens</i>	Annonaceae	Congo	Lawal et al, 2015
334	<i>Piper peltatum</i>	Piperaceae	Brazil	Silva et al, 2011
335	<i>Prosopis africana</i>	Leguminaceae	Nigeria	Lawal et al, 2015
336	<i>Pseudarthria hookeri</i>	Fabaceae	South Africa	Lawal et al, 2015
337	<i>Psiadia punctulata</i>	Asteraceae	South Africa	Lawal et al, 2015
338	<i>Psidium guajava</i>	Myrtaceae	Nigeria/Egypt	Lawal et al, 2015
339	<i>Psoralea pinnata</i>	Fabaceae	South Africa	Lawal et al, 2015
340	<i>Ptaeroxylon obliquum</i>	Rutaceae	South Africa	Lawal et al, 2015
341	<i>Pterocarpus angolensis</i>	Fabaceae	South Africa	Lawal et al, 2015
342	<i>Pulicaria crispa</i>	Asteraceae	Sudan	Lawal et al, 2015
343	<i>Punica granatum</i>	Lythraceae	Egypt	Lawal et al, 2015
344	<i>Pupalia lappacea</i>	Amaranthaceae	Benin	Lawal et al, 2015
345	<i>Pycnanthus angolensis</i>	Myristicaceae	Ivory Coast/São Tomé	Lawal et al, 2015, Silva et al, 2011
346	<i>Pyrenacantha grandiflora</i>	Icacinaceae	South Africa	Lawal et al, 2015
347	<i>Pyrenacantha klaineana</i>	Cacinaceae	Congo	Lawal et al, 2015
348	<i>Quassia africana</i>	Simaroubaceae	Congo	Lawal et al, 2015
349	<i>Quassia amara</i>	Simaroubaceae	Nigeria	Lawal et al, 2015
350	<i>Quercus infectoria</i>	Fagaceae	Egypt	Lawal et al, 2015
351	<i>Ranunculus multifidus</i>	Ranunculaceae	South Africa	Lawal et al, 2015
352	<i>Rapanea melanophloeos</i>	Myrtaceae	South Africa	Lawal et al, 2015
353	<i>Rauvolfia caffra</i>	Apocynaceae	South Africa	Lawal et al, 2015
354	<i>Rauvolfia vomitoria</i>	Apocynaceae	Ivory Coast	Lawal et al, 2015
355	<i>Remijia ferruginea</i>	Rubiaceae	Brazil	Silva et al, 2011
356	<i>Rhigiocarya racemifera</i>	Menispermaceae	Ivory Coast	Lawal et al, 2015
357	<i>Rhizophora mucronata</i>	Rhizophoraceae	South Africa	Lawal et al, 2015
358	<i>Ricinus communis</i>	Euphorbiaceae	Egypt/South Africa	Lawal et al, 2015
359	<i>Rothmannia longiflora</i>	Rubiaceae	Ghana	Lawal et al, 2015
360	<i>Rourea coccinea</i>	Connaraceae	Benin	Lawal et al, 2015
361	<i>Rumex abyssinicus</i>	Polygonaceae	Rwanda	Lawal et al, 2015
362	<i>Rumex bequaertii</i>	Polygonaceae	Rwanda	Lawal et al, 2015

363	<i>Rumex crispus</i>	Polygonaceae	South Africa	Lawal et al, 2015
364	<i>Rumex sagittatus</i>	Poaceae	South Africa	Lawal et al, 2015
365	<i>Agathosma</i>	Rutaceae	South Africa	Lawal et al, 2015
366	<i>Salix suberrata</i>	Salicaceae	Egypt	Lawal et al, 2015
367	<i>Salvia repens</i>	Lamiaceae	South Africa	Lawal et al, 2015
368	<i>Sansevieria liberica</i>	Dracaenaceae	Benin	Lawal et al, 2015
369	<i>Sarcocephalus latifolius</i>	Rubiaceae	Guinea-Bissau	Silva et al, 2011
370	<i>Scaevola plumieri</i>	Goodeniaceae	South Africa	Lawal et al, 2015
371	<i>Schefflera actinophylla</i>	Araliaceae	Mozambique	Lawal et al, 2015
372	<i>Schefflera umbellifera</i>	Araliaceae	South Africa	Lawal et al, 2015
373	<i>Schizogygia coffaeoides</i>	Apocynaceae	Kenya	Lawal et al, 2015
374	<i>Schkuhria pinnata</i>	Asteraceae	South Africa	Lawal et al, 2015
375	<i>Schrankia leptocarpa</i>	Mimosaceae	Benin	Lawal et al, 2015
376	<i>Schumanniphyton magnificum</i>	Rubiaceae	Cameroon	Lawal et al, 2015
377	<i>Scolopia zeyheri</i>	Flacourtiaceae	Kenya	Lawal et al, 2015
378	<i>Scoparia dulcis</i>	Scrophulariaceae	Brazil	Silva et al, 2011
379	<i>Scorodophloeus zenkeri</i>	Leguminosae	Congo	Lawal et al, 2015
380	<i>Securidaca longipedunculata</i>	Polygalaceae	Mali	Lawal et al, 2015
381	<i>Securinega virosa</i>	Euphorbiaceae	Burkina Faso	Lawal et al, 2015
382	<i>Senecio oxyriifolius</i>	Asteraceae	South Africa	Lawal et al, 2015
383	<i>Senna abbreviata</i>	Fabaceae	Mozambique	Silva et al, 2011
384	<i>Senna alexandrina</i>	Fabaceae	Sudan	Lawal et al, 2015
385	<i>Senna didymobotrya</i>	Fabaceae	Mozambique/ South Africa	Lawal et al, 2015
386	<i>Senna occidentalis</i>	Fabaceae	Brazil/Mozambique	Silva et al, 2011
387	<i>Senna petersiana</i>	Fabaceae	South Africa	Lawal et al, 2015
388	<i>Sesamum indicum</i>	Pedaliaceae	Egypt	Lawal et al, 2015
389	<i>Sesbania sesban</i>	Leguminosae	Egypt	Lawal et al, 2015
390	<i>Setaria megaphylla</i>	Poaceae	South Africa	Lawal et al, 2015
391	<i>Sida acuta</i>	Malvaceae	Nigeria	Lawal et al, 2015
392	<i>Sisymbrium irio</i>	Brassicaceae	Egypt	Lawal et al, 2015
393	<i>Solanecio mannii</i>	Asteraceae	Rwanda	Lawal et al, 2015
394	<i>Solanum indicum</i>	Olanaceae	Ivory Coast	Lawal et al, 2015
395	<i>Solanum nigrum</i>	Olanaceae	Ivory Coast	Lawal et al, 2015
396	<i>Solenostemma argel</i>	Apocynaceae	Egypt/Sudan	Lawal et al, 2015
397	<i>Sonchous cornatus</i>	Asteraceae	Sudan	Lawal et al, 2015
398	<i>Spilanthes mauritiana</i>	Asteraceae	South Africa	Lawal et al, 2015
399	<i>Spinacia oleracea</i>	Chenopodiaceae	Egypt	Lawal et al, 2015
400	<i>Staudtia kamerunensis</i>	Myristicaceae	Congo	Lawal et al, 2015
401	<i>Striga hermonthica</i>	Orobanchaceae	Nigeria	Lawal et al, 2015
402	<i>Struchium sparganophorum</i>	Asteraceae	São Tomé	Silva et al, 2011
403	<i>Strychnos henningsii</i>	Strychnaceae	Kenya	Lawal et al, 2015
404	<i>Strychnos icaia</i>	Loganiaceae	Congo	Lawal et al, 2015
405	<i>Strychnos madagascariensis</i>	Strychnaceae	South Africa	Lawal et al, 2015
406	<i>Strychnos potatorum</i>	Strychnaceae	South Africa	Lawal et al, 2015

407	<i>Strychnos pungens</i>	Strychnaceae	South Africa	Lawal et al, 2015
408	<i>Strychnos spinosa</i>	Loganiaceae	Benin/Ivory Coast	Lawal et al, 2015
409	<i>Strychnos usambarensis</i>	Strychnaceae	Kenya	Lawal et al, 2015
410	<i>Stylosanthes erecta</i>	Fabaceae	Mali	Lawal et al, 2015
411	<i>Swartzia madagascariensis</i>	Leguminosae	Burkina Faso	Lawal et al, 2015
412	<i>Symphonia globulifera</i>	Clusiaceae	Congo	Lawal et al, 2015
413	<i>Syzygium cordatum</i>	Myrtaceae	South Africa	Lawal et al, 2015
414	<i>Tabernaemontana elegans</i>	Apocynaceae	South Africa /Mozambique	Lawal et al, 2015
415	<i>Tamarindus indica</i>	Fabaceae	Egypt/Togo	Lawal et al, 2015
416	<i>Tamarix nilotica</i>	Tamaricaceae	Egypt	Lawal et al, 2015
417	<i>Tapinanthus dodoneifolius</i>	Euphorbiaceae	Burkina Faso	Lawal et al, 2015
418	<i>Tapinanthus sessilifolius</i>	Lorantheciae	nigeria	Lawal et al, 2015
419	<i>Tarchonanthus camphoratus</i>	Asteraceae	South Africa	Lawal et al, 2015
420	<i>Tecomaria capensis</i>	Bignoniaceae	South Africa	Lawal et al, 2015
421	<i>Tefracera pogge</i>	Dilleniaceae	Congo	Lawal et al, 2015
422	<i>Terminalia avicennioides</i>	Combretaceae	Burkina, Nigeria	Lawal et al, 2015
423	<i>Terminalia catappa</i>	Combretaceae	Nigeria	Lawal et al, 2015
424	<i>Terminalia ivorensis</i>	Combretaceae	Ghana	Lawal et al, 2015
425	<i>Terminalia mollis</i>	Combretaceae	Rwanda	Lawal et al, 2015
426	<i>Tetradenia riparia</i>	Lamiaceae	South Africa	Lawal et al, 2015
427	<i>Tetrapleura tetraptera</i>	Fabaceae	Congo	Lawal et al, 2015
428	<i>Thomandersia hensii</i>	Acanthaceae	Congo	Lawal et al, 2015
429	<i>Thymus vulgaris</i>	Lamiaceae	Egypt	Lawal et al, 2015
430	<i>Tilia cordata</i>	Tiliaceae	Egypt	Lawal et al, 2015
431	<i>Tinospora bakis</i>	Menispermaceae	Burkina Faso/Sudan	Lawal et al, 2015
432	<i>Tithonia diversifolia</i>	Asteraceae	Nigeria/Rwanda/ São Tomé	Lawal et al, 2015; Silva et al, 2011
433	<i>Toddalia asiatica</i>	Rutaceae	Kenya	Lawal et al, 2015
434	<i>Trema orientalis</i>	Ulmaceae	Nigeria	Lawal et al, 2015
435	<i>Trichilia emetica</i>	Meliaceae	Benin/Mali/Mozambique	Lawal et al, 2015
436	<i>Trichilia rubescens</i>	Meliaceae	Uganda	Krief et al, 2006
437	<i>Triclisia dictyophylla</i>	Menispermaceae	Congo	Lawal et al, 2015
438	<i>Tridax procumbens</i>	Asteraceae	South Africa	Lawal et al, 2015
439	<i>Trifolium alexandrinum</i>	Leguminosae	Egypt	Lawal et al, 2015
440	<i>Trimeria grandifolia</i>	Flacourtiaceae	Rwanda	Lawal et al, 2015
441	<i>Triumfetta welwitschii</i>	Tiliaceae	South Africa	Lawal et al, 2015
442	<i>Turraea floribunda</i>	Meliaceae	South Africa	Lawal et al, 2015
443	<i>Turraea heterophylla</i>	Meliaceae	Ghana	Lawal et al, 2015
444	<i>Uvaria chamae</i>	Annonaceae	Ghana	Lawal et al, 2015
445	<i>Uvariopsis congensis</i>	Annonaceae	Uganda	Krief et al, 2006
446	<i>Vahlia capensis</i>	Vahilaceae	Namibia	Lawal et al, 2015
447	<i>Vangueria infausta</i>	Rubiaceae	South Africa	Lawal et al, 2015
448	<i>Vernonia amygdalina</i>	Asteraceae	Angola/Nigeria /São Tomé	Lawal et al, 2015; Silva et al, 2011
449	<i>Vernonia brasiliana</i>	Asteraceae	Brazil	Silva et al, 2011



450	<i>Vernonia colourata</i>	Asteraceae	Ghana/South Africa	Lawal et al, 2015
451	<i>Vernonia fastigiata</i>	Asteraceae	South Africa	Lawal et al, 2015
452	<i>Vernonia hirsute</i>	Asteraceae	South Africa	Lawal et al, 2015
453	<i>Vernonia mespilifolia</i>	Asteraceae	South Africa	Lawal et al, 2015
454	<i>Vernonia myriantha</i>	Asteraceae	South Africa	Lawal et al, 2015
455	<i>Vernonia natalensis</i>	Asteraceae	South Africa	Lawal et al, 2015
456	<i>Vernonia oligocephala</i>	Asteraceae	South Africa	Lawal et al, 2015
457	<i>Virola surinamensis</i>	Myristicaceae	Brazil	Silva et al, 2011
458	<i>Vitex doniana</i>	Verbenaceae	Nigeria	Lawal et al, 2015
459	<i>Withania somnifera</i>	Solanaceae	Egypt	Lawal et al, 2015
460	<i>Ximenia americana</i>	Olacaceae	South Africa	Lawal et al, 2015
461	<i>Ximenia caffra</i>	Olacaceae	South Africa	Lawal et al, 2015
462	<i>Xylopia parviflora</i>	Annonaceae	South Africa	Lawal et al, 2015
463	<i>Xysmalobium undulatum</i>	Araliaceae	South Africa	Lawal et al, 2015
464	<i>Zanthoxylum chalybeum</i>	Rutaceae	Rwanda	Lawal et al, 2015
465	<i>Zehneria scabra</i>	Cucurbitaceae	South Africa	Lawal et al, 2015
466	<i>Zingiber officinale</i>	Zingiberaceae	Egypt	Lawal et al, 2015
467	<i>Ziziphus mucronata</i>	Rhamnaceae	South Africa	Lawal et al, 2015
468	<i>Ziziphus spina-christi</i>	Rhamnaceae	Egypt	Lawal et al, 2015

*Artemisia annua* (Artemisinin) and *Cinchona calisaya* (Quinine) are not African plants, but were included in the analysis as two known antimalarial plants so as to not overlook potential African relatives; however, none of the OTUs from ape faecal samples matched these two taxa.

**Supplementary Table 9. GenBank accession numbers of ape *Plasmodium* sequences**

Sample <sup>a</sup>	mitochondrial genome							nuclear genome					apicoplast genome			
	<i>cytB</i>	Accession No.	3.4kb	Accession No.	3.3kb	Accession No.	<i>Cox1</i>	Accession No.	<i>eba165</i>	Accession No.	<i>eba175</i>	Accession No.	<i>p47</i>	Accession No.	<i>clpM</i>	Accession No.
TL2pp3888	TL3888_1.3	=TL3905_5.12													TL3888_2.1	=TL3862_1.1
	TL3888_1.4	=TL3812_1.3														
TL2pp3843	TL3843_1.3	=TL3812_1.3													TL3843_2.7	=TL3862_1.1
	TL3843_1.6	KY790529														
	TL3843_1.8	=TL3905_5.12														
	TL3843_1.10	KY790534														
TL2pp3812	TL3812_1.3	KY790530					TL3812_1.4	KY790592							TL3812_1.1	=TL3842_2.8
TL2pp3905	TL3905_5.1	=TL3812_1.3									TL3905_1.3	KY790580			TL3905_2.5	KY790485
	TL3905_5.12	KY790540													TL3905_5.11	=TL3870_5.12
TL2pp3911	TL3911_5.1	KY790541														
	=TL3834_1.7	TL3911_5.10 TL3911_2.4	=TL3862_1.1	KY790477		KY790464		TL3911_5.13 TL3911_5.12		KY790568				KY790590	TL3911_3.4 TL3911_1.1	
						KY790465				KY790569						
	TL3911_5.3	=TL3905_5.12				KY790466				KY790570		TL3911_5.1 TL3911_1.2	KY790581			
	TL3911_5.10	=TL3812_1.3								KY790571		TL3911_5.12 TL3911_1.5	KY790584			
												TL3911_5.24 TL3911_1.6	KY790585			
											TL3911_1.7	KY790586				
											TL3911_1.8	KY790582				
											TL3911_1.9	KY790583				
											TL3911_1.10	=TL3816_1.7				
											TL3911_1.12	=TL3884_1.3				
TL2pp3912	TL3912_5.12	=TL3812_1.3	TL3912_5.13	KY790478					TL3912_5.23	KY790572					TL3912_2.1	=TL3870_5.12
									TL3912_5.24	KY790573					TL3912_2.5	KY790486
															TL3912_2.7	=TL3862_1.1
TL2pp3870	TL3870_3.8	=TL3911_5.1		KY790475		KY790462		TL3870_5.1 TL3870_5.2		KY790567		TL3870_3.11				TL3870_5.11
	=TL3862_1.1			KY790476		KY790463										
	TL3870_3.9	KY790538						TL3870_5.4 TL3870_5.24								TL3870_5.12
KY790483																
	TL3870_3.11	KY790537														
	TL3870_5.5	=TL3812_1.3														
	TL3870_5.11	=TL3834_3.1														
	TL3870_5.16	KY790539														
	TL3870_5.19	=TL3833_5.22														
	TL3870_5.20	=TL3905_5.12														
TL2pp3846	TL3846_3.12	=TL3812_1.3														
TL2pp3882	TL3882_1.4	=TL3812_1.3													TL3882_2.1	=TL3862_1.1
															TL3882_2.2	=TL3931_1.4
TL2pp3826	TL3826_1.3	=TL3812_1.3														
	TL3826_1.11	=TL3905_5.12														
TL2pp3866	TL3866_1.7	=TL3812_1.3													TL3866_1.1	=TL3862_1.1
	TL3866_3.8	=TL3905_5.12														
TL2pp3874	TL3874_1.7	=TL3812_1.3					TL3874_1.8	KY790593							TL3874_1.11	KY790484
TL2pp3853							TL3853_1.2	=TL3812_1.4								
TL2pp3873	TL3873_1.9	=TL3905_5.12														
	TL3873_3.7	=TL3812_1.3														
TL2pp3816	TL3816_5.1	=TL3812_1.3		KY790468		TL3816_5.11 TL3816_5.1	=TL3833_5.23			KY790566		KY790576			TL3816_5.9 TL3816_1.7	
	TL3816_5.1	=TL3831_1.4		KY790469						KY790565						
	TL3816_5.2	=TL3905_5.12				TL3816_5.13 TL3816_5.20	KY790455					TL3816_5.13				TL3816_5.5
=TL3862_1.1																
	TL3816_5.9	=TL3911_5.1	TL3816_5.17	=TL3911_5.13												
			TL3816_5.23	=TL3834_5.13												

TL2pp3834	=TL3862_1.1		KY790528	TL3834_5.13	KY790473	TL3834_3.1 TL3834_5.22 =TL3855_5.19		TL3834_1.5	=TL3884_1.3	TL3834_5.2
	TL3834_5.1		=TL3911_5.1	TL3834_5.22	=TL3850_5.1			KY790577		
	TL3834_5.11		=TL3905_5.12					KY790578		TL3834_5.11
	TL3834_5.20		=TL3812_1.3							TL3834_5.12
TL2pp3850	TL3850_5.1	=TL3905_5.12			KY790474	TL3850_5.1 TL3850_3.11 =TL3870_5.2				
	=TL3862_1.1									TL3850_2.6
							KY790459			
	TL3850_5.6	=TL3812_1.3				TL3850_3.12	KY790460			
	TL3850_5.9	=TL3911_5.1				TL3850_5.3				
TL2pp3948	TL3948_3.12	=TL3905_5.12	TL3948_5.11	=TL3850_5.1	TL3948_5.6	TL3850_5.19	=TL3820_5.17			
							KY790467	TL3948_5.1	=TL3862_1.1	TL3948_5.13
TL2pp3842				TL3948_5.18	KY790479					
	TL3842_1.1	=TL3905_5.12		TL3948_5.21	KY790480					TL3842_2.8
	TL3842_1.2	=TL3812_1.3								KY790481
TL2pp3889	TL3889_1.1	=TL3812_1.3						TL3889_5.8	=TL3911_5.10	
TL2pp3884	TL3884_5.1	=TL3905_5.12						TL3889_5.9	KY790589	
TL2pp3833	TL3833_5.10	=TL3905_5.12			KY790472	TL3833_5.23	TL3833_5.23	KY790458		TL3884_2.6
=TL3870_5.12								TL3884_1.3	KY790579	=TL3870_5.12
	TL3833_5.22	KY790527								TL3833_2.2
TL2pp3915	TL3915_5.1	=TL3812_1.3								
	TL3915_5.24	=TL3905_5.12						TL3915_5.12	KY790574	
TL2pp3856	TL3856_1.1	=TL3812_1.3								
	TL3856_1.3	=TL3905_5.12						TL3915_5.24	KY790575	
TL2pp3820	TL3820_5.2	KY790531			KY790470		KY790456			
					KY790471		KY790457	TL3820_5.13	TL3820_5.17	
=TL3862_1.1										TL3820_5.11
TL2pp3903	TL3820_5.4	=TL3812_1.3	TL3820_5.17		TL3820_5.18					
	TL3820_5.6	=TL3943_1.6	TL3820_5.21	=TL3834_5.13	TL3820_5.20	=TL3833_5.23				
	TL3820_5.8	=TL3905_5.12								
	TL3820_5.9	KY790533								
	TL3820_5.20	=TL3911_5.1								
	TL3820_5.23	KY790532								
	TL3903_5.7	2 (1)								TL3903_5.9
TL2pp3862	TL3862_1.4	KY790535								=TL3862_1.1
	TL3862_1.6	KY790536								TL3903_5.10
	TL3862_1.7		=TL3905_5.12							=TL3870_5.12
	TL3862_3.1	=TL3812_1.3								TL3903_5.12
TL2pp3855	TL3855_3.5	=TL3905_5.12				KY790461				=TL3931_1.4
	TL3855_5.8	=TL3812_1.3						TL3855_5.9	KY790588	TL3855_5.19
TL2pp3943	TL3943_1.2	=TL3812_1.3								TL3855_2.8
TL2pp3918	TL3918_3.9	=TL3911_5.1								TL3918_1.6
	TL3918_3.12	=TL3812_1.3								=TL3862_1.1
TL2pp3931	TL3931_1.11									TL3931_1.1
		KY790542								=TL3862_1.1
TL2pp3932	TL3931_2.12	=TL3812_1.3								TL3931_1.4
	TL3932_5.1	=TL3812_1.3	TL3932_5.3	=TL3911_5.13						KY790487

	TL3932_5.19	=TL3905_5.12	TL3932_5.7	=TL3850_5.1		
TL2pp3936	TL3936_1.2	=TL3812_1.3			TL3936_1.4	=TL3862_1.1
	TL3936_1.8	=TL3905_5.12				
TL2pp3942	TL3942_3.1	=TL3812_1.3			TL3942_2.5	=TL3862_1.1
	TL3942_3.3	=TL3905_5.12				
KRpp10	KR10_1.6	KY790526			KR10_1.1	=TL3862_1.1
Blpts54	Blpts54_1.4	KY790492				
	Blpts54_1.6	=KU665682				
Blpts67	Blpts67_1.4	KY790493				
	Blpts67_1.5	=KT824285				
Blpts93	Blpts93_1.5	=KU665682				
	Blpts93_1.8	KY790494				
Blpts244	Blpts244_1.1	=KU665682				
Blpts245	Blpts245_1.1	=KU665682				
Blpts246	Blpts246_1.1	=KU665682				
Blpts253	Blpts253_1.1	KY790489				
Blpts260	Blpts260_1.1	KY790490				
	Blpts260_1.4	KY790491				
Blpts266	Blpts266_1.1	=Blpts253_1.1				
Blpts2415	Blpts2415_1.1	=KT824285				
	Blpts2415_1.7	KY790488				
Blpts2416	Blpts2416_1.1	=KT824285				
ENpts4388	ENpts4388_1.2	=KU665670				
KSpts201	KSpts201_1.5	KY790495				
	KSpts201_1.8	KY790496				
LUpts2029	LUpts2029_1.2	KY790497				
LUpts2067	LUpts2067_1.1	=KU665682				
LUpts2069	LUpts2069_1.1	=KU665666				
LUpts2070	LUpts2070_1.1	=KT824285				
LUpts2071	LUpts2071_1.1	=KU665682				
	LUpts2071_1.3	=HM235050				
	LUpts2071_1.5	=KT824285				
	LUpts2071_1.8	=KT824296				
LUpts2072	LUpts2072_1.1	=KT824285				
LUpts2073	LUpts2073_1.1	=KT824285				
	LUpts2073_1.3	=KT824283				
	LUpts2073_1.5	=KU665682				
LUpts2074	LUpts2074_1.1	=KT824285				
LUpts2078	LUpts2078_1.1	=KT824285				
LUpts2079	LUpts2079_1.1	=KT824285				
LUpts2084	LUpts2084_1.2	=KT824299				
	LUpts2084_1.4	=KT824285				
LUpts2089	LUpts2089_1.1	=HM235208				
PApts75	PApts75_1.8	KY790507				
PApts369	PApts369_1.1	=KT824283				
PApts370	PApts370_1.1	=KT824285				
	PApts370_1.6	=KT824283				
PApts1039	PApts1039_1.6	=HM235208				
PApts1040	PApts1040_1.2	KY790498				
PApts1041	PApts1041_1.2	=HM235208				
	PApts1041_1.8	KY790499				
PApts1042	PApts1042_1.6	=HM235208				
	PApts1042_1.7	=WApts398_2.1				
PApts1043	PApts1043_1.8	=PApts1041_1.8				
PApts1044	PApts1044_1.2	KY790500				

	PApts1044_1.6	KY790501
PApts1046	PApts1046_1.1	=KT824285
	PApts1046_1.2	=HM234976
	PApts1046_1.8	=HM235208
PApts1047	PApts1047_1.1	=KT824285
	PApts1047_1.2	=HM234976
	PApts1047_1.3	KY790502
PApts1048	PApts1048_1.1	=HM235208
	PApts1048_1.2	=KT824285
PApts1052	PApts1052_1.5	=KU665682
	PApts1052_1.6	=PApts1044_1.6
	PApts1052_1.8	=WApts394_1.8
PApts1053	PApts1053_1.8	KY790503
PApts1054	PApts1054_1.7	=KT824285
PApts1056	PApts1056_1.4	KY790504
	PApts1056_1.8	=Blpts93_1.8
PApts1058	PApts1058_1.6	=WApts398_2.1
PApts1059	PApts1059_1.6	=PApts1040_1.2
	PApts1059_1.7	=KT824283
PApts1060	PApts1060_1.4	=HM235208
PApts1061	PApts1061_1.7	=HM235208
PApts1062	PApts1062_1.8	=WApts398_2.1
PApts1063	PApts1063_1.1	KY790505
	PApts1063_1.2	=Blpts93_1.8
PApts1064	PApts1064_1.2	=HM235208
PApts3143	PApts3143_5.7	=KT824285
PApts3146	PApts3146_1.1	=KU665666

PApts3146\_1.2 =KT824283

PApts3146\_5.1 =KT824285

	PApts3146_5.10	KY790506
WApts1	WApts1_5.8	=HM235208
WApts2	WApts2_1.1	=HM235208
	WApts2_1.4	=KT824285
WApts7	WApts7_1.3	=WApts398_2.1
WApts21	WApts21_1.1	KY790509
	WApts21_1.3	=WApts22_1.8
	WApts21_1.8	=KT824285
WApts22	WApts22_1.1	=HM235402
	WApts22_1.8	KY790510
WApts41	WApts41_1.3	=HM234976
	WApts41_1.5	=PApts1044_1.6
WApts392	WApts392_1.1	=KU665682
	WApts392_1.2	=KU665666
	WApts392_1.7	=Blpts93_1.8
WApts393	WApts393_1.1	=KT824285
	WApts393_1.2	=KU665682
	WApts393_1.3	KY790511
WApts394	WApts394_1.8	KY790512
WApts395	WApts395_1.1	KY790513
WApts396	WApts396_1.8	=KT824285
WApts397	WApts397_1.1	=WApts393_1.3
	WApts397_1.2	=KU665666
	WApts397_1.3	=KT824285
	WApts397_1.4	=KU665682
WApts398	WApts398_2.1	KY790514
WApts399	WApts399_5.4	=KU665682
	WApts399_5.8	=KT824285
WApts467	WApts467_1.7	=HM235050

WApts469	WApts469_1.8	=HM235050
WApts513	WApts513_1.1	KY790515
	WApts513_1.8	=KT824283
WApts519	WApts519_1.1	=HM235208
	WApts519_1.6	=WApts520_5.6
WApts520	WApts520_5.6	KY790516
WApts522	WApts522_1.5	=HM235208
WApts523	WApts523_1.1	=HM235208
WApts525	WApts525_1.1	=WApts398_2.1
WApts527	WApts527_1.2	=KT824283
	WApts527_1.4	=KT824299
WApts529	WApts529_1.2	=HM235208
WApts530	WApts530_1.5	=KT824299
WApts531	WApts531_1.5	=HM235402
	WApts531_1.8	=KT824299
WApts548	WApts548_1.5	=KT824283
	WApts548_1.8	=Blpts93_1.8
WApts555	WApts555_1.3	=KT824299
WApts561	WApts561_1.2	KY790517
WApts563	WApts563_1.1	=WApts398_2.1
WLpts99	WLpts99_1.1	=KT824299
WLpts101	WLpts101_1.1	KY790518
	WLpts101_1.2	=PApts1044_1.6
	WLpts101_1.3	KY790519
	WLpts101_1.7	=HM235208
WLpts103	WLpts103_1.6	=WApts393_1.3
	WLpts103_1.7	KY790520
		KY790508
WLpts104	WLpts104_1.7	=HM235208
WLpts111	WLpts111_1.1	=WLpts120_5.1
WLpts113	WLpts113_1.1	=WLpts120_5.1
WLpts120	WLpts120_5.1	
WLpts125	WLpts125_1.4	=KT824283
		KY790521
WLpts128	WLpts128_1.4	KY790522
WLpts131	WLpts131_1.5	
	WLpts131_5.7	=WLpts120_5.1
WLpts132	WLpts132_1.1	=WLpts120_5.1
	WLpts132_1.6	KY790523
	WLpts132_2.1	KY790524
	WLpts132_2.10	KY790525

<sup>a</sup> Samples are labeled to indicate their field site (see Fig. 1 for location) and ape species (pp; *Pan paniscus*; pts, *P. t. schweinfurthii*), followed by a number.

<sup>b</sup> New GenBank Accession Numbers are coloured yellow for *Laverania* sequences and green for non-*Laverania* sequences.

## Supplementary References

1. Loy, D. E. *et al.* Out of Africa: origins and evolution of the human malaria parasites *Plasmodium falciparum* and *Plasmodium vivax*. *Int. J. Parasitol.* **47**, 87-97 (2017).
2. Guindon, S. *et al.* New algorithms and methods to estimate maximum-likelihood phylogenies: assessing the performance of PhyML 3.0. *Syst. Biol.* **59**, 307-321 (2010).
3. Eriksson, J., Hohmann, G., Boesch, C. & Vigilant, L. Rivers influence the population genetic structure of bonobos (*Pan paniscus*). *Mol. Ecol.* **13**, 3425-3435 (2004).
4. Kawamoto, Y. *et al.* Genetic structure of wild bonobo populations: diversity of mitochondrial DNA and geographical distribution. *PLoS One* **8**, e59660 (2013).
5. Li, Y. *et al.* Eastern chimpanzees, but not bonobos, represent a simian immunodeficiency virus reservoir. *J. Virol.* **86**, 10776-10791 (2012).
6. Liu, W. *et al.* African origin of the malaria parasite *Plasmodium vivax*. *Nat. Commun.* **5**, 3346 (2014).
7. Liu, W. *et al.* Origin of the human malaria parasite *Plasmodium falciparum* in gorillas. *Nature* **467**, 420-425 (2010).
8. National Aeronautics and Space Administration: MODIS. Available at: <http://modis.gsfc.nasa.gov/> (accessed 1st May 2016).
9. Tatem, A. J., Goetz, S. J. & Hay, S. I. Terra and Aqua: new data for epidemiology and public health. *Int. J. Appl. Earth Obs. Geoinf.* **6**, 33-46 (2004).
10. Weiss, D. J. *et al.* Air temperature suitability for *Plasmodium falciparum* malaria transmission in Africa 2000-2012: a high-resolution spatiotemporal prediction. *Malar. J.* **13**, 171 (2014).
11. Hansen, M. C. *et al.* High-resolution global maps of 21st-century forest cover change. *Science* **342**, 850-853 (2013).



12. Adler, R. F. *et al.* The version 2 Global Precipitation Climatology Project (GPCP) monthly precipitation analysis (1979-Present). *J. Hydrometeor.* **4**, 1147-1167 (2003).
13. Krief, S. *et al.* Bioactive properties of plant species ingested by chimpanzees (*Pan troglodytes schweinfurthii*) in the Kibale National Park, Uganda. *Am. J. Primatol.* **68**, 51-71 (2006).
14. Lawal, B. *et al.* Potential antimalarials from African natural products: A review. *J. Intercult. Ethnopharmacol.* **4**, 318-343 (2015).
15. Silva, J. R. *et al.* A review of antimalarial plants used in traditional medicine in communities in Portuguesespeaking countries: Brazil, Mozambique, Cape Verde, Guinea-Bissau, Sao Tome and Principe and Angola. *Mem. Inst. Oswaldo. Cruz.* **106 Suppl 1**, 142-158 (2011).